AD_____

Award Number: DAMD17-02-1-0082

TITLE: The Hinge Region as a Key Regulatory Element of Androgen Receptor Dimerization, DNA Binding and Transactivation

PRINCIPAL INVESTIGATOR: Frank A. Claessens, Ph.D.

CONTRACTING ORGANIZATION: K.U. Leuven Research and Development
B-3000 Leuven, Belgium

REPORT DATE: May 2004

TYPE OF REPORT: Annual

PREPARED FOR: U.S. Army Medical Research and Materiel Command
Fort Detrick, Maryland 21702-5012

BEST AVAILABLE CO.

REPORT DOCUMENTATION PAGE

Form Approved
OMB No. 074-0188

1. AGENCY USE ONLY (Leave blank)	2. REPORT DATE	3. REPORT TYPE AND DATES COVERED
	May 2004	Annual (1 Apr 2003 - 31 Mar 2004)

4. TITLE AND SUBTITLE

The Hinge Region as a Key Regulatory Element of Androgen Receptor Dimerization, DNA Binding and Transactivation

5. FUNDING NUMBERS

DAMD17-02-1-0082

6. AUTHOR(S)

Frank A. Claessens, Ph.D.

7. PERFORMING ORGANIZATION NAME(S) AND ADDRESS(ES)

K. U. Leuven Research and Development
B-3000 Leuven, Belgium

E-Mail: Frank.claessens@med.kuleuven.ac.be

8. PERFORMING ORGANIZATION REPORT NUMBER

9. SPONSORING / MONITORING AGENCY NAME(S) AND ADDRESS(ES)

U.S. Army Medical Research and Materiel Command
Fort Detrick, Maryland 21702-5012

10. SPONSORING / MONITORING AGENCY REPORT NUMBER

11. SUPPLEMENTARY NOTES

Original contains color plates: ALL DTIC reproductions will be in black and white

12a. DISTRIBUTION / AVAILABILITY STATEMENT

Approved for Public Release; Distribution Unlimited

12b. DISTRIBUTION CODE

13. ABSTRACT (Maximum 200 Words)

The androgen receptor binds direct repeats as well as inverted repeats of the 5'-AGAACA-3' core element. This makes this receptor unique in the family of nuclear receptors. The inverted repeats are called canonical AREs, the direct repeats selectiev AREs. In collaboration with the group of Daniel Gewirth (DAMD17-01-1-0050) we were able to solve the crystal structure of the AR DNA binding domain bound to a direct repeat. The data indicate a stronger dimerization interface between the two AR protomers bound to the direct repeat in a unexpected head-to-head conformation. We are currently verifying the implication of several residues in this dimerization.

A carboxyterminal extension of the DNA binding domain of the AR is known to be involved in DNA binding (unfortunately its structure remains unsolved), in nuclear localization and in transactivation control. We have identified an inhibitory region partially overlapping the nuclear localization signal. Surprisingly, deletions which affect DNA binding negatively have a positive effect on transactivation when tested in full size receptors. Mutating the acetylation sites does not affect this phenomenon. The deletion of the inhibitory region affects the MG132 (protease inhibitor) effects on transactivation.

We are continuing the structure-function analysis of this region, and try to unravel the mechanism of potentiation of transactivation.

14. SUBJECT TERMS

Androgen receptor, selectivity, DNA binding, transactivation

15. NUMBER OF PAGES

98

16. PRICE CODE

17. SECURITY CLASSIFICATION OF REPORT	18. SECURITY CLASSIFICATION OF THIS PAGE	19. SECURITY CLASSIFICATION OF ABSTRACT	20. LIMITATION OF ABSTRACT
Unclassified	Unclassified	Unclassified	Unlimited

NSN 7540-01-280-5500

Standard Form 298 (Rev. 2-89)
Prescribed by ANSI Std. Z39-18
298-102

Table of Contents

Annual Report Grant DAMD17-02-1-0082

THE HINGE REGION AS A KEY REGULATORY ELEMENT OF ANDROGEN RECEPTOR DIMERIZATION, DNA BINDING AND TRANSACTIVATION

P.I. Claessens, Frank A.
University of Leuven
Faculty of Medicine
Department of Molecular Cell biology
Laboratory for Molecular Endocrinology
Campus GHB O/N
Herestraat 49
3000 Leuven
Belgium

INTRODUCTION

Androgens play specific key roles, not only in male development (illustrated by the study of De Gendt *et al.* 2004), but also in many normal physiological processes in both sexes and in the development and progression of prostate cancer. The androgen receptor together with the receptors for glucocorticoids, progestagens and mineralocorticoids all bind bipartite hormone response elements organized as inverted repeats of 5'-AGAACA-3'-like core elements separated by three nucleotides (figure 1B, appendix I). However, we discovered that the androgen receptor can bind direct repeats of the same core elements as well (Claessens and Gewirth). This makes this receptor unique in the family of nuclear receptors, although other receptors, like the vitamine D receptor also recognize direct repeats of a different core sequence 5'-AGGTCA-3'. The inverted repeats are called canonical AREs, while the direct repeats will be called selective AREs.

Two zinc coordinating modules that constitute the receptors DNA-binding domain, are involved in the recognition of canonical AREs, but for the high affinity binding to selective AREs, a carboxyterminal extension (CTE) is needed (figure 1A, appendix I). This CTE is not only involved in DNA binding, but is also the acceptor for acetylation. In addition, the CTE is involved in nuclear translocation as well as the transactivating properties of the androgen receptor (Moilanen *et al.* 1997, Wang *et al.* 2001). In this study, we are unraveling the structure-function relationships in the two zinc coordinating modules and the CTE (reviewed in Claessens *et al.* 2001).

BODY

The subject of the here reported research, is **a.** to determine the structure of the DNA-binding domain bound to direct repeats versus inverted repeats (in collaboration with Dr. Daniel Gewirth DAMD17-01-1-0050), and **b.** to analyze the structure-function relationship within the hinge region of the AR. We aim to use the new insights in the development of alternative therapeutic strategies against prostate cancer.

Task I

I.A. Co-crystals of an AR-DBD fragment

Co-crystals of an AR-DBD fragment with double stranded oligonucleotides containing the sequence of a perfect 5'-AGAACA-3' direct repeat were obtained and analyzed in the Gewirth Laboratory. The three dimensional structure of the DBD dimer bound to this element reveals an unexpected head-to-head arrangement, contrary to the expected head-to-tail conformation seen for nuclear receptors bound to response elements of similar geometry (figure 3, appendix I).

Comparison of the dimerization interface between GR-GRE and AR-ARE data, revealed that a glycine to serine change at position 580 in the AR fills a 'glycine hole' present in the GR interface, and results in an additional hydrogen bond between the two serines. The threonines at position 585 in the AR (an isoleucine is found at this position in the GR) forms hydrogen bonds to the carbonyl oxygen of alanines at position 579 in the opposing monomers (figure 4, appendix I).

The AR DBD-DNA interface of the two protomers is not surprisingly slightly different. The cognate AR DBD half-complex binds the consensus 5'-AGAACA-3'. The nonconsensus half-complex, however, has to bind 5'-TGTTCT-3' instead of the inverted repeat as present in the GR-GRE complex. Although the T to A substitution at position 4 (opposite strand, numbering cfr. Appendix I) reduces the number of protein-DNA interactions, no clashes occur which would disfavour AR binding to a direct repeat (figures 5 and 6, appendix I).

These data indicate that the AR-DBD dimerization is stronger than that of the other steroid receptors. A more stable protein-protein interface would allow DNA elements with a less conserved downstream hexamer (like direct repeat elements) to be recognized as response elements by the AR, but not by the other receptors and thus explain the existence of AR-selective elements.

The crystal data have been described and published in Shaffer *et al.* 2004 (Appendix 1), and presented at the Keystone Meeting on Nuclear receptors, steroid sisters (March 2004).

Should we exclude head-to-tail binding by AR to direct repeat elements?

- The crystal data indicate a stronger dimerisation interface for the AR DBD, as compared to other receptors. However, the crystal data do not explain why the AR-DBD has a specifically high affinity for direct repeat-like elements, or natural AR-selective AREs like that described for the probasin promotor (24 nM for PB-ARE-2). A stronger dimerization interface is certainly part of the explanation, but not sufficient to explain all aspects of DNA-selectivity.
- It is unfortunate that the crystal data do not show the structure of the CTE, which has a clear role in DNA-binding and recognition of selective AREs (Schoenmakers *et al.* 2000, Haelens *et al.* 2003). Indeed, swapping the CTEs between GR and AR DBDs resulted in fragments with apparent affinity constants of 200 and 270 nM versus 22 and 21 nM for the PB-ARE-2 and the C3(1)ARE respectively (Schoenmakers *et al.* 1999). In addition, a Gly to Glu substitution in the AR DBD CTE resulted in a decrease of apparent affinity constant from 23 to 340 for the PB-ARE-2, while the affinity for the C3(1)ARE remained unchanged.
- In functional analyses of several mutations in the AR transactivation domains, we observed differential effects depending upon the type of ARE that was tested (see further). This too hints to alternative conformations of full size AR dimers bound to such elements.

We developed two working hypotheses which will be tested in the following year: either head-to-tail binding by the AR is possible, but did not allow crystal growth (yet), or the DNA binding of the AR results in allosteric effects, possibly involving non-specific interactions between the CTE and DNA.

I.B. Translation of the structural data

To confirm the three-dimensional crystal structure of the androgen receptor DNA-binding domain bound to a direct repeat element, we are exchanging the glycine580/serine and the threonine585/isoleucine in the DNA-binding domains of the androgen and glucocorticoid receptors (see table I).

Table I: New constructs needed for the further verification of the structure data

Mutations cloned	as DBD-GST fusion	in full size receptor expression vector
AR DBD Ser to Gly	X	X
Thr to Ile	X	X
Double		X
GR DBD Gly to Ser	X	
Ile to Thr	X	X
Double	X	

X indicates constructs finished at the time of writing

Table II : Sequences of the androgen response elements used in this study

Non-specific motifs

C3(1)ARE	5'-AGTACGtgaTGTTCT-3'
rTAT-GRE	5'-TGTACAtgaTGTTCT-3'
IR	5'-AGAACAtgaTGTTCT-3'

Specific motifs

pb-ARE2	5'-GGTTCTtggAGTACT-3'
slp-HRE2	5'-TGGTCAgccAGTTCT-3'
DRi	5'-GGTTCTtgaTGTTCT-3'
DR(3)	5'-TGTTCTtgaTGTTCT-3'

The effect of the serine 580 to glycine mutation (and vice versa) on the affinity of the AR-DBD (and GR-DBD) was compared with that of wild type receptor fragments. In preliminary band shifts, we could not observe a difference in DNA recognition (figure 1A in annex I). As shown in table I, the same changes were introduced in expression vectors for full size AR and GR. In functional assays (figure 1B), the single mutations did not result in change of specificity in AR or GR when tested on several AREs described in Table II. Although this does not corroborate the crystal data, possibly, we will only see differences when analyzing the double mutants. We will therefore finish the construction of all mutant forms of AR- and GR-DBD (table I) in the next year, and test them in DNA binding and transactivation assays.

Additional experiments are planned to verify the structure of the AR-DBD dimer on selective elements:

a. **Fluorescent resonance energy transfer (FRET) analyses** reveals the proximity of two molecules by a transfer of the energy of a donor fluorophore (linked to a first molecule) to a second fluorophore, called acceptor, linked to a second molecule. We are labeling the ARE in the spacer region with one fluorophore and the AR-DBD at one end with the second fluorophore. In theory, only when bound in a head-to-tail arrangement of the protein dimer, the second fluorophore will be close enough to the spacer region to allow energy transfer.

b. **NMR analyses** are planned in collaboration with Prof. D. Gewirth. They will be performed on AR-DBD (including the CTE) bound to different types of AREs. This should enable us to visualize the CTE in the DNA-bound DBD.

I.C. Deletion study of the hinge region

Initially, we have performed a mutation analysis of the hinge region, analyzing the effect of the mutations in the context of the full size receptor. Three series of deletions were developed (figure 2). The first series was described in the first annual report. Constructs Δ1 en Δ2, but not Δ3 to 5 resulted in a more active AR on C3(1)ARE- or MMTV-based reporter constructs tested in HeLa and COS cells (figure 3B, and results not shown). Surprisingly, DNA binding to the C3(1)ARE and PB-ARE-2 for Δ1 en Δ2 was reduced to almost undetectable amounts in band shift assays (figure 3A). This study defined the left boundary of the inhibitory region at position 629. Further deletion of residues 636 to 642 in Δ8 increased the effects (figure 4B). This is possibly due to the fact that in construct Δ7, due to the deletion of 629 to 636, the lysine 630 and leucine 631 are replaced by lysine 638 and leucine 639.

The second generation of constructs revealed that a deletion of 628 to 636 reduced the affinity for both selective and canonical AREs (figure 4A), while the transactivating potency of the AR was increased up to 6-fold (figure 4B). Construct Δ6 is the only construct for which a reduced DNA binding is not correlated with an increased transactivation, however, the reduction in DNA-binding is not as dramatic as that observed for constructs Δ7 or Δ8 (figure 4 and Table III). Therefore, the right side boundary of the inhibitory region was set at position 636.

In a third generation of constructs, we verified whether the inhibitory region could be further divided. From the results represented in figure 5, we learned that deletion of residues 629 to 636 was necessary and sufficient for decreased DNA binding and increased transactivation.

Table III: Summary of data from figures 3 to 5.

Code	deletion	C3(1)ARE	PB-ARE-2	I.F. on MMTV in HeLa cells
WT		+++	+++	**7.4 ± 0.9**
Δ1	**Δ628-646**	+	-	**24.3 ± 4.8**
Δ2	**Δ629-646**	+	-	**19.5 ± 2.3**
Δ3	**Δ632-646**	++	++	**5.6 ± 1.0**
Δ4	**Δ637-646**	+++	+++	**7.4 ± 1.0**
Δ5	**Δ640-646**	+++	+++	**6.3 ± 4.9**
Δ6	**Δ628-631**	+	-	**18.1 ± 8.5**
Δ7	**Δ628-636**	(+)	-	**50.7 ± 4.6**
Δ8	**Δ628-642**	(+)	-	**106.5 ± 9.6**
Δ9	**Δ629-631**	+++	+++	**14.5 ± 2.0**
Δ10	**Δ632-636**	+++	+++	**13.8 ± 2.3**
Δ11	**Δ629-636**	+	-	**42.1 ± 9.6**

Column 1: codes as used in later figures. Column 2: residues deleted in the full size AR. Columns 3 and 4: relative binding was scored – for no binding, + weak, ++ less than wild type and +++ similar to wild type. The last column gives the induction factors as measured in transient transfection assays in HeLa cells (at least 3 experiments in triplicates, +/- S.E.M.) the data for Δ1 were compiled from figs 3 to 5.

In summary (Table III), those constructs with a reduced affinity for DNA resulted in higher trans-activation, indicating increased potencies, since in Western blot no difference in expression levels were observed (upper panels in figures 3 to 5). This apparent contradiction is even more puzzling when we take into account that the inhibitory region overlaps with part of the bipartite nuclear localization signal. We have fused green fluorescent protein to the carboxy-terminal end of the AR constructs to verify their subcellular localization. Initial observations indicate that the deletion indeed affects the localization, but more elaborate studies will be performed to analyse ligand effects in a quantitative manner (see also further).

I.D. Functional comparison of AR-fragments with or without hinge region

The yeast expression vector for Gal4DBD-AR-HR-LBD was developed, but shown to be inactive in functional assays (see earlier report). Deletion of the hinge region did not affect the outcome.
Similar AR-deletion and Gal4DBD-fusion constructs have been tested in mammalian cells (HeLa cells in figure 6). Preliminary results indicate that the effect of the deletion depends on the way transactivation is measured. In the AR-DBD-H-LBD, the deletion has little effect when tested on C3(1)ARE-based luc-reporters (induction factors 1 to 1.5). When this AR fragment is fused to the DBD of Gal4, the deletion of the hinge region has a more pronounced effect. The presence of the AR-DBD is not necessary for the effect of the deletion of the hinge region as can be deduced from figure 6B (right panel). The differences in activity are not due to differences in expression levels of the AR-derived constructs at the time of luciferase measurement (Figure 6A right panel).
This indicates that **a)** mammalian proteins but not **b)** yeast proteins, are involved in the function(s) of the hinge region and **c)** that the presence of the AR DBD is not necessary.

Task II

II.A. Studies in yeast

Since we did not observe a difference in the activity of the AR-DBD-HR-LBD and the AR-DBD-LBD (in yeast), we did not set up a yeast screening system for activating mutations in the hinge region. However, we want to take these AR-fragments to screen a cDNA expression library for co-regulatory proteins that interact with the hinge region of the AR. The group of Jänne has already described several hinge region-interacting proteins, but these were obtained by screening with a DBD-HR fragment, without the LBD.
To this end we aim to construct yeast strains expressing AR-fragments with or without the inhibitory region, together with reporter genes under control of AREs. Clones, present as activation domain-fusions

in a cDNA library, which code for proteins that interact with the inhibitory region will then be screened for. For the construction of these yeast strains, we will start from constructs made available to us by Dr. Ceraline (Laboratoire de Cancerologie Experimentale et de Radiobiologie-EA/ULP 3430, IRCAD, Strasbourg, France)

II.B. Define a minimal part of the hinge region

The minimal part of the hinge region necessary for correct functioning of the AR was defined in mammalian cells rather than yeast, as described in part I.C.

An amphipathic α-helix is predicted in the inhibitory region (from position 629 to 636) described in section I.C.

- Is the amphipatic nature of this putative helix involved in the inhibitory effect?

The effects of point mutations that changed leucines 631 and 634 into lysines had a (less then 2-fold) negative effect on the functionality of the AR on the MMTV reporter (figure 7A), which is contrary to the expected potentiation. The effect is only marginal and does not compare to the positive effect of the deletion on the activity of the full size receptor.

- Is the helical nature involved in the inhibitory effect?

Mutations of leucine 631, lysine 633 or leucine 634 into helix breaking prolines (as inferred from computational helix predictions), had no effect on the functionality of the AR (figure 7A). This clearly shows that the helical nature of this section is not necessary for the inhibitory effect.

Further point mutation analysis of this region is described in the following paragraphs.

Role of hinge region: acetylation of the AR

The group of Pestell has demonstrated that the AR can be acetylated *in vivo*, and that Lysines 630, 632 and 633 in the hinge region of the AR can be acetylated *in vitro* (Fu *et al.* 2000, 2002). Lysine 630 was proposed to be involved in transcriptional regulation through an enhanced recruitment of p300 and reduced affinities for N-CoR and Smad3 after its acetylation (Fu *et al.* 2003). In their study, the mutation of this lysine to glutamine or threonine (mimics acetylation), when expressed in DU145 cells promoted cell survival and growth of cancer cells in soft agar and nude mice.

We have analyzed point mutations in lysine 630, 632 and 633. Surprisingly, when tested in transactivation on the mouse mammary tumor viral enhancer in HeLa cells, only mutating lysine 633 to arginine reduced the transactivating properties of the AR to about half that of wild type AR. Changing lysine 630 to threonine (cfr Fu *et al.* 2003) did not have any effect either, nor did changing arginine to glutamine at 629 (figure 7B).

We have mutated the three lysine residues, but could not see any effect in our transient transfection assays (figure 7B). Since the group of Pestell has elaborated on the acetylation of these residues, and since we have difficulties in reproducing the published effects, we will focus on other aspects of the hinge region. We will however, pursue the possible roles of the lysines and their acetylation by comparing effects of deletions of the histon acetylase domain of CBP on androgen responses. To this end, we obtained expression constructs from Erik Kalkhoven (Department of Molecular Cell Biology, Leiden University Medical Centre, The Netherlands)

Role of the hinge region: sumoylation of the AR (figure 4 in appendix II)

The AR is substrate for a recently described posttranslational modification, i.e. covalent attachment of a small ubiquitin-like modifier (sumo) (Poukka *et al.* 2000). Two sumo acceptor sites have been described in the aminoterminal domain as documented in Callewaert *et al.* (2004). Two enzymes involved in sumoylation have been reported to interact with the AR hinge region: the sumo-conjugating enzyme Ubc9 and the sumo-ligase PIAS 1xa (protein inhibitor of activated STAT) (Poukka *et al.* 1999; Kotaja *et al.* 2000). In our assays, Ubc9 interacts much stronger with the aminoterminal domain as compared to the hinge region (figure 2 in appendix II). However, PIAS 1xa binds to the hinge region (results not shown), although the AR in which the hinge region has been deleted is sumoylated as efficiently as wild type receptor (figure 2A in appendix II).

Role of the hinge region: stability of the AR

The deletion of the region 628-646 in the human AR did not affect the steady state levels of the AR in transfected cells as measured by Western blot (compare lanes 1 in figure 8).

MG 132 is an inhibitor of the proteasome. It was shown to be necessary for mobility of the ER, as well as the transcriptional control by this receptor (Reid *et al.* 2003). In the case of the AR, we analyzed the role of proteasome in the function of AR versus ARΔ1 by measuring the effect of 18 hrs and 24 hrs addition of MG132 to the medium of transfected cells (figure 8 and Tanner *et al.* submitted). While MG132 did not seem to affect AR levels, it resulted in an increase in the signal for the Δ1 construct. This contrasts with the observed transactivations, since MG132 reduced the activity of the Δ1 construct. We can not exclude indirect effects of MG132 on transcription, but possibly, the deletion results in a relieve of inhibition on a function which is proteasome-dependent. As a matter of course, we need to verify this hypothesis by more extensive time-courses and refined monitoring of AR-stability, -mobility and recycling (see appendix III for more details).

Role of the hinge region: cellular localization of the AR

We have cloned the AR and Δ1 fused to EGFP (first clone obtained from Dr. Knudsen, Department of Cell Biology, University of Cincinnati, Ohio). This fusion contained a $(Gly\text{-}Ala)_5$ linker which was necessary to obtain a functional fusion product. Indeed, this fusion is active in transactivation assays. The deletion of the hinge region increased the activity of this AR-fusion very similar to what was observed for the AR.

The intracellular localization of these constructs will be analyzed during the third year. This is an important control, since it can be expected that deleting part of the NLS results in a different intracellular distribution of the AR. In addition, contacts have been made with Gordon Hager to express AR and mutant ARs in a cell line containing an array of the MMTV-HRE. This array enables direct visualization of GR-GFP recruited to this array in living cells. We want to analyze the effect of hinge region mutation on these events. In addition, this collaboration should enable us to study the role of the hinge region in the mobility of the AR, which can be studied by the FRAP technique (fluorescence recovery after photo-bleaching).

II.C. High level expression of the mutant DBD-LBD constructs

GST-fused fragments of the AR containing the DBD-HR-LBD with complete hinge region or small deletions in it have been developed for expression in *E. coli*. Unfortunately, the expression levels of these fragments were very low and difficult to reproduce, due to the fact that the *E. coli* clones seem to loose the insert very fast.

III.C. Translate the data into strategy for control of androgen response in cells

As an initial experiment (figure 9) to search for dominant negative peptides based on the hinge region of the AR, we performed co-transfection experiments. In this assay we followed the functionality of the androgen receptor via a C3(1)ARE-based luciferase reporter. An AR-fragment covering part of the DBD and the hinge region (589-669), or this fragment with a deletion of the hinge region (confer Δ1) were tested. Although we clearly observe a negative effect of both fragments on the function of the AR as well as construct Δ1, this is clearly not a dominant negative effect, since 10 ng expression vector for the fragment did not abolish the androgen response. In fact, if the hinge region is inhibitory by recruiting a negative co-regulator, we would expect a positive effect of co-transfection of this fragment. It is more likely though that for the inhibitory effect a larger part of the AR is involved. We certainly need more information on the structure-function relations within the hinge region of the AR that should allow more targeted design of dominant negative peptides.

Key research accomplishments

- The crystal structure of the DNA-binding domain of the AR bound to a selective element has been solved, and this detailed knowledge can be used to analyze the effect of the many mutations described in androgen insensitivity syndromes.
- The crystal data led to new insights into the dimerization of the AR DBD: the surface is larger, and there are three additional hydrogen bonds compared to the GR DBD.
- This dimerization interface of the AR predicted by the crystal has been partially analyzed by mutation analyses. At present, the prediction is not corroborated (but is not contradicted either) by these new data.
- The minimal inhibitory motif in the hinge region has been determined to be located between 628 and 637. The amphipatic α-helix predicted in this region is not necessary for the inhibitory function.
- There is a strong inverse correlation between DNA binding and transactivation.
- The study of the sumoylation of the AR revealed that the sumo-conjugating enzyme Ubc9 does not bind to the hinge region, but to the aminoterminal domaion of the AR. The sumo-ligase PIAS1Xa does bind to the hinge region, but does not seem required for sumoylation.
- The acetylation of the hinge region does not seem involved in the inhibitory effect of the hinge region seen in or assays, since mutations did not result in a more active AR.
- Fragments of the AR containing this inhibitory region are not dominant negative over the androgen response measured in transient transfection experiments, irrespective of the presence of the inhibitory region (629-645).

Reportable outcomes

- The structural data on the AR DNA-binding domain bound to a direct repeat element has been reported by Shaffer, P., Jivan, A., Dollins, D.E., Claessens, F., Gewirth, D. Structural basis of androgen receptor binding to selective androgen response elements. Proc. Natl. Acad. Sci U.S.A. (2004) 101:4758-4763. (see annex I),
  and by Claessens F. and Gewirth D. as a poster (nr 179) at the Keystone Joint Meetings on Nuclear receptors: Orphan brothers (J7) and Steroid Sisters (J8) Februari 28 to March 4
- A 'inhibitory motif' in the hinge region of the AR was defined (work in progress). The initial experiments were reported (oral presentation by F. Claessens) at the Jensen Symposium on Nuclear Receptors and Endocrine Disorders december 5-7, 2003 at Cincinnatti, Ohio.
- The sumoylation of the AR and its relation to the hinge region as recruitment surface for Ubc9 or PIAS Ixa was reported by Callewaert, L., Verrijdt, G., Haelens, A., Claessens, F. (2004) Differential effect of sumoylation of the androgen receptor in the control of cooperativity on selective versus canonical response elements. Mol. Endocrinol. *In press.* (annex II). This was also a chapter of the PhD thesis of Leen Callewaert entitled 'Structure-function analysis of the aminoterminal domain of the androgen receptor' and presented at 29 March 2004 at the Universitary Press of the University of Leuven
- The sensitivity to MG132 of the AR compared to a mutant AR in which the inhibitory region was deleted has been reported and submitted by Tanner *et al.* 2004 (see annex III).

Conclusions

The grant has provided us with the necessary means to study the structure-function relations in the hinge region of the AR. This led to the description of a minimal inhibitory region and we will use the remaining year to focus on the further elucidation of the mechanisms of action responsible for this apparent inhibition.

- The structure of a dimer of the AR DBD bound to a direct repeat of the hexamer 5'-AGAACA-3' was solved in collaboration with the group of Prof. D. Gewirth. This revealed that the AR DBD has a stronger dimerization interaction due to a glycine/serine and a threonine/isoleucine difference with the glucocorticoid, progesterone and mineralocorticoid receptors. We are verifying these data by swapping experiments between the full size AR and GR, as well as their isolated DBDs.
- In future experiments, we will try to determine the structure of the carboxyterminal extension of the DBD that is also involved in the DNA-recognition by the AR.
- We have made considerable progress in our knowledge of the structure-function relations within the hinge region of the androgen receptor. The deletion of a minimal fragment from residues 629 to 636 is shown to be sufficient to potentiate the AR activity as a transcription factor. We postulate that the deleted fragment acts as an inhibitory motif.
- The inhibitory fragment overlaps with part of the nuclear localization signal. A first series of mutations that destruct the amphipatical or even the helical nature of the motif, did not result in a potentiation of the AR. Further mutational analyses to reveal the role of each individual residue in the activation/inhibition, are necessary for a better understanding.
- We will use the combination of the information on the yeast and mammalian assays to screen for inhibitory-region-interacting partners.

References

Callewaert, L., Verrijdt, G., Haelens, A., Claessens, F. (2004) Differential effect of sumoylation of the androgen receptor in the control of cooperativity on selective versus canonical response elements. Mol. Endocrinol. *In press.*

Ceraline J, Erdmann E, Erbs P, Deslandres-Cruchant M, Jacqmin D, Duclos B, Klein-Soyer C, Dufour P, Bergerat JP. (2003) A yeast-based functional assay for the detection of the mutant androgen receptor in prostate cancer. Eur J Endocrinol. 148: 99-110.

Claessens, F., Gewirth, D. (2004) Essays in Biochemistry Volume 40: The nuclear receptor superfamily. *In press*

Claessens F, Verrijdt G, Schoenmakers E, Haelens A, Peeters B, Verhoeven G, Rombauts W (2001) Selective DNA binding by the androgen receptor as a mechanism for hormone-specific gene regulation. J. Steroid. Biochem. Mol. Biol. 76:23-30.

De Gendt, K., Swinnen, J.V., Saunders, P.T.K., Schoonjans, L., Dewerchin, M., Devos, A., Tan, K., Atanassova, N., Claessens, F., Lécureuil, C., Heyns, W., Carmeliet, P., Guillou, F., Sharpe, R.M., Verhoeven, G. (2004) A sertoli cell-selective knock out of the androgen receptor causes spermatogenic arrest in meiosis. Proc. Natl. Acad. Sci U.S.A. 101: 1327-1332.

Evans RM (1988) The steroid and thyroid hormone receptor superfamily. Science 240:889-895.

Fu, M., Rao, M., Wang, C., Sakamaki, T., Wang, J., Di Vizio D., Zhang, X., Albanese, C., Balk, S., Chang, C., Fan, S., Rosen, E., Palvimo, J., Janne, O.A., Muratoglu, S., Avantaggiati, M.L., Pestell, R.G. (2003) Acetylation of androgen receptor enhances coactivator binding and promotes prostate cancer cell growth. Mol. Cell. Biol. 23: 8563-8575.

Fu, M., Wang, C., Reutens, A.T., Wang, J., Angeletti, R.H., Siconolfi-Baez, L., Ogryzko, V., Avantagiatti, M.L., Pestell R.G. (2000) p300 and p300/cAMP-response element-binding protein-associated factor acetylate the androgen receptor at sites governing hormone-dependent transactivation. J. Biol. Chem. 275: 20853-860.

Fu, M., Wang, C., Wang, J., Zhang, X., Sakamaki, T., Yueng, Y.G., Chang, C., Hopp, T., Fuqua, S.A.W., Jaffray, E., Hay, R.T., Palvimo, J., Janne, O.A., Pestell, R.G. (2002) Androgen receptor acetylation governs trans activation and MEKK1-induced apoptosis without affecting in vitro sumoylation and trans-repression function Mol. Cell. Biol. 22:3373-3388.

Haelens A., Verrijdt, G., Callewaert, L., Christiaens, V., Schauwaers, K., Peeters, B., Rombauts, W., Claessens, F. (2003) DNA recognition by the androgen receptor: evidence for an alternative DNA-dependent dimerization, and active role of sequences flanking the response element on transactivation. Biochem. J. 369: 141-151.

Kotaja N, Aittomaki S, Silvennoinen O, Palvimo JJ, Janne OA (2000) ARIP3 (androgen receptor-interacting protein 3) and other PIAS (protein inhibitor of activated STAT) proteins differ in their ability to modulate steroid receptor-dependent transcriptional activation. Mol. Endocrinol. 14:1986-2000.

Moilanen A, Rouleau N, Ikonen T, Palvimo JJ, Janne OA (1997) The presence of a transcription activation function in the hormone-binding domain of androgen receptor is revealed by studies in yeast cells. FEBS Lett. 412:355-358.

Poukka H, Karvonen U, Janne OA, Palvimo JJ (2000) Covalent modification of the androgen receptor by small ubiquitin-like modifier 1 (SUMO-1). Proc. Natl. Acad. Sci. U S A. 97:14145-14150.

Poukka H, Aarnisalo P, Karvonen U, Palvimo JJ, Janne OA (1999) Ubc9 interacts with the androgen receptor and activates receptor-dependent transcription. J. Biol. Chem. 274:19441-19446.

Reid G, Hubner MR, Metivier R, Brand H, Denger S, Manu D, Beaudouin J, Ellenberg J, Gannon F (2003) Cyclic, proteasome-mediated turnover of unliganded and liganded ERalpha on responsive promoters is an integral feature of estrogen signaling. Mol. Cell. 11:695-707.

Schoenmakers, E., Verrijdt, G., Peeters, B., Verhoeven, G., Rombauts, W. and Claessens F. (2000) Differences in DNA binding characteristics of the androgen and glucocorticoid receptor can determine hormone specific responses. J. Biol. Chem. 275, 12290-12297.

Shaffer, P., Jivan, A., Dollins, D.E., Claessens, F., Gewirth, D. Structural basis of androgen receptor binding to selective androgen response elements. Proc. Natl. Acad. Sci U.S.A. (2004) 101:4758-4763.

Wang Q, Lu J, Yong EL (2001) Ligand- and coactivator-mediated transactivation function (AF2) of the androgen receptor ligand-binding domain is inhibited by the cognate hinge region. J. Biol. Chem.276:7493-7499.

Appendices

I. Shaffer, P., Jivan A., Dollins, D.E., Claessens, F. and Gewirth, D.T. (2004) Structural basis of androgen receptor binding to selective androgen response elements *Proc. Natl. Acad. Sci U.S.A.* **101**, 4758-4763

II. Callewaert, L., Verrijdt, G., Haelens, A., Claessens, F. (2004) Differential effct of sumoylation of the androgen receptor in the control of cooperativity on selective versus canonical response elements. Mol. Endocrinol. *In press.* Is also a chapter of the PhD thesis of Leen Callewaert.

III. Tamzin, T., Claessens, F., Haelens, A. The hinge region of the androgen receptor plays a role in proteasome mediated transcriptional activation. Submitted for Annals of the New York Academy of Sciences, and presented as a poster at a Meeting on Chromatine structure and gene expression mechanisms as therapeutic targets 'Chromatin 2004', Luxembourg, january 28-31, 2004.

Figure legends

Figure 1. Verification of the structural data on AR-DBD dimerisation surface.
A. Oligonucleotides with sequences given in Table II (codes indicated) were used as a radiolabeled probes (10^4 cpm) for binding to the DNA-binding domains and mutated versions, produced in *E. coli* (Schoenmakers *et al.* 1999). Binding reactions were performed with increasing amounts (0.2, 0.4, 1, 2, 4, 10, 20, 40 and 100 ng in the upper panel and 2, 4, 10, 20, 40, 100, 200, 400 and 800 ng in the lower panel) of purified recombinant protein named at the bottom of each experiment. Constructs ARmutS-G and GRmutG-S are described in table I as AR DBD Ser to Gly and GR DBD Gly to Ser resp.
B. Transient transfections were performed on 10^4 HeLa cells plated in 96-well plates. 100 ng of the indicated luciferase reporter construct was co-transfected with 1 ng of receptor expression plasmid (pCMV-based) and 10 ng of a pCMV-b-galactosidase construct. Cells were stimulated with 1 nM R1881 (a synthetic androgen) or 10 nM dexamethasone (a synthetic glucocorticoid) as appropriate. Cells were harvested and luciferase and b-galactosidase values were measured. Induction factors are the ratio's of the luciferase values (means of at least three experiments in triplicate, corrected for b-galactosidase expression levels) in extracts of stimulated and unstimulated.
Reporter constructs (indicated below each graph) contain two copies of the response element (sequence in Table II) upstream of a minimal promoter. Bars to the left of the dotted lines are the results of the control transfections.

Figure 2. Representation of AR and derived constructs

Schematic representation of the androgen receptor, with functional domains indicated (top). The amino acid sequence of the hinge region fragment under study is given. The carboxyterminal extension and the inhibitory region are indicated. Below: a schematic presentation of the three series of deletions used in this study, the codes and the numbers of fragments which were deleted are given at the right.

Figure 3 Binding and transactivation characteristics of first AR derived constructs.

A. The first series of constructs (AR, Δ1 to 5) depicted in figure 2 were expressed in COS cells. Cell extracts were assayed for presence of the AR or the AR-derived proteins by Western blotting. A self made rabbit antibody raised against an aminoterminal peptide was used at 5000-fold dilution as primary antibody.

The AR constructs were incubated with either C3(1)ARE (at the left) or PB-ARE-2 (at the right) and bound probe (arrowhead) was separated from free probe (dot) by non-denaturing polyacrylamide gel electrophoresis. Supershifts were induced by addition of antibody against AR before addition of the probe.

B. Functional analysis: Expression constructs (10 ng) were co-transfected with the MMTV-based luciferase reporter (100 ng) in HeLa cells (data presentation as described in the legend of figure 1B).

Figure 4 Binding and transactivation characteristics of second AR derived constructs.

Confer legend figure 3. The constructs Δ1, Δ6 to 8 are described in Figure 2.

Figure 5 Binding and transactivation characteristics of third AR derived constructs.

Confer legend figure 3. The constructs Δ1, Δ9 to 11 are described in Figure 2.

Figure 6. Role of hinge region in AR fragments tested in mammalian cells.

A. Schematic representation of the constructs with indication of the boundaries of the functional domains. At the right, the expression of the constructs in HeLa cells is demonstrated by Western blotting. For this, a Flag epitope was added to the fusion proteins and the Western blot was developped with a monoclonal antibody against this epitope (cfr legend figure 8). The position of marker proteins with given molecular weight are indicated by arrowheads. DHL is the code for the DBD-HR-LBD fragment of the human AR; G4HL: fusion of the Gal4 DBD with the HR-LBD region of the AR; G4DHL: fusion of the Gal4 DBD with the DBD-HR-LBD fragment of the AR. The suffix Δh indicates that the region between 628 and 646 has been deleted.

B. Functional assays of the constructs were performed as described in Figure 1B. The reporter construct used is indicated on top. Gal4UAS is a luciferase reporter construct containing five Gal4 upstream activating sequences. The AR-derived constructs are indicated at the bottom of each histogram.

Figure 7. Point mutation analysis of the inhibitory region in the AR hinge.

A. Functional analysis of full size AR with mutations in residues in the inhibitory region. The left panel shows results of mutations which lead to destruction of a possible amphipatic nature of an alpha-helix.

The right panel shows the effect of mutations that would disrupt an alpha-helix. The AR-construct activities were measured in transient transfections as described in the legend of figure 1B.
B. Effect of the mutations of the lysines in the inhibitory region on the activity of the AR. The induction factors obtained in two sets of experiments are given. The activities were tested as in A.

Figure 8. Amino acids 628-646 of the hinge region play a role in proteasome-mediated transcriptional activation of the AR

A. Western blot. HeLa cells were seeded into 24-well plates at 10^5 cells/well. After 24 hours, cells were transiently transfected with 200 ng of the appropriate flag-tagged receptor expression vector using FuGene6 reagent. Twenty-four hours later, cells were stimulated with or without 1 nM R1881 in the presence of increasing concentrations MG132 (Calbiochem). MG132 was added either 1 hr before, simultaniously or 6 hrs after the hormone, resulting in an incubation of 24 and 18 h, respectively. Equal amounts of extracts were loaded onto a 10% SDS-polyacrylamide gel, electrophoresed and blotted onto Hybond-P nitrocellulose membrane (Amersham Biosciences). Membranes were probed with anti-Flag antibody, receptor proteins detected by ECL and autoradiography performed. B. HeLa cells were transfected and data were obtained and analyzed as in Figure 1B. The effect of increasing concentrations of MG132 on AR or Δ1 activity was assayed.

Figure 9. Assay for dominant negative effects of hinge-region containing AR fragments on the androgen response.

A. representation of the AR fragments used. Boundaries are indicated at the right.
B. The androgen response was measured as luciferase induction in cells transiently transfected with the C3(1)ARE-luciferase reporter construct and AR or Δ1 expression construct. (Beta-gal expression construct was added as described in figure 1B) Indicated amounts of AR-fragment expression constructs were co-transfected. Amount of total transfected DNA was kept constant. Data were obtained and analyzed as described in the legend of figure 1B.

Figure 1

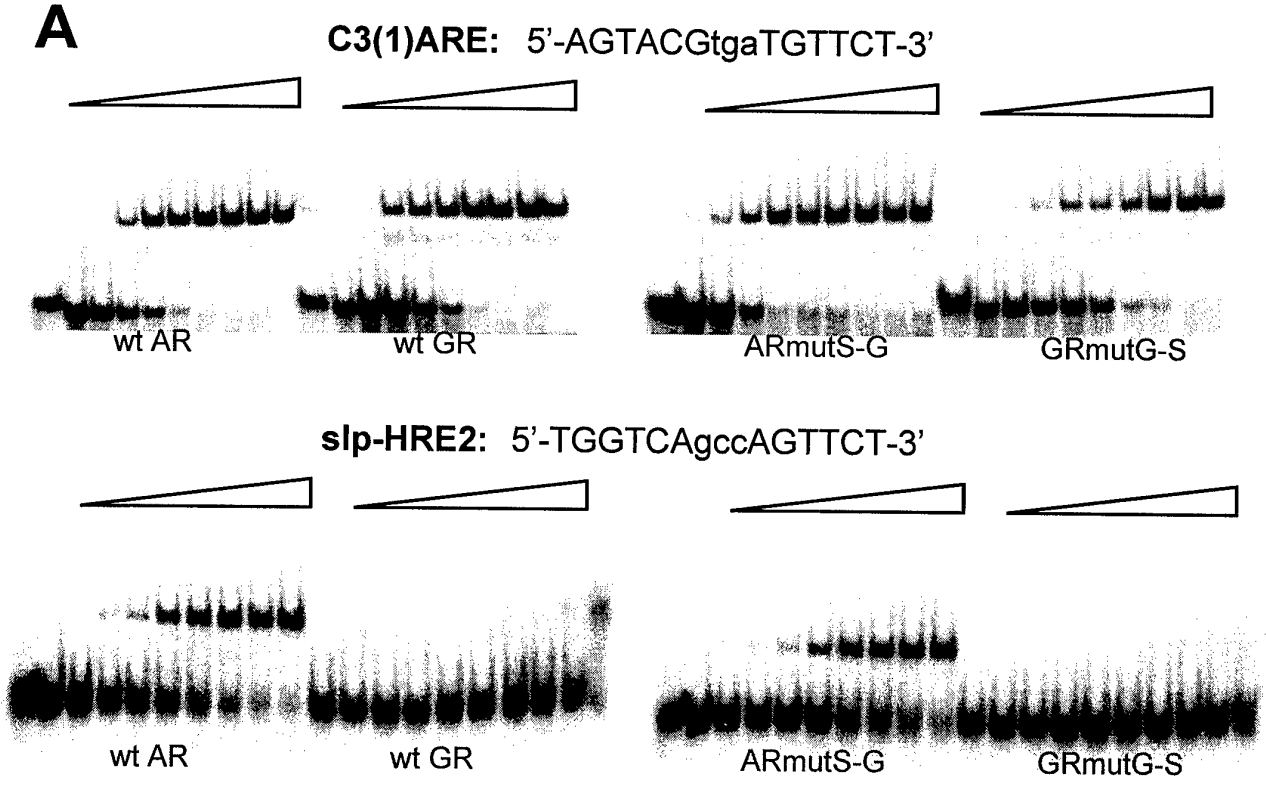
A
C3(1)ARE: 5'-AGTACGtgaTGTTCT-3'
wt AR
wt GR
ARmutS-G
GRmutG-S
Slp-HRE2: 5'-TGGTCAgccAGTTCT-3'
wt AR
wt GR
ARmutS-G
GRmutG-S

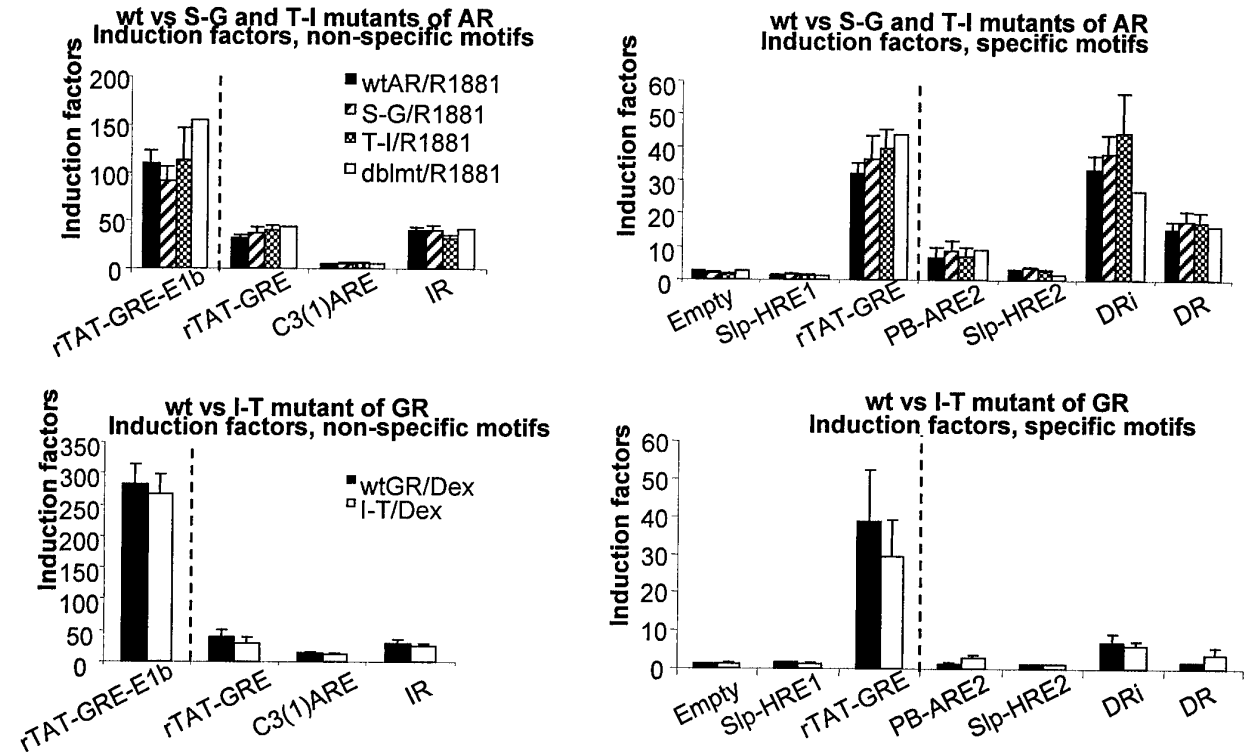
B
wt vs S-G and T-I mutants of AR
Induction factors, non-specific motifs
Induction factors
wtAR/R1881
S-G/R1881
T-I/R1881
dblmt/R1881
rTAT-GRE-E1b
rTAT-GRE
C3(1)ARE
IR
wt vs S-G and T-I mutants of AR
Induction factors, specific motifs
Induction factors
Empty
Slp-HRE1
rTAT-GRE
PB-ARE2
Slp-HRE2
DRi
DR
wt vs I-T mutant of GR
Induction factors, non-specific motifs
Induction factors
wtGR/Dex
I-T/Dex
rTAT-GRE-E1b
rTAT-GRE
C3(1)ARE
IR
wt vs I-T mutant of GR
Induction factors, specific motifs
Induction factors
Empty
Slp-HRE1
rTAT-GRE
PB-ARE2
Slp-HRE2
DRi
DR

Figuur 2

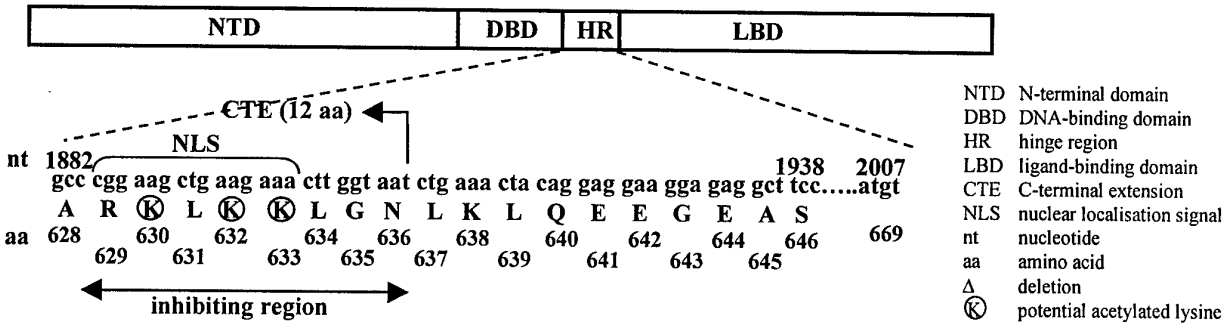
NTD
DBD
HR
LBD
CTE (12 aa)
NLS
nt 1882
1938 2007
gcc cgg aag ctg aag aaa ctt ggt aat ctg aaa cta cag gag gaa gga gag gct tcc.....atgt
A R K L K K L G N L K L Q E E G E A S
aa 628 630 632 634 636 638 640 642 644 646 669
629 631 633 635 637 639 641 643 645
inhibiting region
NTD N-terminal domain
DBD DNA-binding domain
HR hinge region
LBD ligand-binding domain
CTE C-terminal extension
NLS nuclear localisation signal
nt nucleotide
aa amino acid
Δ deletion
K potential acetylated lysine

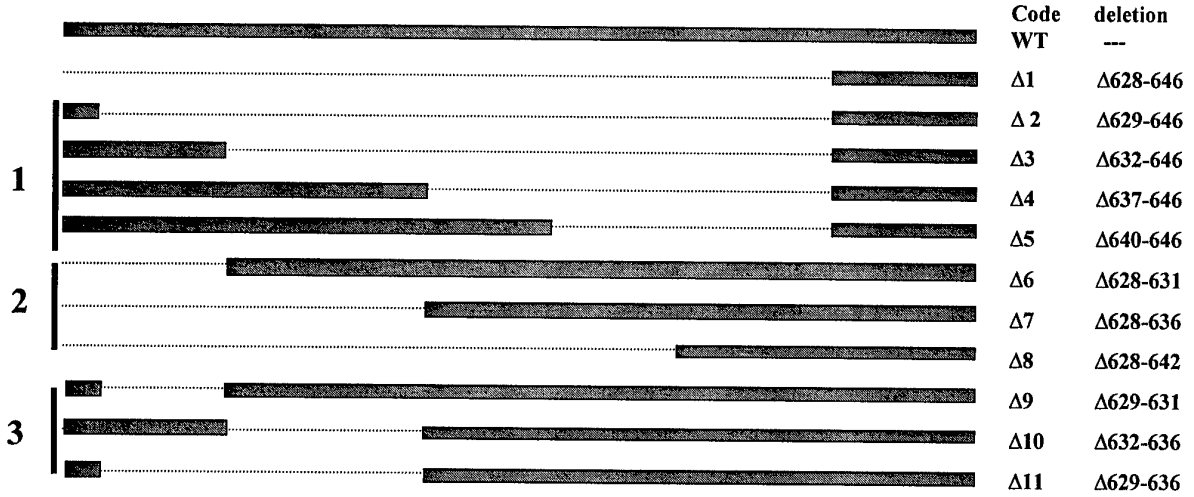
1
2
3
Code deletion
WT ---
Δ1 Δ628-646
Δ 2 Δ629-646
Δ3 Δ632-646
Δ4 Δ637-646
Δ5 Δ640-646
Δ6 Δ628-631
Δ7 Δ628-636
Δ8 Δ628-642
Δ9 Δ629-631
Δ10 Δ632-636
Δ11 Δ629-636

Figure 3

A

Band shift assays

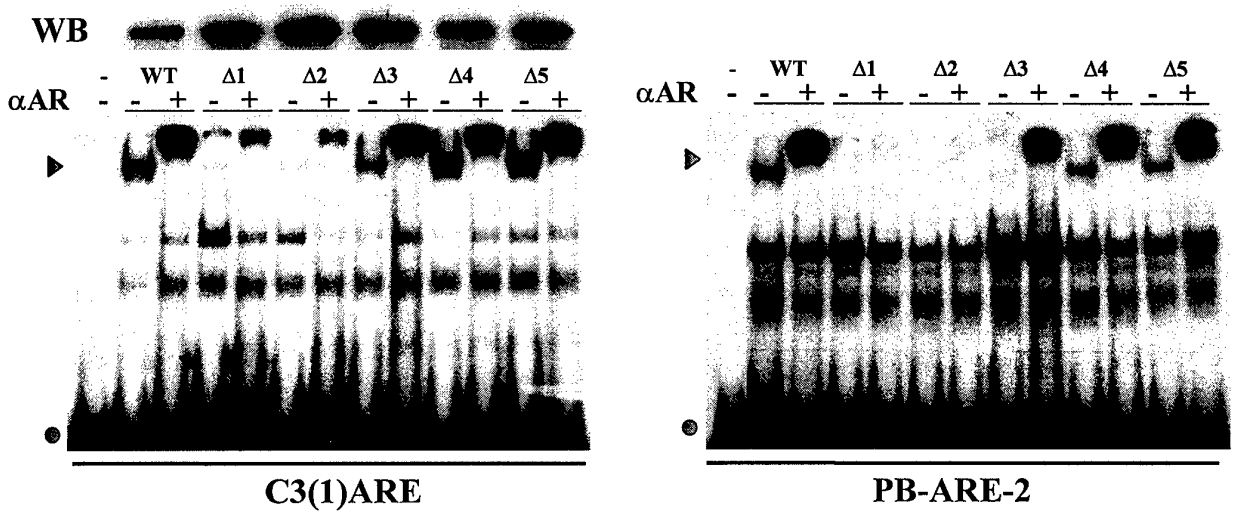

B

Induction factors

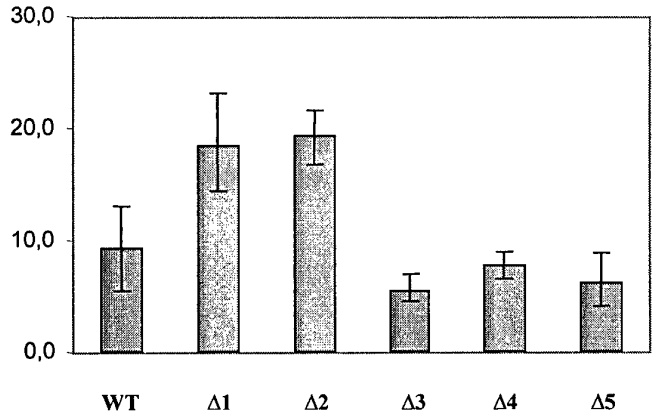

Figure 4

A

Band shift assays

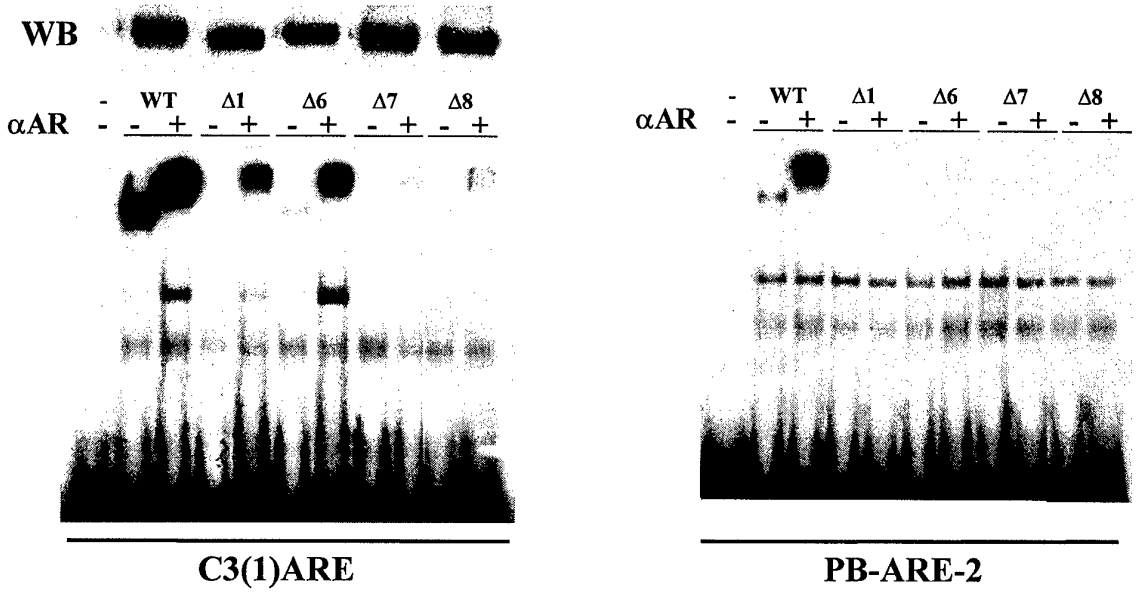

B

Induction factors

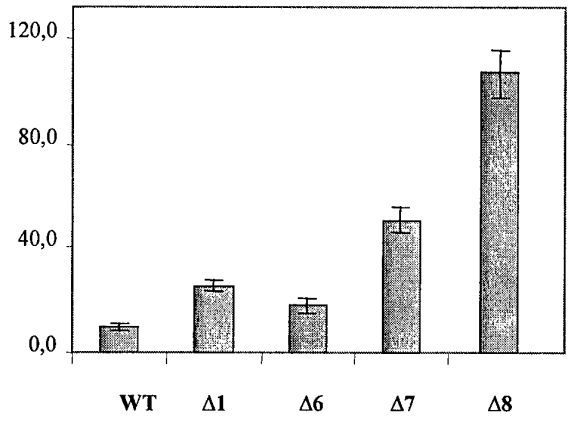

Figure 5

A

Band shift assays

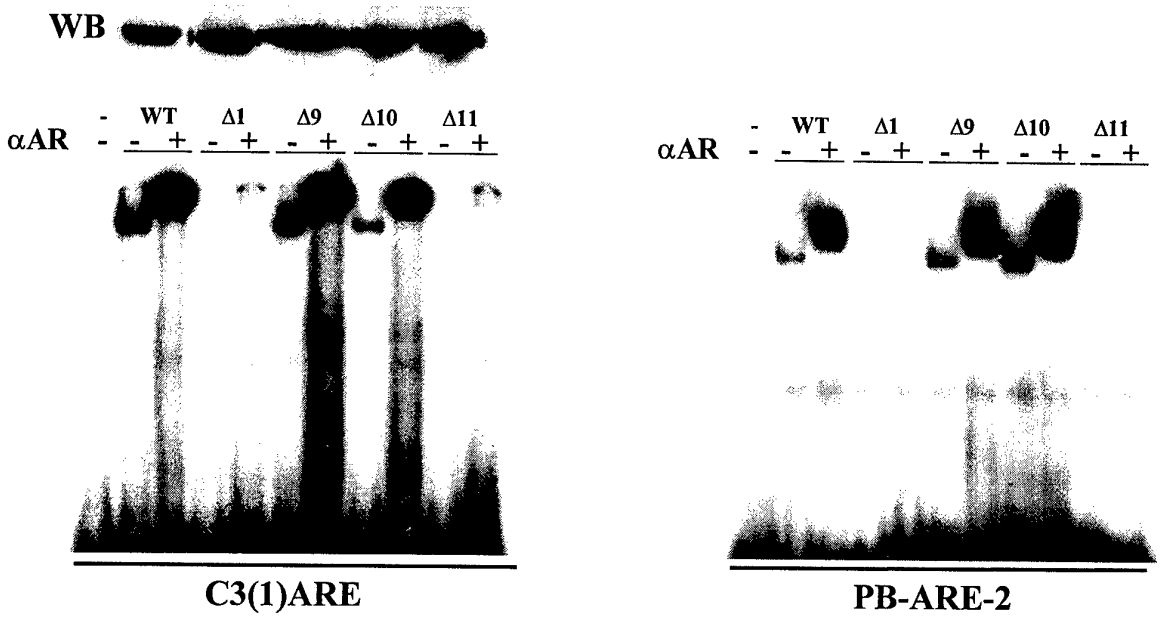

B

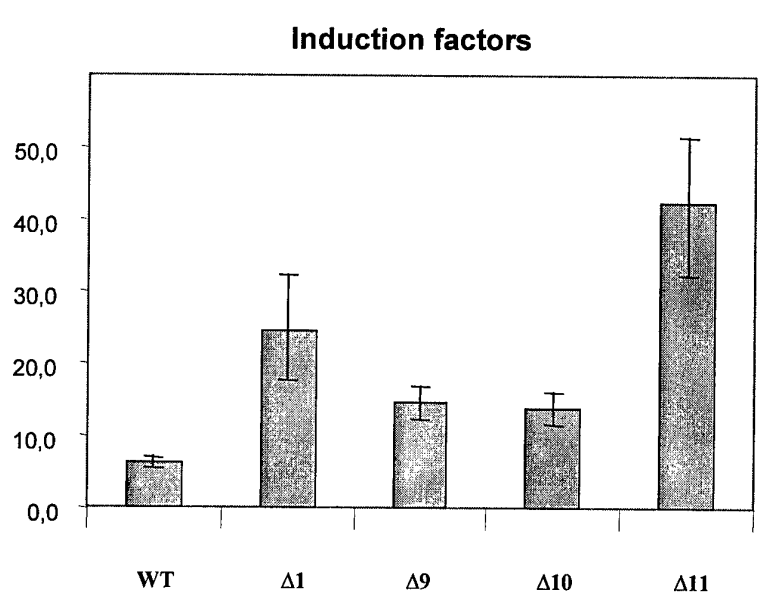

Figure 6

A

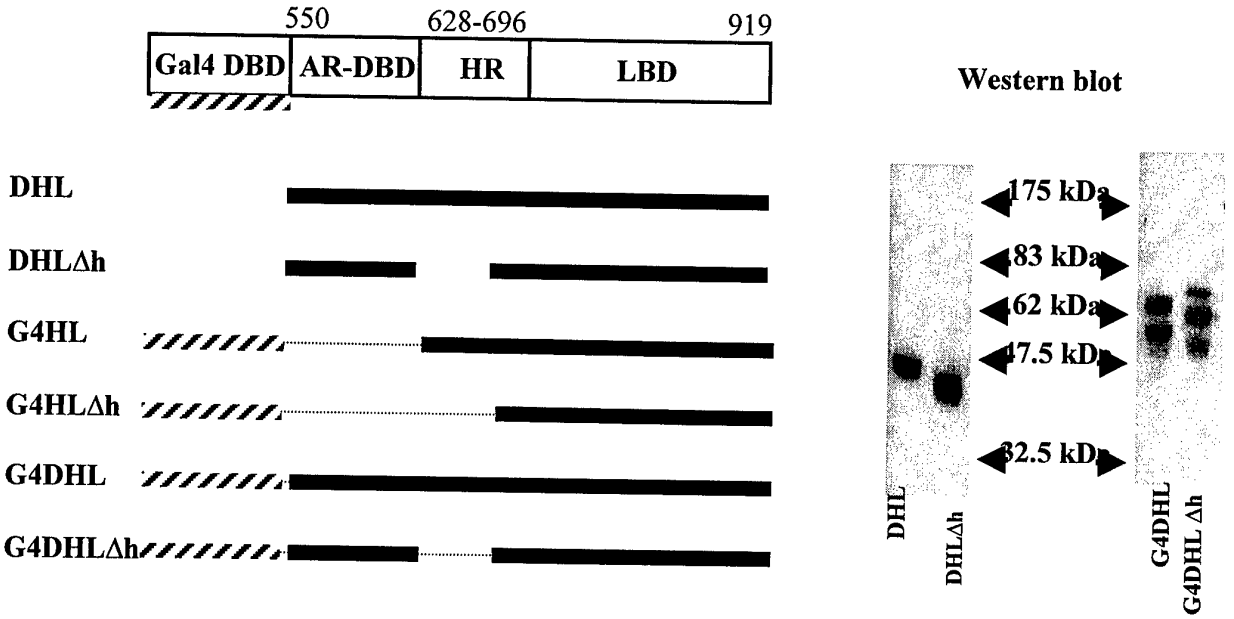

B Functional assay of AR-derived constructs

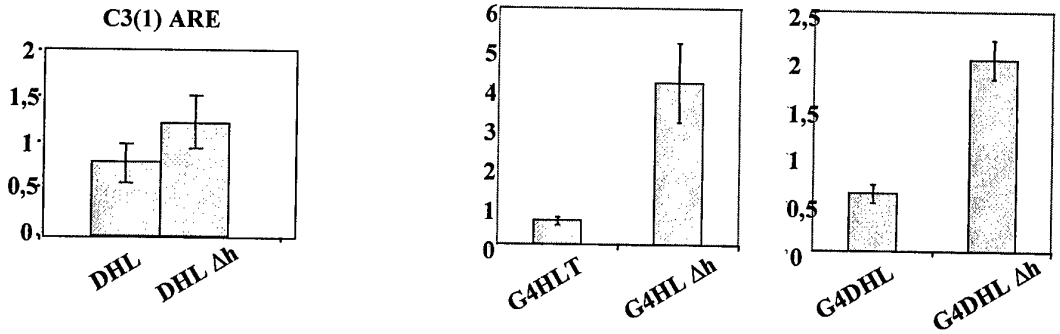

Figure 7

A.

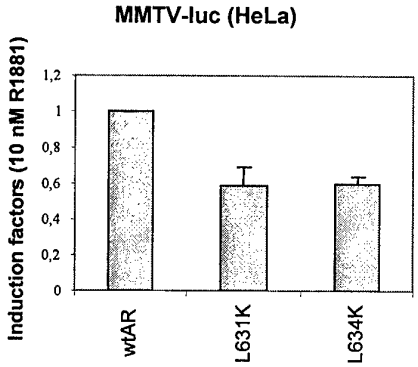

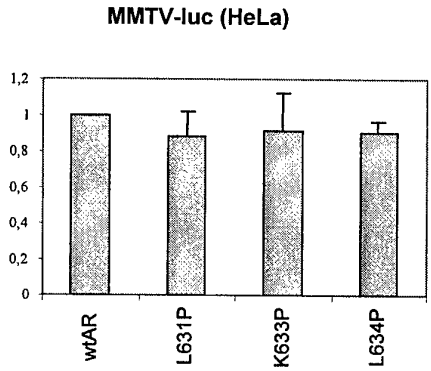

B.

Mutation	Average induction factors in two independent sets of experiments	
	Exp.1	Exp. 2
WT	12.0 +/- 3.8	8.1 +/- 2.2
K630R	11.7 +/-2.9	
K632R	13.8 +/- 3.6	
K633R	7.4 +/- 1.1	
K630-632-633R	6.8 +/- 3.6	
K630T		13.8 +/- 2.3
R629Q		11.0 +/- 2.5

Figure 8

A.

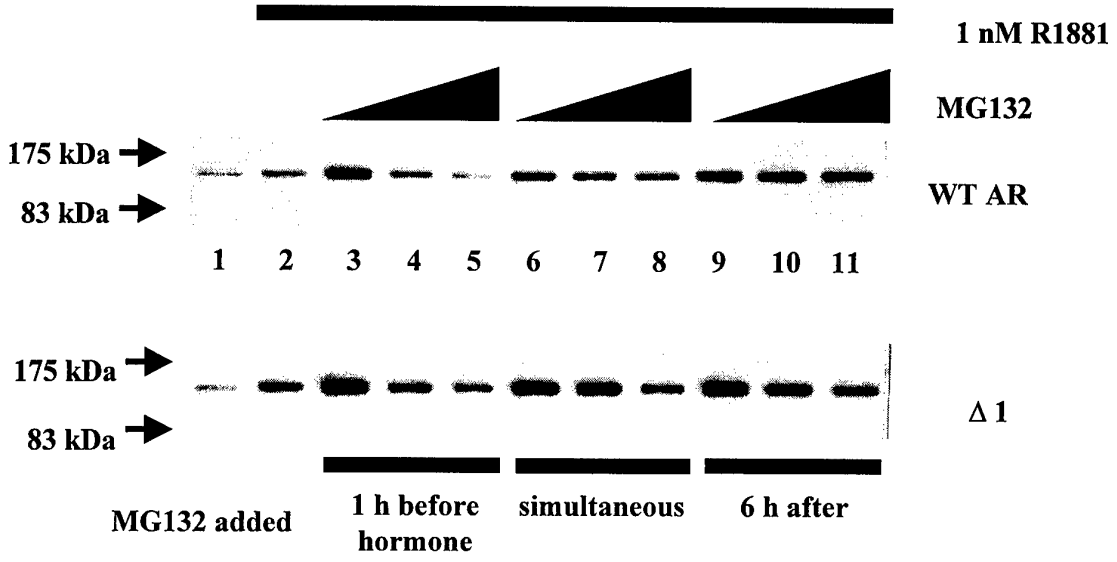
1 nM R1881
MG132
175 kDa
83 kDa
WT AR
1 2 3 4 5 6 7 8 9 10 11
175 kDa
83 kDa
Δ 1
MG132 added
1 h before hormone
simultaneous
6 h after

B.

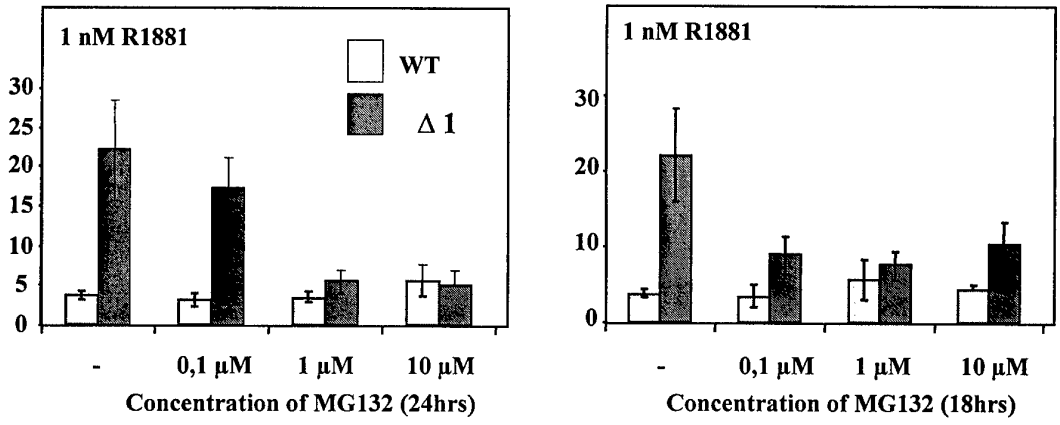
1 nM R1881
WT
Δ 1
30
25
20
15
10
5
0
- 0,1 μM 1 μM 10 μM
Concentration of MG132 (24hrs)
1 nM R1881
30
20
10
0
- 0,1 μM 1 μM 10 μM
Concentration of MG132 (18hrs)

Figure 9

A **AR fragments cloned in mammalian expression vector pSG5**

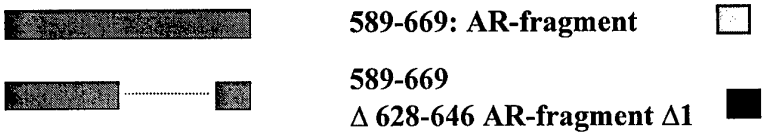

B **Effect of expression of AR fragments on the androgen responses mediated by AR and Δ1**

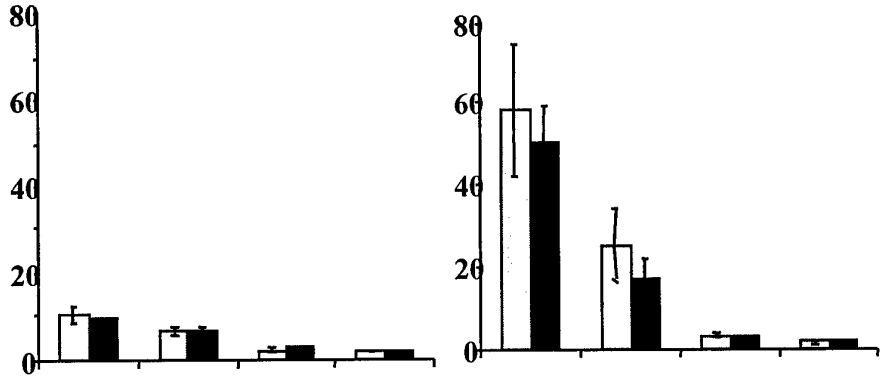

100 ng C3(1)ARE-luc	+	+	+	+	+	+	+	+	+	+	+	+	+	+	+	+
10ng CMV-betagal	+	+	+	+	+	+	+	+	+	+	+	+	+	+	+	+
10 ng AR	+		+		+		+		+		+		+		+	
10ng Δ1		+		+		+		+		+		+		+		+
ng AR-fragment	0		10		100		200		0		10		100		200	
ng AR-fragment Δ1		0		10		100		200		0		10		100		200

Structural basis of androgen receptor binding to selective androgen response elements

Paul L. Shaffer*†, Arif Jivan*†, D. Eric Dollins*, Frank Claessens‡, and Daniel T. Gewirth*§

*Department of Biochemistry, Duke University Medical Center, Durham, NC 27710; and ‡Division of Biochemistry, Faculty of Medicine, Campus Gasthuisberg, University of Leuven, 3000 Leuven, Belgium

Communicated by Jane S. Richardson, Duke University Medical Center, Durham, NC, February 17, 2004 (received for review October 29, 2003)

Steroid receptors bind as dimers to a degenerate set of response elements containing inverted repeats of a hexameric half-site separated by 3 bp of spacer (IR3). Naturally occurring selective androgen response elements have recently been identified that resemble direct repeats of the hexameric half-site (ADR3). The 3D crystal structure of the androgen receptor (AR) DNA-binding domain bound to a selective ADR3 reveals an unexpected head-to-head arrangement of the two protomers rather than the expected head-to-tail arrangement seen in nuclear receptors bound to response elements of similar geometry. Compared with the glucocorticoid receptor, the DNA-binding domain dimer interface of the AR has additional interactions that stabilize the AR dimer and increase the affinity for nonconsensus response elements. This increased interfacial stability compared with the other steroid receptors may account for the selective binding of AR to ADR3 response elements.

The androgen receptor (AR) is a ligand-activated transcription factor that plays a central role in male sexual development and in the etiology of prostate cancer (1, 2). It is a member of the steroid and nuclear hormone receptor superfamily, which also includes receptors for glucocorticoids (GR), mineralocorticoids (MR), progesterone (PR), estrogens (ER), and vitamin D (VDR) (3). Members of this family contain conserved, discrete, DNA-binding domains (DBDs) and ligand-binding domains. The amino-terminal domain and the hinge region connecting the central DBD to the C-terminal ligand-binding domain diverge among family members.

The hormone receptor DBD consists of a highly conserved 66-residue core made up of two zinc-nucleated modules, shown schematically in Fig. 1*A* (4, 5). With VDR as the only reported exception (6), the isolated DBD and associated C-terminal extension are necessary and sufficient to generate the same pattern of DNA response element selectivity, partner selection, and dimerization as the full-length receptor from which it is derived (6–11).

Although ligand binding elicits distinct hormone-specific responses, all classical steroid receptors (AR, PR, MR, and GR) recognize identical DNA response elements, which consist of two hexameric half-sites (5′-AGAACA-3′) arranged as inverted repeats with 3 bp of separating DNA, producing the 2-fold IR3 sequence pattern (Fig. 1*B*) (12). A question that continues to engage the steroid receptor field is how these transcription factors achieve DNA target specificity despite this degeneracy. As seen in the structures of the GR and ER DBDs bound to IR3 elements (4, 13), the receptors bind as "head-to-head" homodimers whose symmetric displacement across the DNA pseudodyad reflects the underlying half-site arrangement. Differences in steroid metabolism, receptor expression, local chromatin structure, and the availability of cofactors all contribute to steroid-specific responses (14–17). However, recent work has now also identified selective androgen response elements (AREs). The AREs consist of two hexameric half-sites arranged as an androgen direct repeat separated by 3 bp of spacer (ADR3) (18–21), with the half-site repeating on the same strand (Fig. 1*B*). The expanded binding repertoire of AR, including both the common IR3 and specific ADR3 elements, breaks the degeneracy of the steroid response elements, allowing specific AR activation from certain response elements but disfavoring interaction with PR, MR, or GR. This finding could further account for steroid-specific actions *in vivo*.

The crystal structures of nuclear receptors bound to direct-repeat elements, including the VDR DBD bound to a similar DR3 element, reveal a "head-to-tail" protein dimer bound to the DNA (6, 22–24). For AR to bind to ADR3-type elements in a head-to-tail orientation, the DBD would require a second dimerization interface that is distinct from the canonical D box region used to dimerize on IR3 elements (25). To visualize this unusual homodimeric assembly, we have solved the crystal structure of an AR DBD homodimer bound to an ADR3 response element. The structure we report here reveals that the proteins do not adopt the expected head-to-tail orientation on the DNA, but, instead, they retain the symmetric mode of dimerization observed previously for the GR DBD bound to an IR3 DNA element. We describe the protein–protein and protein–DNA interactions that allow for this unexpected arrangement, and we propose that AR-specific dimerization contacts account for the AR specificity of ADR3 elements.

Materials and Methods

Protein and DNA Purification. The rat AR DBD (residues 533–637, C552A) was expressed in *Escherichia coli* BL21/DE3 cells as a GST fusion and purified with a glutathione-Sepharose column (Sigma). The GST was cleaved with thrombin at 4°C overnight. Further purification was performed with SP Sepharose FastFlow (pH 7.4) and Source 15S (pH 6.9) columns. Protein concentration and purity was determined by UV absorbance and SDS/PAGE.

Synthetic oligonucleotides (W. M. Keck Facility, Yale University) were detritylated and purified by reversed-phase HPLC (Rainin Dynamax-300). Concentrated, purified strands were annealed by heating to 95°C and slowly cooling to room temperature.

Crystallization and Data Collection. Samples for cocrystallization contained DNA and protein concentrations of 0.15 and 0.30 mM, respectively, in 5 mM Tris (pH 7.6)/150 mM LiCl/10 mM DTT. Crystals were grown by hanging drop vapor diffusion at 18°C with the addition of 2 μl of the complex to an equal volume of reservoir solution (50 mM Mes, pH 5.6/0–20 mM $MgCl_2$/0–2% polyethylene glycol 400). Diffraction quality crystals (0.15 × 0.15 × 0.4 mm) grew in 2–6 weeks.

Crystals were equilibrated into reservoir solution supplemented with 35% glycerol before being flash-cooled in liquid

Abbreviations: AR, androgen receptor; GR, glucocorticoid receptor; MR, mineralocorticoid receptor; PR, progesterone receptor; ER, estrogen receptor; VDR, vitamin D receptor; DBD, DNA-binding domain; ARE, androgen response element.

Data deposition: The atomic coordinates have been deposited in the Protein Data Bank, www.pdb.org (PDB ID code 1R4I).

†P.L.S. and A.J. contributed equally to this work.

§To whom correspondence should be addressed. E-mail: gewirth@duke.edu.

www.pnas.org/cgi/doi/10.1073/pnas.0401123101

nitrogen. Diffraction data were collected at −180°C on beamline 22ID at the Advanced Photon Source with a CCD detector (Marresearch, Norderstedt, Germany). Data were indexed and reduced by using HKL2000 (26).

Structure Determination and Refinement. Four zinc sites were found by using SOLVE (27) and data from the peak anomalous wavelength. Experimental phases were generated with these sites; and, in the anomalous difference Fourier maps, the four zinc sites had peaks of >30 σ, whereas the next highest peak was 3 σ, indicating one AR dimer was in the asymmetric unit. Only one of the two possible enantiomeric space group choices yielded zinc sites that corresponded to possible AR dimers. Visual inspection of the zinc sites revealed that the proteins were arranged in a palindromic orientation. This finding led to construction of a molecular replacement model by using the ER DBD-IR3 structure (13) (PDB ID code 1HCQ). Because of its higher sequence homology to AR, the ER DBD was replaced with the core GR DBD (4) (PDB ID code 1GLU) by using least-squares fitting. A molecular replacement solution was obtained by using MOLREP (28).

Multiwavelength anomalous dispersion phases were calculated by using the remote and peak wavelength data to 3.4 Å and also used in refinement, which was done in CNS (29) by using the maximum likelihood Hendrickson–Lattman target. Model building was done by using O (30). Even at 3.1 Å, the number of unique reflections used was eight times the number of modeled atoms because of the very large (>80%) solvent content of the crystal, allowing for restrained individual B factor refinement in later rounds. Visualization of hydrogen bonds, van der Waals interactions, and clashes was aided by use of all atom contacts in KING and PROBE (31). Graphics used RIBBONS (32) and PYMOL (DeLano Scientific, San Carlos, CA).

Results

Crystallization and Structure Solution. Initial crystals of AR DBD–ADR3 complexes grew as thin needles from complexes containing AR DBD (residues 533–619) and diffracted to 4 Å with synchrotron radiation. These crystals were resistant to dissolution, suggesting crosslinking within the lattice. The AR DBD contains a nonconserved cysteine at position 552[11] (common receptor DBD numbering is given in brackets), which was predicted to be solvent-exposed based on modeling from the GR DBD structure. When Cys-552[11] in the AR DBD was changed to alanine, complexes containing this mutant yielded bar-shaped crystals that were isomorphous with the initial crystal form. These crystals were used to determine the structure of the AR DBD–DNA complex (PDB ID code 1R4I).

The structure of AR DBD(533–637)Cys552Ala in complex with ADR3 DNA (Fig. 1) was determined at 3.1 Å by a combined MAD and molecular replacement approach with diffraction data collected at the zinc anomalous edge. The arrangement of the proteins on the ADR3 DNA was determined from zinc anomalous data that revealed the location of the four zinc atoms in the complex. Data collection and refinement statistics are presented in Table 1, and representative electron density maps are shown Fig. 7, which is published as supporting information on the PNAS web site.

Anomalous difference Fourier maps confirmed that the asymmetric unit consists of just one AR DBD homodimer–DNA complex, yielding a Matthews number of 6.9 and a solvent content of 82%. The main crystal-packing interactions are made by the junction near protomer A, which contains neither a pseudocontinuous DNA interaction nor a biologically plausible alternative protein dimer interface. The downstream AR DBD (protomer B) makes only two crystal contacts by residues Phe-589[48] and Arg-590[49] and, except for the interaction with protomer A and the DNA, it is otherwise completely exposed to the large solvent channels (Fig. 2).

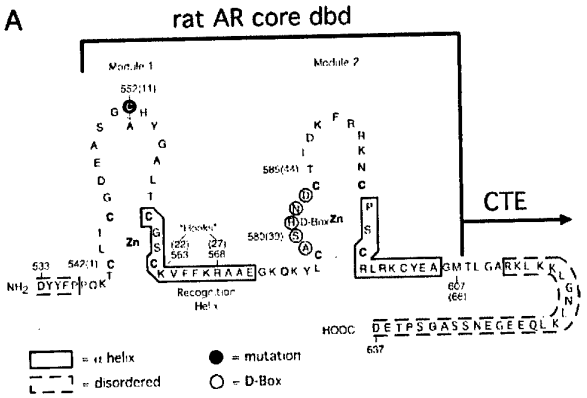

Fig. 1. Protein and DNA constructs. (*A*) The rat AR DBD. Sequence numbers in parentheses refer to the common receptor DBD-numbering scheme. Residues in dashed boxes are disordered in both protomers of the homodimeric complex. (*B*) The DNA used in cocrystallization, labeled ADR3, two naturally occurring AR response elements, PB-ARE-2 and C3 (1)-ARE, and a canonical IR3 steroid response element. Differences from the IR3 sequence are shaded gray.

Examination of the crystal-packing interactions can explain the refractory effect of C552[11] on crystallization. Residue

Table 1. Summary of data collection and refinement

Diffraction data		
Space group,*† Å	$P3_221$ 137.89, 85.71	
Data set	Native/remote	Zn peak
Wavelength, Å	1.0000	1.2831
Resolution, Å	50–3.1	50–3.4
Last shell, Å	3.21–3.1	3.52–3.4
Unique reflections	17,313	25,060
Completeness, % (last shell)	99.7 (99.1)	99.5 (98.9)
Average I/σ_σ (last shell)	20.4 (2.5)	19.6 (2.0)
R_{merge}, % (last shell)	9.6 (62)	7.8 (58)
FOM (after DM)‡	0.41 (0.96)	
Crystallographic refinement		
Resolution range, Å	50–3.1	
Reflections ($F > 2\sigma_F$)	14,839 (12,418)	
Atoms	1,813	
rms bond lengths, Å	0.0076	
rms bond angles, °	1.29	
R value ($F > 2\sigma_F$)†	24.6 (22.7)	
R_{free} ($F > 2\sigma_F$)	26.4 (24.9)	

*$R_{merge} = \Sigma_{hkl}\Sigma_i|I_{i(hkl)} - \langle I_{(hkl)}\rangle|/\Sigma_{hkl}\Sigma_i I_{(hkl)}$.
†$R = \Sigma||F_o| - |F_c||/\Sigma|F_o|$. 5% of the reflections were used for R_{free}.
‡Figure of merit = $\langle|\Sigma P(\alpha)e^{i\alpha}/\Sigma P(\alpha)|\rangle$, where α is the phase and $P(\alpha)$ is the phase-probability distribution.

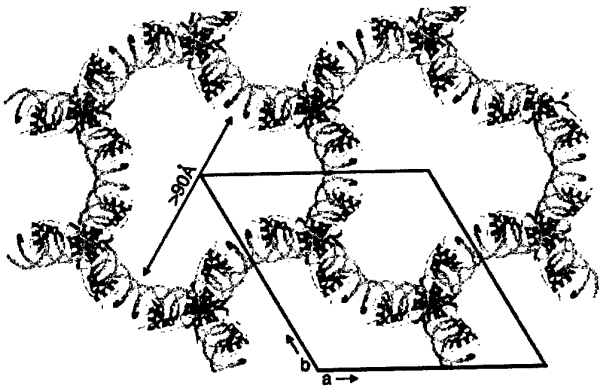

Fig. 2. Crystal packing of the AR DBD–ADR3 complex. Red and blue ribbons are the upstream and downstream subunits, respectively, with the DNA backbone shown in gold. The view is parallel to the *c* axis of the crystal, and the unit cell is shown.

552[11] from protomer A is in position to crosslink with Cys-578[37] of protomer A in the adjacent symmetry-related complex. Cys-578[37] coordinates a zinc atom in the first Zn module. Formation of a C552[11]-C578[37] disulfide link is likely to disrupt the native AR DBD conformation and adversely affect crystal order.

The AR DBDs Are Arranged as an Inverted Repeat on a Direct-Repeat DNA Target. In all the dimeric hormone receptor DBD–DNA complexes determined to date, the two DBDs adopt the same relative orientation as that of the underlying DNA target. Surprisingly, however, in the structure of AR DBD bound to ADR3 DNA, the two AR DBD protomers are not arranged as a head-to-tail dimer, as would be expected of receptors bound to a direct-repeat DNA element. Instead, the proteins form a symmetric, head-to-head dimer that is nearly identical with the dimer seen in the ER DBD–DNA and GR DBD–DNA structures (rms deviation for α-carbons of 1.09 and 0.89 Å, respectively) (4, 13). This finding was confirmed unambiguously by inspection of the positions of the four zinc sites determined from anomalous difference maps calculated from single wavelength anomalous dispersion phases (Fig. 3). The arrangement of the AR dimer is unlikely to be an artifact of crystal packing, because there are only two small crystal contacts between the downstream DBD (protomer B) and the neighboring molecules in the crystal lattice (Fig. 2).

The AR DBD Homodimer Interface. The subunit interface of the AR DBD homodimer is symmetric and closely resembles that seen in the GR DBD–DNA complex (4). As in the GR DBD– and ER DBD–DNA complexes, the majority of the cross-subunit contacts are made in the D box region of the second zinc module. In the GR homodimer, the subunit interface is stabilized both by a network of hydrogen bonds between D box residues and by an extensive complementary surface. As seen in Fig. 4*B*, however, the GR interface contains a void formed where the Gly-478[39] from the opposing subunits face each other. This "glycine hole" is also a feature of the MR and PR. In the AR DBD, however, glycine is replaced by Ser-580[39]. This serine packs into the glycine hole of the dimer interface, filling the void and making van der Waals contact with its counterpart in the other subunit. In addition, the arrangement of the two serines is optimal for the formation of a hydrogen bond across the molecular pseudodyad. The substitution of serine for glycine in the AR D box is likely

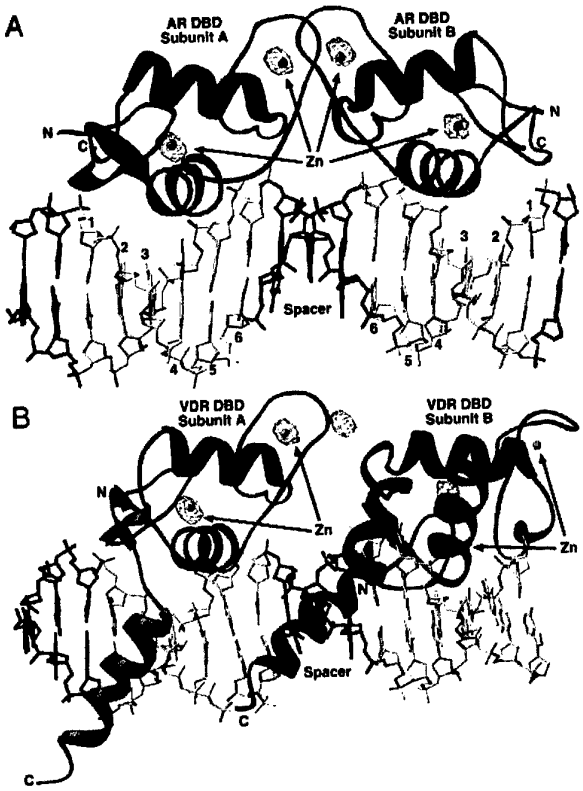

Fig. 3. Overall architecture of the AR DBD–ADR3 and VDR DBD–DR3 complexes. (*A*) The AR DBD–ADR3 complex. The two protomers are in red and blue, the hexameric half-site DNA is gold, and the spacer and flanking base pairs are black. In brown is a 20-σ contour of the experimental anomalous Fourier difference map. (*B*) The VDR DBD–DR3 complex. VDR DBD protomer A is shown in the same orientation as the AR DBD subunit A in *A*. The zincs of subunit B fail to occupy the peaks in the anomalous difference Fourier map in this dimeric arrangement, indicating the AR DBD does not form a head-to-tail dimer.

to increase the relative strength of the dimer interface of the AR DBD.

The AR DBD also makes an additional pair of symmetrical contacts between Thr-585[44] and the carbonyl oxygen of Ala-579[38] in the opposing protomer. In the GR DBD the residue at this position is an isoleucine, and replacement with a threonine as seen in the AR is likely to increase the stability of the dimer because of the enthalpic contribution of the additional two hydrogen bonds. In addition, the change from Ile in GR to Thr in AR removes a nonpolar residue from the solvent-exposed surface of the DBD, thus entropically stabilizing the AR as well.

The AR DBD (P.L.S. and D.T.G., unpublished work) and GR DBD (33) are monomers in solution. Because cooperative dimerization greatly increases the affinity of receptors for their bipartite response elements, these two changes should also increase the relative affinity of the AR for a given response element compared with GR. In support of this hypothesis, GR DBD mutants containing a serine in place of Gly-478[39] in the D box or a threonine in place of GR Ile-483[44] show increased affinity for both palindromic and direct-repeat response elements compared with wild type (34), confirming the importance of these interactions for dimer stability.

Protein–DNA Interactions. The DNA used for cocrystallization has a DR3 arrangement of hexameric half-sites, with the sense strand

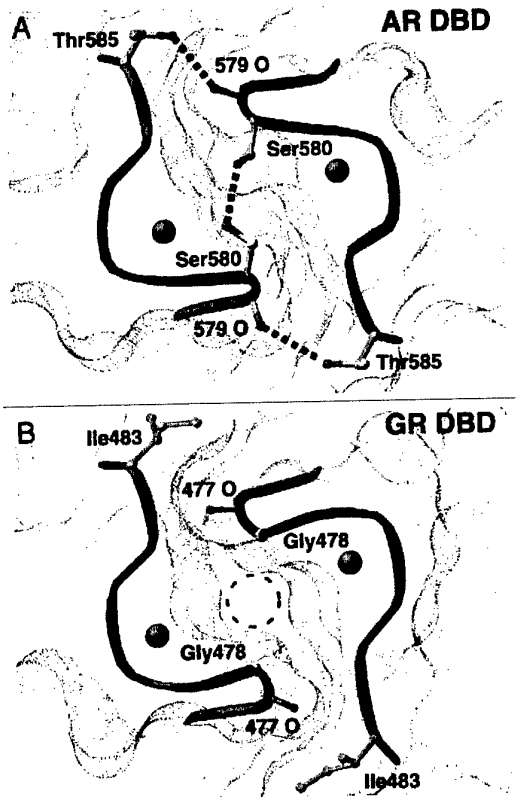

Fig. 4. (*A*) The AR DBD dimer interface. The molecular surfaces of the AR subunits are shown in red and blue. Dashed black lines are hydrogen bonds. (*B*) A similar view of the GR DBD dimer interface. The "glycine hole" is noted by the dashed circle.

sequence 5′-CC **AGAACA** TCA **AGAACA** G-3′. However, the AR proteins were observed to bind in a symmetric, head-to-head arrangement, as was seen with steroid receptors bound to an IR3 response element (symmetrized consensus sequence of 5′-**AGAACA** NNN **TGTTCT**-3′). One half-site, bound by protomer A and shown here as upstream, is common to both DR3 and IR3 elements and is a high-affinity, consensus-binding site for steroid DBDs. Protomer B, on the other hand, binds to the downstream half-site that contains the consensus IR3-type bases at only the second and fifth positions. Experimentally phased electron density maps were used to identify the length of the asymmetric flanking sequences and unambiguously assign the orientation of the DNA. Within the limitations imposed by the diffraction resolution, the DNA does not exhibit significant deviations from B form.

Backbone DNA contacts are similar for both AR protomers (Fig. 5) and show the pattern seen previously in structures of steroid receptor–DNA complexes (4, 35). The base-specific contacts between the AR DBD and the consensus half-site are also nearly identical with those of the GR DBD to its cognate half-site and are shown in Fig. 5*A*. In addition to these previously described interactions, we also note that the aliphatic portion of the Arg-568[27] side chain makes additional van der Waals contacts with Val-564[23] and the C5 methyl group of the thymine at the sixth position of the consensus half-site. Thymine is the only base that can form the second half of this van der Waals "sandwich," and this specific contact likely explains why an A:T base pair is commonly observed at the sixth position of AR-specific half-sites (Fig. 6). Because the interaction between the conserved arginine and thymine is also present in consensus half-sites in the GR, ER, 9-*cis*-retinoic acid receptor, and other steroid and nuclear hormone receptor DBD structures, this can explain the preference for the A:T base pair at the sixth position in these protein–DNA complexes as well.

The nonconsensus half-site interaction seen in the AR DBD–ADR3 structure contains the top strand sequence 5′-AGAACA-3′, with the two bases that match the consensus for a downstream IR3 half-site underlined. These two bases lie at the correct IR3 positions because they are symmetric within the hexameric half-site. This serendipitous match to the consensus IR3 half-site allows Lys-563[22] and Arg-568[27] of protomer B to recapitulate the hydrogen bonds to the GC base pairs at positions 2 and 5 of the hexameric half-site, as seen in the upstream element. These two "hooks" are common elements that position the recognition helix within the major groove of the hexameric half-site (36).

In the cognate AR DBD half-complex, the side chain of Val-564[23] makes van der Waals contact with the 5-methyl group of the T4 of the antisense strand. This interaction between the two nonpolar substituents is the discriminating feature of specific steroid receptor–DNA interfaces, and the resulting dehydration of the protein–DNA interface contributes entropic stabilization to the binding (35, 37). In the nonconsensus AR half-complex, A replaces the T at position 4 of the sense strand, resulting in the loss of the Val-564[23]-T4 contact. Although this replacement reduces the number of specific, stabilizing, interactions with the DNA half-site, the substitution of an A base for the consensus T does not cause a steric clash that might disfavor binding to this element. As befits the reduced complementarity between the AR DBD and the nonconsensus half-site, the cognate half-complex buries slightly more surface area from solvent (1,230 Å^2) than the noncognate one (960 Å^2).

AR Mutations. Mutations in the AR DBD associated with partial or complete androgen insensitivity (see ww2.mcgill.ca/androgendb) can be understood mechanistically in light of the structure determined here. Many of these were correctly analyzed earlier based on the structure of the GR DBD (38). More recently, within the D box, Ala579Thr (39–41) and Ser580Thr (42) mutations have been reported to lead to loss of AR dimerization. Modeling the Ser580Thr mutation on the AR DBD dimer leads to bad steric clashes in any possible Thr conformation, forcing backbone shifts that presumably disfavor dimerization. Modeling of the Ala579Thr substitution is more problematic, because the Thr side chains can each be accommodated with modest steric overlaps of 0.3–0.4 Å. However, that may be enough to force structural changes in the interface, and the imprecision of low resolution may underestimate the problem. The Ala579Thr mutation can be relieved by a compensatory change in Thr-585 to Ala (43), close to residue 579 across the dimer interface. This further change may relieve strains in the dimer interface or in the Zn ligand geometry caused by the Ala579Thr mutation.

Discussion

We have determined the structure of the AR DBD bound to an idealized steroid DR3 response element. Based on studies of the VDR DBD (6), which also binds to a DR3-type response element, we expected the tandem arrangement of half-sites to direct head-to-tail binding of the AR DBD to the DNA. Surprisingly, however, the AR DBDs bind to the direct-repeat response element as head-to-head symmetrical dimers. This mismatch between receptor dimer- and response element-arrangement results in one AR DBD bound to a high-affinity cognate half-site, and the partner DBD bound to a lower-affinity half-site. This finding indicates that the energetic penalty in-

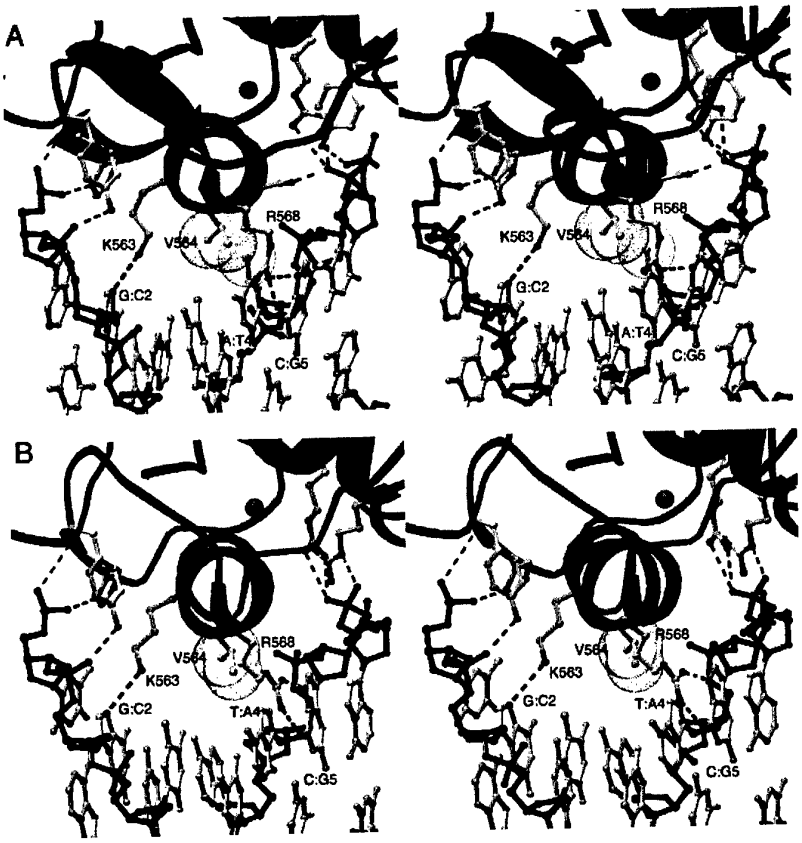

Fig. 5. Stereoview of the AR DBD–DNA interfaces. (*A*) The upstream, cognate, protein–DNA interface. (*B*) The downstream, noncognate interface. The protein is shown in the same orientation as in *A*.

curred by binding to a less favored half-site sequence is more than offset by maintaining the preferred IR3-type dimer interface. This finding is analogous to an earlier observation that the GR DBD maintains the IR3 dimer interface and spacing even when challenged with an IR4 response element (4).

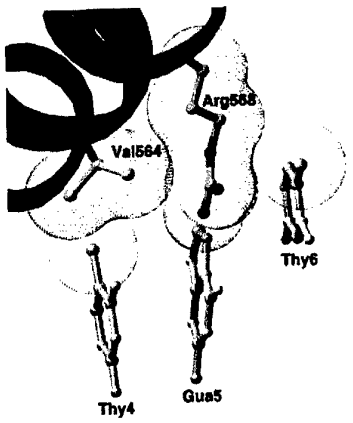

Fig. 6. The arginine "sandwich." Val-564 and Arg-568 of the AR DBD subunit along with bases T4, G5, and T6 of the antisense strand of the upstream, cognate half-site are shown. The C5 methyl group of T6 forms van der Waals interactions with one face of Arg-568, whereas the other side packs against Val-564.

Both the AR and the GR exhibit similar interactions with steroid response elements, yet the AR exhibits consistently stronger binding to direct repeat-type response elements than does the GR. Some of this difference in affinity may be attributable to differences in the C-terminal extension of each DBD, although in both GR and AR these regions were disordered in the crystal structure and may contribute only general electrostatic interactions without affecting selectivity or discrimination. Within the core of the DBD, however, the protein–DNA interactions are nearly identical for both receptor DBDs, and much of the difference in response element affinity is therefore likely to reside in the ability of each receptor to cooperatively form head-to-head dimers on bipartite response elements where the interaction with one or both hexameric half-sites is nonoptimal.

The second zinc module has been shown to be necessary for AR to bind cooperatively to ADR3s (44). The steroid receptor DBD dimerization interface is contained within this module, and between AR and GR it differs at just four positions. The increased AR dimer affinity can be explained by two of these four substitutions, one in the D box, and the other two residues beyond. In the D box, AR is the only steroid receptor that has a Ser residue at the second position, Ser-580[39], and this serine packs into the core of the dimer interface, making both van der Waals interactions and a cross-subunit hydrogen bond. All other steroid receptors have a Gly at this position, which lacks this additional hydrogen bond and leaves a void in the interface. Two residues beyond the D box, an Ile-to-Thr substitution in AR allows both a favorable cross-subunit side chain-to-backbone

hydrogen bond and removes the nonpolar Ile side chain from exposure to solvent. Together these two substitutions appear to account for the stronger AR dimer interface. These substitutions in turn allow the receptor to bind to a more diverse set of response elements with higher affinity and cooperativity than the GR.

Biochemical evidence for the increased cooperativity of the AR DBD dimer correlates with these structural observations. All the steroid receptors (MR, PR, GR, and AR) show a 5- to 10-fold lower affinity for the naturally occurring PB-ARE-2 DR3-type element than the C3 (1) IR3-type element (34). However, the AR DBD binds 3- to 10-fold better to both elements relative to the other steroid receptors. Thus, the binding constant for AR on an apparent DR3 target (23 ± 5 nM) is the same as that of the other receptors for the more optimal IR3 element (the average of the other three is 23 ± 9 nM) (44). Because the concentration of individual steroid receptors in the cell is approximately nanomolar, differences in binding constants of this order are likely to be significant. AR substitutions in the GR dimerization interface, including Gly483Ser and Ile483Thr, show higher affinity binding to both DR3 and IR3 response elements (34), thus mimicking the behavior of the AR. Together with the structural data, these observations suggest a model where, because of the increased strength of the AR dimer interface, AR-selective gene activation arises from the ability of the AR to bind to IR3 response elements that have a greater deviation from the consensus half-site sequence. The reverse cross-activation of GR-responsive genes by the AR would likely be disfavored by the highly tissue-specific expression pattern of the AR compared with the GR.

The structure of the AR DBD bound as an inverted repeat to a direct-repeat response element highlights the fact that DNA target recognition by hormone receptors is strongly governed by the dimerization behavior of the two interacting protomers, even at the cost of losing specific interactions with the target DNA. With the exception of the Ecdysone receptor, which binds to IR1 rather than IR3 targets consisting of AGGTCA rather than AGAACA half-sites (45), no physiologically relevant dimerization interface within the classical steroid receptor DBDs, other than the primary one, has been observed to date in structural studies. Moreover, attempts to capture such potential alternative interfaces, as described in this report, and previously for GR (4), have been unfruitful. This in turn implies that selective hormone response elements that appear to have alternative arrangements of their hexameric half-sites, such as the pemARE with a proposed 5-bp spacer between half-sites (46), may instead simply be further examples of the ability of these receptors to exploit the strength of their DBD dimerization interfaces to accommodate suboptimal protein–half-site interactions. This ability is likely to be not only a mechanism of response element discrimination, but also an effective way of modulating transcription from different hormone-responsive genes.

We thank Nikki Fetter and Jenna Vanliere for help with crystallization and Karen Soldano for preparative assistance. This work was supported by U.S. Army Prostate Cancer Research Program grants (to D.T.G. and F.C.).

1. McPhaul, M. J. (1999) *J. Steroid Biochem. Mol. Biol.* **69,** 315–322.
2. Gottlieb, B., Lehvaslaiho, H., Beitel, L. K., Lumbroso, R., Pinsky, L. & Trifiro, M. (1998) *Nucleic Acids Res.* **26,** 234–238.
3. Mangelsdorf, D. J., Thummel, C., Beato, M., Herrlich, P., Schutz, G., Umesono, K., Blumberg, B., Kastner, P., Mark, M., Chambon, P., *et al.* (1995) *Cell* **83,** 835–839.
4. Luisi, B. F., Xu, W. X., Otwinowski, Z., Freedman, L. P., Yamamoto, K. R. & Sigler, P. B. (1991) *Nature* **352,** 497–505.
5. Khorasanizadeh, S. & Rastinejad, F. (2001) *Trends Biochem. Sci.* **26,** 384–390.
6. Shaffer, P. L. & Gewirth, D. T. (2002) *EMBO J.* **21,** 2242–2252.
7. Mader, S., Chen, J. Y., Chen, Z., White, J., Chambon, P. & Gronemeyer, H. (1993) *EMBO J.* **12,** 5029–5041.
8. Perlmann, T., Rangarajan, P. N., Umesono, K. & Evans, R. M. (1993) *Genes Dev.* **7,** 1411–1422.
9. Towers, T. L., Luisi, B. F., Asianov, A. & Freedman, L. P. (1993) *Proc. Natl. Acad. Sci. USA* **90,** 6310–6314.
10. Zechel, C., Shen, X. Q., Chambon, P. & Gronemeyer, H. (1994) *EMBO J.* **13,** 1414–1424.
11. Zechel, C., Shen, X. Q., Chen, J. Y., Chen, Z. P., Chambon, P. & Gronemeyer, H. (1994) *EMBO J.* **13,** 1425–1433.
12. Beato, M., Herrlich, P. & Schutz, G. (1995) *Cell* **83,** 851–857.
13. Schwabe, J. W., Chapman, L., Finch, J. T. & Rhodes, D. (1993) *Cell* **75,** 567–578.
14. Strahle, U., Boshart, M., Klock, G., Stewart, F. & Schutz, G. (1989) *Nature* **339,** 629–632.
15. Funder, J. W. (1993) *Science* **259,** 1132–1133.
16. Muller, J. M., Isele, U., Metzger, E., Rempel, A., Moser, M., Pscherer, A., Breyer, T., Holubarsch, C., Buettner, R. & Schule, R. (2000) *EMBO J.* **19,** 359–369.
17. List, H. J., Lozano, C., Lu, J., Danielsen, M., Wellstein, A. & Riegel, A. T. (1999) *Exp. Cell Res.* **250,** 414–422.
18. Claessens, F., Alen, P., Devos, A., Peeters, B., Verhoeven, G. & Rombauts, W. (1996) *J. Biol. Chem.* **271,** 19013–19016.
19. Rennie, P. S., Bruchovsky, N., Leco, K. J., Sheppard, P. C., McQueen, S. A., Cheng, H., Snock, R., Hamel, A., Bock, M. E. & MacDonald, B. S. (1993) *Mol. Endocrinol.* **7,** 23–36.
20. Verrijdt, G., Schoenmakers, E., Alen, P., Haelens, A., Peeters, B., Rombauts, W. & Claessens, F. (1999) *Mol. Endocrinol.* **13,** 1558–1570.
21. Verrijdt, G., Schoenmakers, E., Haelens, A., Peeters, B., Verhoeven, G., Rombauts, W. & Claessens, F. (2000) *J. Biol. Chem.* **275,** 12298–12305.
22. Rastinejad, F., Perlmann, T., Evans, R. M. & Sigler, P. B. (1995) *Nature* **375,** 203–211.
23. Rastinejad, F., Wagner, T., Zhao, Q. & Khorasanizadeh, S. (2000) *EMBO J.* **19,** 1045–1054.
24. Zhao, Q., Chasse, S. A., Devarakonda, S., Sierk, M. L., Ahvazi, B. & Rastinejad, F. (2000) *J. Mol. Biol.* **296,** 509–520.
25. Verrijdt, G., Haelens, A. & Claessens, F. (2003) *Mol. Genet. Metab.* **78,** 175–185.
26. Otwinowski, Z. & Minor, W. (1997) *Methods Enzymol.* **276,** 307–326.
27. Terwilliger, T. C. & Berendzen, J. (1999) *Acta Crystallogr. D* **55,** 849–861.
28. Vagin, A. A. & Isupov, M. N. (2001) *Acta Crystallogr. D.* **57,** 1451–1456.
29. Brunger, A. T., Adams, P. D., Clore, G. M., DeLano, W. L., Gros, P., Grosse-Kunstleve, R. W., Jiang, J. S., Kuszewski, J., Nilges, M., Pannu, N. S., *et al.* (1998) *Acta Crystallogr. D* **54,** 905–921.
30. Jones, T. A., Zou, J. Y., Cowan, S. W. & Kjeldgaard, M. (1991) *Acta Crystallogr. A* **47,** 110–119.
31. Word, J. M., Lovell, S. C., LaBean, T. H., Taylor, H. C., Zalis, M. E., Presley, B. K., Richardson, J. S. & Richardson, D. C. (1999) *J. Mol. Biol.* **285,** 1711–1733.
32. Carson, M. (1991) *J. Appl. Crystallogr.* **24,** 958–961.
33. Freedman, L. P., Yamamoto, K. R., Luisi, B. F. & Sigler, P. B. (1988) *Cell* **54,** 444 (lett.).
34. Schoenmakers, E., Verrijdt, G., Peeters, B., Verhoeven, G., Rombauts, W. & Claessens, F. (2000) *J. Biol. Chem.* **275,** 12290–12297.
35. Gewirth, D. T. & Sigler, P. B. (1995) *Nat. Struct. Biol.* **2,** 386–394.
36. Nelson, C. C., Hendy, S. C., Shukin, R. J., Cheng, H., Bruchovsky, N., Koop, B. F. & Rennie, P. S. (1999) *Mol. Endocrinol.* **13,** 2090–2107.
37. Lundback, T., Cairns, C., Gustafsson, J. A., Carlstedt-Duke, J. & Hard, T. (1993) *Biochemistry* **32,** 5074–5082.
38. Luisi, B. F., Schwabe, J. W. & Freedman, L. P. (1994) in *Vitamins and Hormones*, ed. Litwack, G. (Academic, New York), Vol. 49, pp. 1–47.
39. Gast, A., Neuschmid-Kaspar, F., Klocker, H. & Cato, A. C. (1995) *Mol. Cell Endocrinol.* **111,** 93–98.
40. Holterhus, P. M., Wiebel, J., Sinnecker, G. H., Bruggenwirth, H. T., Sippell, W. G., Brinkmann, A. O., Kruse, K. & Hiort, O. (1999) *Pediatr. Res.* **46,** 684–690.
41. Lundberg Giwercman, Y., Nikoshkov, A., Lindsten, K., Bystrom, B., Pousette, A., Knudtzon, J., Alm, J. & Wedell, A. (2000) *Horm. Res.* **53,** 83–88.
42. Nordenskjold, A., Friedman, E., Tapper-Persson, M., Soderhall, C., Leviav, A., Svensson, J. & Anvret, M. (1999) *Urol. Res.* **27,** 49–55.
43. Kaspar, F., Klocker, H., Denninger, A. & Cato, A. C. (1993) *Mol. Cell. Biol.* **13,** 7850–7858.
44. Schoenmakers, E., Alen, P., Verrijdt, G., Peeters, B., Verhoeven, G., Rombauts, W. & Claessens, F. (1999) *Biochem. J.* **341,** 515–521.
45. Devarakonda, S., Harp, J. M., Kim, Y., Ozyhar, A. & Rastinejad, F. (2003) *EMBO J.* **22,** 5827–5840.
46. Geserick, C., Meyer, H. A., Barbulescu, K. & Haendler, B. (2003) *Mol. Endocrinol.* **17,** 1738–1750.

Molecular Endocrinology. First published March 18, 2004 as doi:10.1210/me.2003-0313

Differential effect of SUMOylation of the androgen receptor in the control of cooperativity on selective *versus* canonical response elements.

Abbreviated title : SUMOylation of the AR

Callewaert, L., Verrijdt, G[§]., Haelens, A[§]. and Claessens, F[*].

Division of Biochemistry, Faculty of Medicine, Campus Gasthuisberg, University of Leuven, Herestraat 49, B-3000 Leuven, Belgium

*To whom correspondence should be addressed: F. Claessens
K.U.Leuven, Campus Gasthuisberg,
O/N, Herestraat 49
3000 Leuven
Belgium
Tel.: +32-16-345770
Fax: +32-16-345995
frank.claessens@med.kuleuven.ac.be

Key words: posttranslational modification, SUMO-1, androgen receptor, cooperativity, transactivation, Ubc9

[*] This work was supported in part by the 'Geconcerteerde Onderzoeksactie van de Vlaamse Gemeenschap' and by grants from the 'Fonds voor Wetenschappelijk Onderzoek, Vlaanderen' and by a grant of the Association for International Cancer Research.

[§] Holders of a Postdoctoral Fellowship of the 'Fonds voor Wetenschappelijk Onderzoek-Vlaanderen'.

Summary

The androgen receptor (AR) can be SUMOylated in its amino-terminal domain at lysines 385 and 511. This SUMOylation is responsive to several agonists, but is not induced by the pure antagonist hydroxyflutamide. We show that the main site of interaction of Ubc9, the SUMO-1 conjugating enzyme, resides in the transcription activation unit tau-5.

Overexpression of SUMO-1 represses the AR-mediated transcription and this effect is abolished after mutating both SUMO-1 acceptor sites. On the other hand, the mutation of lysine 385 clearly affects the cooperativity of the receptor on multiple hormone response elements. Lysine 511 is not implicated in this function. Surprisingly, these effects on cooperativity clearly depend on the nature of the response elements. When selective AREs, which are organised as direct repeats of 5'-TGTTCT-3'-like sequences, were tested the lysine 385 mutation did not increase the androgen response. Point mutations changing the direct repeat elements into inverted repeat elements restored the effects of the lysine 358 mutation on cooperativity. In conclusion, SUMOylation of the AR might have a differential function in the control of cooperativity, depending on the conformation of the AR-dimer bound to DNA.

Introduction

The androgen receptor (AR) is a ligand-dependent transcription factor and belongs to the family of the nuclear receptors (NRs). Like all other NRs, the AR consists of three major functional domains: an amino-terminal domain (NTD), a DNA-binding domain (DBD) and a ligand-binding domain (LBD) (1). The DBDs of the class I steroid receptors (AR, glucocorticoid receptor (GR), progesterone receptor (PR) and mineralocorticoid receptor) recognize similar inverted repeats of 5'-TGTTCT-3'-like core sequences, spaced by three nucleotides. These elements will be referred to as canonical androgen responsive elements (AREs). However, several elements have been described to be recognized by the AR, but by no other NR. This proposed to contribute to the AR specificity of transcriptional responses (2). Such elements will be referred to as selective AREs. The three-dimensional structures of the LBDs of NRs are quite similar (3). In contrast to the other NR-LBDs, however, only a weak activation function 2 (AF-2) is observed in the AR-LBD (1, 4).

The AR-mediated response involves the recruitment of coactivators of which the group of the p160 or NR-interacting proteins are the best studied (5). Steroid receptor coactivator-1 (SRC-1), human and rat transcription-intermediary factor 2 and its mouse orthologue glucocorticoid receptor-interacting protein 1 (GRIP1), and receptor-associated coactivator 3 belong to this group (6-9). They interact with the NR-LBDs via highly conserved α-helical LxxLL motifs, arranged in a centrally located NR-interacting region (5, 10). For the AR, however, a glutamine-rich region of SRC-1 (Qr) is the main interaction site for the AR-NTD (11-13).

The NTD of the AR is about 530 amino acids long and contains a strong hormone-dependent transactivation unit 1, called Tau-1, residing between aa 100-370. When the LBD is deleted,

this activation domain shifts more C-terminally and is called the autonomous transactivation unit Tau-5 (aa 360-529) (14, 15). A strong amino-carboxy terminal (N/C)- interaction is necessary for AR-mediated activation on canonical but not selective androgen response elements (16-18).

The transcriptional activity of the NRs can be controlled or at least modulated by posttranslational modifications like phosphorylation and acetylation (19-23). Another posttranslational modification is ubiquitination (24, 25). Covalent attachment of at least four ubiquitin molecules targets the substrates to the proteasome where they undergo degradation. Recently, a new posttranslational modification system was discovered which resembles, but is distinct from the ubiquitination system. It was called SUMO-1 (small ubiquitin-like modifier-1) modification or SUMOylation. The lysine residue where SUMOylation can occur, resides in a consensus motif φKxE where φ is a large hydrophobic residue, K the lysine of SUMO-1 attachment, x any amino acid and E a glutamic acid (26-30). The conjugation pathway is mediated by three types of enzymes: an activating enzyme consisting of the Aos1/Uba2 dimer, a conjugation enzyme Ubc9 and ligation enzymes (26-30). Only one conjugating enzyme for SUMO-1 is known, but several SUMO-1 ligating enzymes have been discovered recently, *e.g.* the Protein Inhibitor of activated STAT (PIAS) (31-32). Moreover, both Ubc9 and PIASxα/ARIP3 have been demonstrated to interact with the AR (32).

A wide range of proteins are subject to SUMOylation, *e.g.* PML, IκBα, p53-related p73α protein, PIAS proteins, and RanGap1 (26-32). Recently, several steroid receptors have also been reported to be conjugated with SUMO-1. The glucocorticoid receptor has three major SUMO-1 attachment sites, two of which are situated in the NTD and one in the LBD (33,

34). The progesteron receptor can be SUMOylated in the NTD, and this modification is thought to regulate its autoinhibition and transrepression (35). The AR-NTD has two SUMO-1 consensus modification sites at positions 385 and 511 (36). In this paper, we analyse the SUMO-1 conjugation of the AR, and its impact on AR-mediated transcriptional activity.

Results

The two SUMOylation acceptor sites in the hAR differ in their abilities to be conjugated by SUMO-1

Poukka *et al.* described AR SUMOylation at lysine 386 and 520 (36). We can confirm these as the SUMO-1 targets in the AR. The numbering of the residues in this study is based on the AR cDNA sequence of the clone obtained from Brinkmann *et al.* (37).

We mutated one or both lysines of the SUMO-1 attachment sites in the hAR into arginines (K385R and K511R) and compared the SUMOylation efficiency to that of the wtAR in the presence of AR agonist methyltrienolone (R1881), pure AR antagonist hydroxyflutamide (OH-F) or partial AR antagonists medroxyprogesterone acetate (MPA) and cyproterone acetate (CPA). Clearly, both lysines are independent SUMO-1 acceptor sites, and the modification status of the AR depends on the nature of the ligand (figure 1).

In figure 1A, Flag-tagged hAR and mutant ARs were transiently expressed in COS-7 cells and coexpressed with c-myc-tagged SUMO-1 in the presence or absence of R1881 (10^{-8}M). When wtAR is coexpressed with SUMO-1, two major bands appear on Western blot in the absence of hormone (figure 1A, *upper* panel, *lane* 1). The fastest migrating band corresponds with the unmodified AR, while the slower band is dependent on coexpression with SUMO-1. As described by Poukka *et al.*, stimulation of the cells with R1881 enhances the SUMO-1 modification of the AR, whereby three bands appear (figure 1A, *upper* panel, *lane* 2) (36). From immunoprecipitation with anti-Flag antibody and subsequent immunoblotting with anti-c-myc antibody, we can conclude that the slower migrating bands are the SUMOylated AR forms (figure 1A, *lower* panel). We assume that the middle band is explained by mono-SUMOylation, while the slowest band corresponds with di-SUMOylated

AR. It is clear that these lysines are the only SUMO-1 conjugation targets in the wtAR since no modification is observed when both sites are mutated (K385R/K511R, *lanes 7 and 8*). When lysine 385 is mutated, mono-SUMOylation takes place only after stimulation with R1881 (*lane* 4 compared to *lane* 3). However, SUMOylation of the K511R construct already takes place in the absence of R1881 (*lane* 5), but is much more pronounced in the presence of the agonist (*lane* 6).

The SUMOylation pattern of the AR and AR mutants in the presence of 10^{-8}M OH-F is shown in figure 1B. The Western blots have been overexposed to detect low SUMOylation efficiencies. Clearly, SUMO-1 attachment to the wtAR or the K385R and K511R constructs is only very weakly enhanced by OH-F.

When the cells are treated with the partial antagonists MPA (figure 1C) or CPA (data not shown), SUMOylation of the AR constructs resembles the pattern obtained with agonist R1881.

Ubc9-binding sites in the hAR

Many of the proteins that can be SUMOylated interact with Ubc9, the SUMO-1 conjugating enzyme. The hinge region of the AR has been implicated in Ubc9 interaction (38). Therefore, we predicted that the deletion of the hinge region of the AR (ARΔH) should affect the SUMOylation efficiency. However, the Western blot in figure 2A shows that the SUMO-1 pattern for both wtAR and ARΔH are superimposable. To identify the Ubc9-interacting part of the AR, two-hybrid assays were performed in COS-7 cells (figures 2B&C). Surprisingly, no interaction is observed between Ubc9 and the DBD/H/LBD under condition where a good interaction is observed between the NTD and the DBD/H/LBD. We therefore looked for additional Ubc9 interaction sites in the AR. Coexpression of AR-NTD

fused to the DBDGal4 domain with Ubc9 fused to the VP16 activation domain clearly shows that Ubc9 binds well to the AR-NTD (figure 2C). There is already a high luciferase activity measured in the presence of the AR-NTD alone because of a strong constitutive active activation domain. To verify this interaction and to analyze the interaction of AR with Ubc9 *in vitro*, we performed GST pull-down experiments. Bacterially expressed GST or GST-Ubc9, immobilized on glutathion-Sepharose beads, were incubated with *in vitro* translated and ^{35}S-methionine labeled hAR-NTD$_{1\text{-}529}$ or deletions hAR-NTD$_{\Delta 1\text{-}360}$ and hAR-NTD$_{\Delta 360\text{-}529}$ (figure 2D). The first deletion construct still contains both SUMO-1 consensus motifs in contrast to the latter deletion construct, which lacks both sites. In this assay the hAR-NTD bound specifically to GST-Ubc9 but not to GST alone. Besides the wtAR-NTD, only the fragment of the NTD encompassing the Tau-5 domain and the SUMO-1 sites (hAR-NTD$_{\Delta 1\text{-}360}$) showed an interaction with Ubc9, while the mutant AR NTD$_{\Delta 360\text{-}529}$ is not able to interact with the conjugating enzyme.

SUMOylation of the hAR-NTD

Next to the study of SUMO-1 conjugation to the K385R and K511R constructs in context of the full size AR (figure 1), we have analysed the SUMOylation of the separated NTD of the AR (figure 3). Flag-tagged hAR-NTD or its mutants (NTDK385R, NTDK511R and NTDK385R/K511R) are transiently expressed in COS-7 cells and coexpressed with either c-myc-tagged SUMO-1 or SUMO-1mut. SUMO-1mut lacks the two carboxy-terminal glycines so that SUMO-1 modification does not occur. The extracts were immunoprecipitated with anti-Flag antibody and subsequently immunoblotted with anti-Flag (figure 3, *upper* panel) or anti-c-myc antibody (figure 3, *lower* panel). After cotransfection of the AR-NTD with SUMO-1, a slower migrating band appears, indicating that the AR-

NTD, when tested in isolation, is also SUMOylated. We can only detect mono-SUMOylation at lysine 385 (figure 3, *lane* 6). However, when both Ubc9 and SUMO-1 are overexpressed with wtAR, we could detect di-SUMOylation (data not shown).

SUMOylation of the AR does not depend on N/C-interactions

We and others demonstrated that an amphipatic helix N-terminally of the hAR-NTD, consisting of the FQNLF-motif, is nessessary for N/C-interaction and AR-function (16-18). We investigated whether the SUMO-1 conjugation of the AR depends on the N/C-interaction within the AR. Therefore, we compared the SUMOylation status of wtAR with that of ARΔFQNLF and ARG21E (figure 4), two mutants for which we know the N/C-interaction is abolished (18). Immunoblotting transfected COS-7 cells with a monoclonal M2 anti-Flag antibody shows that the SUMO-1 pattern for ARΔFQNLF and ARG21E is the same as for wtAR and hence, SUMOylation of the AR is independent of the N/C-interaction.

SUMOylation does not affect DNA-binding

We investigated whether SUMO-1 could affect the DNA-binding of the AR. Gel retardations were performed using either wtAR or ARK385R/K511R (figure 5A). COS-7 cells were transfected with expression vectors for wtAR or ARK385R/K511R in the presence of pSG5SUMO-1 or pSG5SUMO-1mut. As DNA-probe, we used oligonucleotides covering the rTAT-GRE sequence. The band shift assays showed no decreased binding of wtAR when cotransfected with SUMO-1. Also no difference in DNA-binding is observed for the mutant ARs. The SUMOylation status of the AR in the extracts was verified by Western blot analysis (data not shown).

We subsequently investigated whether the SUMOylated AR-form is still able to bind the DNA (figure 5B). The extracts were obtained from COS-7 cells, transfected with expression vectors for non-Flag-tagged wtAR in the presence of Flag-tagged SUMO-1 or SUMO-1mut. Western blot confirmed the presence of SUMOylated wtAR (data not shown). Anti-Flag antibody induced a partial supershift of the retarded rTAT-GRE probe, indicating that SUMOylated AR indeed binds DNA (figure 5B, *lane 5* compared to *lane 3*).

SUMO-1-effect on the transcriptional activity of the AR

It has already been suggested that SUMO-1 modification negatively regulates the AR transactivation capacity (36). We analysed this by cotransfecting wtAR or its mutants (K385R, K511R and K385R/K511R) with an expression vector for either SUMO-1 or SUMO-1mut and the reporter construct 2×rTAT-GRE(E1b)-Luc (figure 6A). Indeed, the transcriptional activity of wtAR or the single mutants decreases with approximately 50% when SUMO-1 is coexpressed. The repressive effect of SUMO-1 for the double mutant (ARK385R/K511R), however, is much smaller. We further investigated this using several other HREs (figure 6B). As selective AREs, we used *slp*-HRE2 and *sc*-ARE1.2 (table 1). As canonical AREs, we introduced mutations in *slp*-HRE2 (*slp*-HRE2 mut-4T-A; +2A-T) and *sc*-ARE1.2 (*sc*-ARE1.2 mut-4T-A;-2T-A), leading to a loss of selectivity of these elements (39). Here too, SUMO-1 overexpression leads to a decrease in AR activity.

Role of the synergy control motif in AR transactivation through canonical versus selective HREs

Initially, the SUMO-1 consensus sites in GR and AR have been described as synergy control motifs. The disruption of the SUMO-1 consensus sites was shown to lead to enhancement of the NR-dependent transcription on promotors with an increasing number of HREs (36, 40).

We tested reporter constructs containing several different AREs. First, COS-7 cells were transfected with constructs expressing wtAR or mutated ARs together with a luciferase reporter construct driven by the minimal thymidine kinase promotor and containing one, two or four copies of the rTAT-GRE. No effect of the lysine mutations on AR activity is seen when one copy of the rTAT-GRE was used (results not shown). In agreement with previous studies, a small increase in AR activity is observed on two copies of the rTAT-GRE when lysine 385 (K385R) or both lysines (K385R/K511R) were mutated (36, 40). Those effects are even more pronounced when studying a reporter containing four HRE copies, as shown in figure 7. Clearly, mutating lysine 511 does not affect the androgen responses.

We tested whether the same is true for reporters containing multiple copies of the androgen-selective AREs, *slp*-HRE2 and *sc*-ARE1.2 (figure 8A). For four copies of *slp*-HRE2, there is a more than 10-fold increase in wild type AR activity compared to two copies (*upper* panel). Also a 5-fold higher androgen induction is observed for 4×*sc*-ARE1.2 compared to 2×*sc*-ARE1.2 (*lower* panel). However, in contrast to multiple copies of canonical AREs, mutating the SUMO-1 acceptor sites separately or together did not affect this synergistic effect.

Interestingly, as shown in figure 8B, the loss of specificity after mutation of the AR-specific HREs (*slp*-HRE2 mut-4T-A; +2A-T and *sc*-ARE1.2 mut-4T-A;-2T-A) indeed correlates with an increased transactivation by ARK385R and K385R/K511R in comparison to wtAR activity.

Discussion

The AR has two SUMO-1 consensus sites in its amino-terminal domain, at lysine 385 and lysine 511 (36). Mutation of one of these sites prevents di-SUMOylation, while mutating both sites abolishes SUMO-1 conjugation (figure 1). SUMOylation of lysine 511 is agonist-dependent. SUMOylation of lysine 385, although partly hormone-independent, certainly is also a ligand-responsive event. Lysine 385 is the main site, but both lysines 385 and 511 can be SUMOylated independently from each other. In the presence of the pure antagonist hydroxyflutamide, there is no SUMO-1 conjugation at lysine 511, nor enhanced SUMO-1 conjugation at lysine 385. Interestingly, we observed that the SUMOylation of the AR mutant T877A, seen in LNCaP cells is comparable to that of wtAR (data not shown).

Most of the SUMO-1 protein targets interact with Ubc9 and it is likely that substrate recognition is achieved by Ubc9 (41, 42). For the AR, it has been suggested that the hinge region is implicated in Ubc9 interaction since it was isolated in double hybrid screening with this region as a bait (38). Our assays, however, did not reveal clear interaction between Ubc9 and AR-DBD/H/LBD. Moreover, an AR in which the hinge region has been deleted is as efficiently SUMOylated as the wild-type receptor (figure 2A). In addition, SUMOylation assay of the AR-NTD in figure 3 confirms that SUMO-1 attachment at lysine 385 can happen in the absence of the hinge region. We concluded that Ubc9 must interact with the AR-NTD. It has been reported that SUMO-1 consensus motifs are not only necessary for the covalent binding of SUMO-1, but they can also serve as the site of interaction with Ubc9 (43). Indeed, from mammalian double hybrid assays as well as GST-pull downs, we deduce that the major interaction site for Ubc9 in the AR resides in the Tau-5 constitutive active activation domain (figure 2). Remarkably, the two consensus motifs for SUMOylation

which lie in Tau-5 are predicted to form a loop structure, which might fit in the catalytic cleft of Ubc9, as demonstrated in the RanGAP1-Ubc9 complex (44).

Ubc9 has been reported to be a potent coactivator of the AR (38), while in other studies Ubc9 was shown to enhance AR activity modestly on some reporter constructs but not on others (45). In our hands, cotransfection of low amounts of Ubc9 increased the AR activity only moderately on all constructs tested, but increasing amounts of Ubc9 lead to a repressive effect. Whether this correlates directly with the intrinsic transcription repressing functions of Ubc9 when fused to Gal4DBD is not clear (data not shown).

PIASxα has been shown to function as a E3-type SUMO-1 protein ligase and enhances SUMOylation of the AR *in vitro* (31, 32). In COS-7 cells, we could not show enhanced AR-SUMOylation after cotransfecting the AR with PIASxα, although a clear interaction of PIASxα with ARDBD/H/LBD is seen in a two-hybrid assay (data not shown). This may be explained by the fact that SUMOylation of the AR is already optimal in COS-7 cells even in the absence of overexpressed PIASxα. In functional assays, PIASxα represses or activates AR activity on the canonical TAT-GRE and *slp*-HRE2 mut-4T-A;-2A-T respectively, while on the selective *slp*-HRE2, no effect is observed (data not shown). We therefore agree with literature that overexpressing the SUMOylation ligase PIASxα can affect AR activity to different extents depending on the response elements tested (45, 46). We postulate that the PIASxα-mediated effects are indirect since we could not see a correlation with the SUMOylation status of the AR.

We then examined the effect of SUMOylation on the transcriptional activity of the AR by coexpression of SUMO-1. The observed effect was dependent on the presence of one or

both SUMO-1 acceptor sites (figure 6). Similar to Poukka *et al.* (36), SUMO-1, but not SUMO-1mut, has a negative effect on AR activity.

For the progesterone receptor, the repression of the transcriptional activity by SUMOylation of its NTD requires the liganded LBD, suggesting that the N/C-interaction is involved (35). For the AR, the ligand-dependent interaction of the LBD with the NTD is strongly agonist-dependent, whereas OH-F, MPA and CPA fail to induce N/C-interaction (47). The SUMOylation pattern of the AR after stimulation with MPA and CPA resembles that after stimulation with agonist (R1881) and not after stimulation of antagonist OH-F (figure 1). It is therefore not surprising that in contrast to the PR, SUMOylation efficiency of the AR is not influenced by N/C-interaction nor by the enhanced recruitment of the p160s, induced by the G21E mutation (figure 4) (18). Whether the ligand-responsiveness of the SUMOylation is indirectly a result of a conformational change of the AR-NTD, induced by a ligand-occupied LBD, or whether other modulating proteins are recruited by the latter is still an open question.

One possible explanation for the observed reduction in AR transactivation by SUMOylation would be that SUMO-1 modification alters its DNA-binding ability. This has been demonstrated for heat shock transcription factor 2 (HSF2), a transcription factor that regulates heat shock protein gene expression. SUMO-1 attachment to HSF2 converts this factor to the active DNA-binding form (48). However, the DNA-binding assays in figures 5 show that the reduced AR activity seen when SUMO-1 is coexpressed does not reduce the DNA-binding. Indeed, the amount of retarded probe is even slightly higher when the AR is SUMOylated.

More recently, the p160 co-activators GRIP1 and SRC-1 have been shown to be SUMOylated at a site in the nuclear receptor interaction domain (49, 50). The group of Jänne (49) has shown that mutation of the SUMO-1 attachment sites in this domain of GRIP1 is correlated with a decreased colocalization of GRIP1 with the AR, a diminished coactivator capacity and a diminished ARLBD/GRIP1 interaction. It seems unlikely that such SUMOylation of GRIP1 or SRC-1 could be responsible for the decreased AR activity seen in our experiments, since the disruption of the SUMO-1 attachment sites (K385R/K511R) in the AR leads to reversal of the negative effects. It could, however, provide an explanation for the residual repression of the AR double mutant by overexpressed SUMO-1 on all AREs tested (figures 6A and 6B).

The possibility that AR-stability, and thus the outcome of these transfection experiments is affected by SUMOylation was contradicted by the immunoblotting results, which revealed no increased proteolysis of the SUMO-1 modified AR and no change in steady state levels (figure 1).

The SUMO-1 consensus modification sites of the glucocorticoid receptor (GR) overlap with the synergy control motifs (33, 40). Disrupting these motifs increases the transcriptional activity of the GR on promotors containing more that one hormone response element. Also the substitutions in the SUMO-1 acceptor sites affect AR activity on reporter constructs with multiple HREs (36). In our experiments, mutation of lysine 385 and the double mutation indeed lead to an increased activity on the reporter construct containing two copies of the rTAT-GRE, and this is even more pronounced when four copies are present (figure 7). It seems that lysine 385 plays an important role in this synergy control, while lysine 511 is not implicated in synergy.

We further characterized this synergy control in AR transactivation. From earlier experiments, we concluded that the AR transactivation mechanisms on canonical AREs differ from these on selective AREs, since the disruption of the N/C-interaction or deletion of the glutamine repeat has a negative effect on AR activity on canonical AREs while no change is seen on selective elements (18, 51). Here, we observed cooperativity of the AR on reporter constructs containing multiple selective motifs (figure 8A), but when the SUMOylation sites in the AR were mutated, no increase in transactivation was seen. It is difficult to compare the experimental data obtained after overexpression of SUMO-1 (figure 6), which will affect a multitude of factors, with those obtained when single SUMOylation sites are mutated (figure 8).

Clearly, lysine 385 is not acting as a synergy control element on selective AREs (figure 8A). However, when the selective AREs are mutated into canonical AREs, mutation of the SUMOylation sites again resulted in an increased synergy in the androgen response (figure 8B). This indicates that the underlying mechanism for cooperation and/or transcription activation and the role of SUMOylation in it on selective AREs might be different from that on canonical response elements.

In conclusion, we provide evidence that SUMOylation of lysines 385 and 511 is non-cooperative, and independent from N/C-interactions and the hinge region. We give evidence that Tau-5 of the AR-NTD is the main interaction site for Ubc9 rather than the AR hinge region. This is important since the hinge region is also involved in the recognition of selective AREs (2), and we report differences in the role of SUMOylation of lysine 385 in cooperativity on AR-selective *versus* canonical elements. These observations have to be taken into account in future experiments e.g. on co-activators and co-repressors. It has

recently been suggested that both AR SUMOylation sites are involved in the binding of SMRT (52, 53) and SRC1 to the AR-NTD (12, 13). The cell-specific levels of SUMO-1, Ubc9 and PIASxα, co-repressors and co-activators, as well as the nature of the response elements, will determine the extend of the androgen responses. Future experiments will also have to direct the issues of the chronological order of events and the regulatory role of SUMOylation at the level of AREs integrated into chromatin.

Materials and Methods

Plasmid constructs. The expression vectors pSG5AR (expressing full-length hAR either Flag tagged or not), pSG5ARG21E, pSG5ARΔFQNLF, pSG5AR-DBD/H/LBD$_{538\text{-}919}$ and the fusion constructs NTD with VP16 or DBDGal4 are described elsewhere (18, 54). The point mutations K385R, K511R and K385R/K511R were made by site-directed mutagenesis using the PCR-based method. The generated fragments were cloned into the pSG5(Flag)$_3$ (expression of the full-size AR or AR-NTDs) or pABGal4 (gererating AR-DBDGal4NTD fusions) vector. The expression vector for SUMO-1 and Ubc9 was a kind gift of Dr. A. Dejean (Unité de Recombinaison et Expression Génétique, Institut Pasteur, France). A c-myc-tagged or Flag-tagged SUMO-1 and SUMO-1mut (lacking the two C-terminal glycines) and the expression vector for flag-tagged ARΔH (hAR lacking the first 56 nucleotides of exon 4) were made by a PCR-cloning method. Similarly, Ubc9 was cloned into the GST expression vector, pGEX-5X-1 (Amersham Pharmacia Biotech.) and the VP16 expression vector pSNATCHII (15).

Restriction and modifying enzymes were obtained from MBI Fermentas GmbH. The luciferase reporter constructs containing the isolated elements TAT-GRE, *slp*-HRE2, *sc*-ARE1.2, *slp*-HRE2 mut-4T-A; +2A-T and *sc*-ARE1.2 mut-4T-A;-2A-T (table 1) are driven by the thymidine kinase (TK) minimal promotor or the E1b promotor, and have been described elsewhere (41 and references herein). The pCMV-βGal vector was obtained from Stratagene.

Transfections. All transfections were performed in COS-7 African green monkey kidney cells, obtained from the American Type Tissue Culture Collection (A.T.C.C., Manassas, VA, U.S.A.). The cells were seeded in 96-well culture plates and transfected as described

elsewhere (18). The amount of luciferase reporter construct was fixed at 100 ng per well and the amount of pCMV-β-Gal was fixed at 5 ng per well. After transfection, the cells were incubated for 24 h with medium containing 5% DCC and supplemented or not with 10^{-8} M of the synthetic androgen R1881 (methyltrienolone) (Dupont-New England Nuclear, Boston, Mass. USA), the antagonist OH-F (a kind gift of Dr. Neri, Schering Plough, Kelinworth, NJ) or the partial antagonist MPA (Sigma Aldrich). After 24 h, the cells were lysed in 25 µl of passive lysis buffer (Promega). The luciferase and β-galactosidase activities were measured in 2.5 µl of the extracts using the assay systems from Promega and Tropix (Westburg, the Netherlands), respectively. The luciferase activity in cell extracts was corrected for transfection efficiency by normalizing it according to the corresponding β-galactosidase activity. The values shown are the averages of at least three independent experiments performed in triplicate. Error bars indicate the standard error of the mean (SEM) values.

Preparation of COS-7 whole cell extracts. COS-7 cells were plated in 6-well culture plates (6 cm Petri Disches for immunoprecipitation experiments) and were transiently transfected with 0.5 µg of Flag-tagged AR or AR mutants (full-size AR or AR-NTDs) and 1.0 µg of c-myc-tagged SUMO-1 or SUMO-1mut. At 24 h after transfection, cells were stimulated for 24 h with or without hormone. The cells were treated and lysed as described earlier (51).

Immunoprecipitation and Western Blots. For immunoprecipitation, each protein extract was incubated with anti-Flag M2 agarose beads (10 µl) for 2 h at 4°C. After centrifugation (1 min. 5000 rpm), the supernatant was removed and the cells were washed 3 times with TBS (Tris bufferd saline, 10 mM Tris-HCl, pH 8.0, 150 mM NaCl). The bound proteins were released fom the beads in 2 × SDS sample buffer. For Western blotting, equal amounts of protein extracts were separated on a 6% or a 8% SDS-PAGE gel (for full-size AR or AR-

NTDs respectively) and blotted onto polyvinylidene difluoride membranes (Amersham Pharmacia Biotech.). The membranes were probed with a monoclonal M2 anti-Flag antibody (Stratagene) or with c-Myc antibody 9E10 (Santa Cruz Biotechnology). Immunoreactive proteins were visualized with the chemiluminescence reagent plus (NEN™ Life science) or with the chromogenic reagent for HRP detection (4CN reagent, NEN™ Life science).

DNA-binding assays and supershift assays. Synthetic complementary oligonucleotides were hybridized, radioactively labelled, and used in band-shift assays as described previously (52). In brief, 15 µg of total cell extract was preincubated with 1 µl poly(dI:dC) (1 µg/µl), 10 µl D100 (20 mM Hepes, 5 mM $MgCl_2$, 0.1 mM EDTA, 17% glycerol, 100 mM NaCl), 1 µl DTT (20 mM), 1 µl Triton X100 (1%) and 1 µl of water. Subsequently, the probe is added and incubated for 20 min. on ice. Bound probe was separated from the free by non-denaturing electrophoresis for two hours at 120 V in a 5% polyacrylamide gel. To obtain supershifts, a rabbit antiserum against human AR (55) or the monoclonal M2 anti-Flag antibody was added prior to the probe.

Protein expression and in vitro binding assay. In vitro transcription and translation of full size AR or AR fragments were performed in rabbit reticulocyte lysate in the presence of ^{35}S-methionine in a total volume of 25 µl as described by the manufacturer (Promega). The *in vitro* translated proteins were diluted to 500 µl with binding buffer (20 mM Tris pH 7.5, 150 mM NaCl and 0.1% Tween 20). GST or GSTUbc9 were expressed in the BL21 bacterial strain and bound to glutathion-Sepharose beads (Amersham Pharmacia biotech.). Nonspecific protein-binding sites were blocked by incubation with 2% BSA for 1 h at 4°C. 50 µl of each *in vitro* translated protein was incubated with the beads in 250 µl of binding

buffer for 30 min. at room temperature. Beads were washed three times with binding buffer. Bound proteins were eluted with 2 × SDS sample buffer. After SDS-PAGE electrophoresis, the gel was fixed in 10% acetic acid/25% isopropanol for 30 min., incubated in Amplify NAMP 100 (Amersham Pharmacia biotech.) for another 30 min., dried and finally labelled proteins were visualized by exposure to autoradiographic film (Hyperfilm ECL, Amersham, pharmacia).

Acknowledgements

We thank R. Bollen, H. Debruyn and K. Bosmans for their excellent technical assistance. We are indebted to Dr. A. Dejean for providing plasmids.

abbreviations

The abbreviations used are: AR/PR/GR/NR, androgen, progesterone, glucocorticoid, nuclear receptor; ARE, androgen response element; NTD, amino-terminal domain; DBD, DNA-binding domain; LBD, ligand-binding domain; AF, activation function; N/C, amino/carboxy; SRC-1, steroid receptor coactivator-1; GRIP1, glucocorticoid receptor-interacting protein 1; Qr, glutamine rich; Tau, transcription activation function; SUMO-1, small ubiquitin-like modifier-1; PIAS, Protein Inhibitor of Activated STAT; OH-F, hydroxyflutamine; MPA, medroxyprogesterone acetate; CPA, cyproterone acetate; TK, thymidine kinase; CMV, cytomegalovirus; rTAT, rat tyrosine aminotransferase; wt, wild-type

References

1. Evans RM 1988 The steroid and thyroid hormone receptor superfamily. Science 240:889-895

2. Claessens F, Verrijdt G, Schoenmakers E, Haelens A, Peeters B, Verhoeven G, Rombauts W 2001 Selective DNA binding by the androgen receptor as a mechanism for hormone-specific gene regulation. J Steroid Biochem Mol Biol 76:23-30

3. Kumar R, Thompson EB 1999 The structure of the nuclear hormone receptors. Steroids 64:310-319

4. Moilanen A, Rouleau N, Ikonen T, Palvimo JJ, Janne OA 1997 The presence of a transcription activation function in the hormone-binding domain of androgen receptor is revealed by studies in yeast cells. FEBS Lett 412:355-358

5. Heinlein CA, Chang C 2002 Androgen receptor (AR) coregulators: an overview. Endocr Rev 23:175-200

6. Voegel JJ, Heine MJ, Zechel C, Chambon P, Gronemeyer H 1996 TIF2, a 160 kDa transcriptional mediator for the ligand-dependent activation function AF-2 of nuclear receptors. EMBO J 15:3667-3675

7. Hong H, Kohli K, Garabedian MJ, Stallcup MR 1997 GRIP1, a transcriptional coactivator for the AF-2 transactivation domain of steroid, thyroid, retinoid, and vitamin D receptors. Mol Cell Biol 17:2735-2744

8. Bevan C, Parker M 1999 The role of coactivators in steroid hormone action. Exp Cell Res 253:349-356

9. Leo C, Chen JD 2000 The SRC family of nuclear receptor coactivators. Gene 245:1-11

10. Heery DM, Kalkhoven E, Hoare S, Parker MG 1997 A signature motif in transcriptional co-activators mediates binding to nuclear receptors. Nature 387:733-736

11. Onate SA, Boonyaratanakornkit V, Spencer TE, Tsai SY, Tsai MJ, Edwards DP, O'Malley BW 1998 The steroid receptor coactivator-1 contains multiple receptor interacting and activation domains that cooperatively enhance the activation function 1 (AF1) and AF2 domains of steroid receptors. J Biol Chem 273:12101-12108

12. Bevan CL, Hoare S, Claessens F, Heery DM, Parker MG 1999 The AF1 and AF2 domains of the androgen receptor interact with distinct regions of SRC1. Mol Cell Biol 19:8383-8392

13. Christiaens V, Bevan CL, Callewaert L, Haelens A, Verrijdt G, Rombauts W, Claessens F 2002 Characterization of the two coactivator-interacting surfaces of the androgen receptor and their relative role in transcriptional control. J Biol Chem 277:49230-49237

14. Jenster G, van der Korput HA, van Vroonhoven C, van der Kwast TH, Trapman J, Brinkmann AO 1991 Domains of the human androgen receptor involved in steroid binding, transcriptional activation, and subcellular localization. Mol Endocrinol 5:1396-1404

15. Alen P, Claessens F, Verhoeven G, Rombauts W, Peeters B 1999 The androgen receptor amino-terminal domain plays a key role in p160 coactivator-stimulated gene transcription. Mol Cell Biol 19:6085-6097

16. He B, Kemppainen JA, Wilson EM 2000 FXXLF and WXXLF sequences mediate the NH2-terminal interaction with the ligand binding domain of the androgen receptor. J Biol Chem 275:22986-22994

17. Steketee K, Berrevoets CA, Dubbink HJ, Doesburg P, Hersmus R, Brinkmann AO, Trapman J 2002 Amino acids 3-13 and amino acids in and flanking the 23FxxLF27 motif

modulate the interaction between the N-terminal and ligand-binding domain of the androgen receptor. Eur J Biochem 269:5780-5791

18. Callewaert L, Verrijdt G, Christiaens V, Haelens A, Claessens F 2003 Dual function of an amino-terminal amphipatic helix in androgen receptor-mediated transactivation through specific and nonspecific response elements. J Biol Chem 278:8212-8218

19. Fu M, Wang C, Reutens AT, Wang J, Angeletti RH, Siconolfi-Baez L, Ogryzko V, Avantaggiati ML, Pestell RG 2000 p300 and p300/cAMP-response element-binding protein-associated factor acetylate the androgen receptor at sites governing hormone-dependent transactivation. J Biol Chem 275:20853-20860

20. Wang C, Fu M, Angeletti RH, Siconolfi-Baez L, Reutens AT, Albanese C, Lisanti MP, Katzenellenbogen BS, Kato S, Hopp T, Fuqua SA, Lopez GN, Kushner PJ, Pestell RG 2001 Direct acetylation of the estrogen receptor alpha hinge region by p300 regulates transactivation and hormone sensitivity. J Biol Chem 276:18375-19383

21. Lee H, Bai W 2002 Regulation of estrogen receptor nuclear export by ligand-induced and p38-mediated receptor phosphorylation. Mol Cell Biol 22:5835-5845

22. Wang, Z., Frederick, J. and Wang Z, Frederick J, Garabedian MJ 2002 Deciphering the phosphorylation "code" of the glucocorticoid receptor in vivo. J Biol Chem 277:26573-26580

23. Gioeli D, Ficarro SB, Kwiek JJ, Aaronson D, Hancock M, Catling AD, White FM, Christian RE, Settlage RE, Shabanowitz J, Hunt DF, Weber MJ 2002 Androgen receptor phosphorylation. Regulation and identification of the phosphorylation sites. J Biol Chem 277:29304-29314

24. Pickart CM 2001 Mechanisms underlying ubiquitination. Annu Rev Biochem 70:503-533

25. Glickman MH, Ciechanover A 2002 The ubiquitin-proteasome proteolytic pathway: destruction for the sake of construction. Physiol Rev. 82:373-428

26. Yeh ET, Gong L, Kamitani T 2000 Ubiquitin-like proteins: new wines in new bottles. Gene 248:1-14

27. Melchior F 2000 SUMO--nonclassical ubiquitin. Annu Rev Cell Dev Biol 16:591-626

28. Rodriguez MS, Dargemont C, Hay RT 2001 SUMO-1 conjugation in vivo requires both a consensus modification motif and nuclear targeting. J Biol Chem 276:12654-12659

29. Muller S, Hoege C, Pyrowolakis G, Jentsch S 2001 SUMO, ubiquitin's mysterious cousin. Nat Rev Mol Cell Biol 2:202-210

30. Seeler JS, Dejean A 2001 SUMO: of branched proteins and nuclear bodies. Oncogene 20:7243-7249

31. Nishida T, Yasuda H 2002 PIAS1 and PIASxalpha function as SUMO-E3 ligases toward androgen receptor and repress androgen receptor-dependent transcription. J Biol Chem 277:41311-41317

32. Kotaja N, Karvonen U, Janne OA, Palvimo JJ 2002 PIAS proteins modulate transcription factors by functioning as SUMO-1 ligases. Mol Cell Biol 22:5222-5234

33. Tian S, Poukka H, Palvimo JJ, Janne OA 2002 Small ubiquitin-related modifier-1 (SUMO-1) modification of the glucocorticoid receptor. Biochem J 367:907-911

34. Le Drean Y, Mincheneau N, Le Goff P, Michel D 2002 Potentiation of glucocorticoid receptor transcriptional activity by sumoylation. Endocrinology 143:3482-3489

35. Abdel-Hafiz H, Takimoto GS, Tung L, Horwitz KB 2002 The inhibitory function in human progesterone receptor N termini binds SUMO-1 protein to regulate autoinhibition and transrepression. J Biol Chem 277:33950-33956

36. Poukka H, Karvonen U, Janne OA, Palvimo JJ 2000 Covalent modification of the androgen receptor by small ubiquitin-like modifier 1 (SUMO-1). Proc Natl Acad Sci U S A 97:14145-14150

37. Trapman J, Klaassen P, Kuiper GG, van der Korput JA, Faber PW, van Rooij HC, Geurts van Kessel A, Voorhorst MM, Mulder E, Brinkmann AO 1988 Cloning, structure and expression of a cDNA encoding the human androgen receptor. Biochem Biophys Res Commun. 153:241-248

38. Poukka H, Aarnisalo P, Karvonen U, Palvimo JJ, Janne OA 1999 Ubc9 interacts with the androgen receptor and activates receptor-dependent transcription. J Biol Chem 274:19441-19446

39. Verrijdt G, Schoenmakers E, Haelens A, Peeters B, Verhoeven G, Rombauts W, Claessens F 2000 Change of specificity mutations in androgen-selective enhancers. Evidence for a role of differential DNA binding by the androgen receptor. J Biol Chem 275:12298-12305

40. Iniguez-Lluhi JA, Pearce D 2000 A common motif within the negative regulatory regions of multiple factors inhibits their transcriptional synergy. Mol Cell Biol 20:6040-6050

41. Lin D, Tatham MH, Yu B, Kim S, Hay RT, Chen Y 2002 Identification of a substrate recognition site on Ubc9. J Biol Chem 277:21740-21748

42. Tatham MH, Chen Y, Hay RT 2003 Role of two residues proximal to the active site of Ubc9 in substrate recognition by the Ubc9.SUMO-1 thiolester complex. Biochemistry 42:3168-3179

43. Sampson DA, Wang M, Matunis MJ 2001 The small ubiquitin-like modifier-1 (SUMO-1) consensus sequence mediates Ubc9 binding and is essential for SUMO-1 modification. J Biol Chem 276:21664-21669

44. Bernier-Villamor V, Sampson DA, Matunis MJ, Lima CD 2002 Structural basis for E2-mediated SUMO conjugation revealed by a complex between ubiquitin-conjugating enzyme Ubc9 and RanGAP1. Cell 108:345-356.

45. Geserick C, Meyer HA, Barbulescu K, Haendler B 2003 Differential Modulation of Androgen Receptor Action by DNA Response Elements. Mol Endocrinol Jun 5 [in press]

46. Kotaja N, Aittomaki S, Silvennoinen O, Palvimo JJ, Janne OA 2000 ARIP3 (androgen receptor-interacting protein 3) and other PIAS (protein inhibitor of activated STAT) proteins differ in their ability to modulate steroid receptor-dependent transcriptional activation. Mol Endocrinol 14:1986-2000

47. Berrevoets CA, Umar A, Brinkmann AO 2002 Antiandrogens: selective androgen receptor modulators. Mol Cell Endocrinol 198:97-103

48. Goodson ML, Hong Y, Rogers R, Matunis MJ, Park-Sarge OK, Sarge KD 2001 Sumo-1 modification regulates the DNA binding activity of heat shock transcription factor 2, a promyelocytic leukemia nuclear body associated transcription factor. J Biol Chem 276:18513-18518

49. Kotaja N, Karvonen U, Janne OA, Palvimo JJ 2002 The nuclear receptor interaction domain of GRIP1 is modulated by covalent attachment of SUMO-1. J Biol Chem 277:30283-30288

50. Chauchereau A, Amazit L, Quesne M, Guiochon-Mantel A, Milgrom E 2003 Sumoylation of the progesterone receptor and of the steroid receptor coactivator SRC-1. J Biol Chem 278:12335-12343

51. Callewaert L, Christiaens V, Haelens A, Verrijdt G, Verhoeven G, Claessens F 2003 Implications of a polyglutamine tract in the function of the human androgen receptor. Biochem Biophys Res Commun 306:46-52

52. Dotzlaw H, Moehren U, Mink S, Cato AC, Iniguez Lluhi JA, Baniahmad A 2002 The amino terminus of the human AR is target for corepressor action and antihormone agonism. Mol Endocrinol 16:661-673

53. Dotzlaw H, Papaioannou M, Moehren U, Claessens F, Baniahmad A 2003 Agonist-antagonist induced coactivator and corepressor interplay on the human androgen receptor. Mol Cell Endocrinol [in press]

54. Haelens A, Verrijdt G, Callewaert L, Christiaens V, Schauwaers K, Peeters B, Rombauts W, Claessens F 2003 DNA recognition by the androgen receptor: evidence for an alternative DNA-dependent dimerization, and an active role of sequences flanking the response element on transactivation. Biochem J 369:141-151

55. Marivoet S, Hertogen M, Verhoeven G, Heyns W 1990 Antibodies against synthetic peptides recognize the human and rat androgen receptor. J Steroid Biochem Mol Biol 37:39-45

Figure legends

Figure 1. **Analysis of the ligand-dependency of the two SUMO-1 acceptor sites** (A) The effect of the mutation of the SUMO-1 acceptor sites was analysed in immunoprecipitation assays. COS-7 cells were transfected with Flag-tagged wtAR, ARK385R, ARK511R or ARK385R/K511R and cotransfected with c-myc-tagged SUMO-1. After 24 h, cells were incubated with or without agonist R1881 (10^{-8} M) as indicated on top. 10% of the protein extracts were subjected to Western blotting and AR was detected using the monoclonal M2 anti-Flag antibody (*upper* panel). AR was immunoprecipitated from 90% of the extracts with the anti-Flag antibody agarose, subjected to Western blotting and probed with anti-c-Myc antibody to detect the SUMOylated AR-forms (*lower* panel). The non-modified ARs and the SUMOylated ARs are indicated on the right by an asterisk or a double asterisk, respectively. Non-specific bands are indicated by an empty circle. (B and C) Experiments are performed as in figure 1A. Cells were stimulated with OH-F (10^{-8} M) (panel B) or MPA (10^{-8} M) (panel C).

Figure 2. **Ubc9 interaction with hAR and effect on AR activity.** (A) SUMOylation of wtAR and ARΔH. COS-7 cells were transfected with Flag-tagged AR or ARΔH and cotransfected with either empty vector pSG5 or with pSG5SUMO-1 and stimulated with or without hormone after 24 h. The extracts were resolved on a 6% SDS polyacrylamide gel and immunoblotted with monoclonal M2 anti-Flag antibody. The positions of non-modified AR and SUMOylated AR are indicated by an asterisk or a double asterisk, respectively. (B) Two-hybrid assay. PSG5AR-DBD/H/LBD (538-919aa) (50 ng/well) was coexpressed in COS-7 cells with either the empty pSNATCH-II expression vector or the same expression vector containing Ubc9 or AR-NTD (50 ng/well). Assays were performed using the 2×TAT-

GRE(E1b)-Luc reporter (100 ng) and the CMV-β-Gal reporter (5 ng/well). Bars represent the luciferase/β-galactosidase values. (C) Two-hybrid assay. Empty pABGal4 or pABGal4AR-NTD (50 ng/well) was coexpressed in COS-7 cells with 50 ng of empty pSNATCH-II or pSNATCHIIUbc9. Assays were performed using the $(Gal4)_5$-TATA-Luciferase reporter (100 ng). Activities are depicted relative to the activity of the wtAR-NTD construct in the presence of empty vector, which was set to 100. (D) GST-pull down assay. Wild-type AR-NTD (*lanes* 1-3) and the deletion mutants $NTD_{\Delta 1\text{-}360}$ and $NTD_{\Delta 360\text{-}529}$ (*lanes* 4-6 and 7-9, respectively) were transcribed and translated in rabbit reticulocyte lysates in the presence of ^{35}S-methionine and incubated with GST or GSTUbc9 beads. Elution was performed with SDS sample buffer and analysed by SDS-PAGE followed by autoradiography. The amount of protein loaded in the input lane is equivalent to 10% of the amount of protein assayed in each binding experiment.

Figure 3. **SUMO-1 conjugation of ARNTD and its mutants.** COS-7 cells were transfected with Flag-tagged wtAR-NTD, NTDK385R, NTDK511R or NTDK385R/K511R and cotransfected with c-myc-tagged SUMO-1 or SUMO-1mut. Protein extracts were immunoprecipitated with the anti-Flag antibody agarose, subjected to Western blotting and probed with the monoclonal M2 anti-Flag antibody (*upper* panel) or anti-c-Myc antibody (*lower* panel). The non-modified ARs and the SUMOylated ARs are indicated on the right by an asterisk or a double asterisk, respectively.

Figure 4. **SUMOylation of wtAR, ARΔFQNLF and ARG21E.** COS-7 cells were transfected with Flag-tagged AR, ARΔFQNLF or ARG21E and cotransfected with either empty vector pSG5 or with pSG5SUMO-1. Cells were treated, extracts were made and analysed as dictated for figure 1 and detected with the monoclonal M2 anti-Flag antibody.

The positions of non-modified AR and SUMOylated AR are indicated by an asterisk or a double asterisk, respectively.

Figure 5. **DNA-binding analysis of SUMOylated AR.** (A) DNA-binding assay of the rTAT-GRE with wtAR or ARK385R/K511R. Labelled probe was incubated with similar amounts of COS-7 extracts containing wtAR or ARK385R/K511R indicated at the top in the presence of SUMO-1 or SUMO-1mut as indicated at the bottom. Cells were stimulated with hormone (R1881, 10^{-8} M) for 24 h. Free probe and bound probes are indicated on the right by an open arrow or a black arrow, respectively. (B) DNA-binding analysis and super shift assays of the SUMOylated AR-forms. The same labelled probe was used as in figure 5A and was incubated with equal amount of COS-7 extracts containing wtAR (non Flag-tagged) cotransfected with Flag-tagged SUMO-1 or SUMO-1mut, as indicated at the bottom. Cells were stimulated with hormone (R1881, 10^{-8} M) for 24 h. For the super shifts, the M2 anti-Flag antibody to detect SUMO-1 (*lanes 4 and 5*) and a rabbit antiserum against human AR (*lanes 6* and *7*) were used. Free probe and shifted complexes are indicated on the right by an open arrow or a black arrow, respectively. Supershifts are marked by an asterisk.

Figure 6. **SUMO-1 affects AR activity.** (A) 100 ng luciferase reporter construct driven by the E1b promotor containing 2 copies of the rTAT-GRE and 5 ng CMV-βGal reporter construct were transiently transfected into COS-7 cells. Cotransfection was performed with 20 ng of empty vector pSG5, pSG5wtAR, pSG5ARK385R, pSG5ARK511R or pSG5ARK385R/K511R as indicated and with 20 ng pSG5SUMO-1 or pSG5SUMO-1mut. Cells were incubated for 24 h without or with hormone (R1881, 10^{-8} M). Bars represent the luciferase/β-galactosidase values. (B) The transfection assays were performed as in figure 6A, using luciferase reporter constructs (100 ng) as indicated on top. The sequences of the

AREs are given in table 1. Bars represent the luciferase/β-galactosidase values measured in extracts, relative to the activity in the extracts of cells transfected with wtAR, which was set on 100.

Figure 7. **Effect of mutation of the SUMO-1 acceptor sites on AR activity on 2×rTAT-GRE and 4×rTAT-GRE.** TK minimal promotor-driven luciferase reporter constructs (100 ng) containing 2 or 4 copies of the response element, indicated on the top, were transiently transfected into COS-7 cells and cotransfected with 20 ng of empty vector, pSG5wtAR, pSG5ARK385R, pSG5ARK511R or pSG5ARK385R/K511R as indicated. Cells were incubated for 24 h without hormone or with hormone (R1881, 10^{-8} M). Bars represent the luciferase/β-galactosidase values measured in extracts, relative to the activity in the extracts of cells transfected with wtAR and the luciferase reporter construct containing four copies of the response element, which was set on 100.

Figure 8. **Synergy control motif in AR-transactivation through canonical *versus* selective HREs.** (A) Effect of mutation of the SUMO-1 acceptor sites on AR activity on selective AREs. TK minimal promotor-driven luciferase reporter constructs (100 ng) containing either 2 or 4 copies of the AR-selective response elements *slp*HRE2 or *sc*ARE1.2 (*upper* and *lower* panel respectively), were transiently transfected into COS-7 cells and cotransfected with 20 ng of empty vector, pSG5wtAR, pSG5ARK385R, pSG5ARK511R or pSG5ARK385R/K511R as indicated. Cells were incubated for 24 h without hormone or with hormone (R1881, 10^{-8} M). The sequences of the AREs are given in table 1. The experimental values are presented as in figure 7. (B) Effect of mutation of the SUMO-1 acceptor sites on AR-activity on mutant AREs. Luciferase reporter constructs containing 4 copies of the mutated *slp*-HRE2 and *sc*-ARE1.2 motifs, indicated on the right, were

transiently transfected into COS-7 cells and cotransfected with 20 ng of empty vector, pSG5wtAR, pSG5ARK385R, pSG5ARK511R or pSG5ARK385R/K511R as indicated. The sequences of the AREs are given in table 1. The experimental values are presented as in figure 7.

Table 1

Name	Sequence	Specificity
TAT-GRE	5'TGTACAggaTGTTCT3'	Canonical
*slp*HRE2	5'TGGTCAgccAGTTCT3'	AR-selective
*slp*HRE2 mut-4T-A;+2T-A	5'TGGACAgccTGTTCT3'	Canonical
*sc*ARE1.2	5'GGCTCTttcAGTTCT3'	AR-selective
*sc*ARE1.2mut-4T-A;-2T-A	5'GGCACAttcAGTTCT3'	Canonical

Table 1. **Canonical and AR-selective steroid receptor binding motifs.** Trivial names and sequences of the different motifs, used in this study, are indicated. Numbering of the nucleotides is relative to the central nucleotide of the three-nucleotide spacer. Mutated nucleotides are *underlined*.

Figure 1A

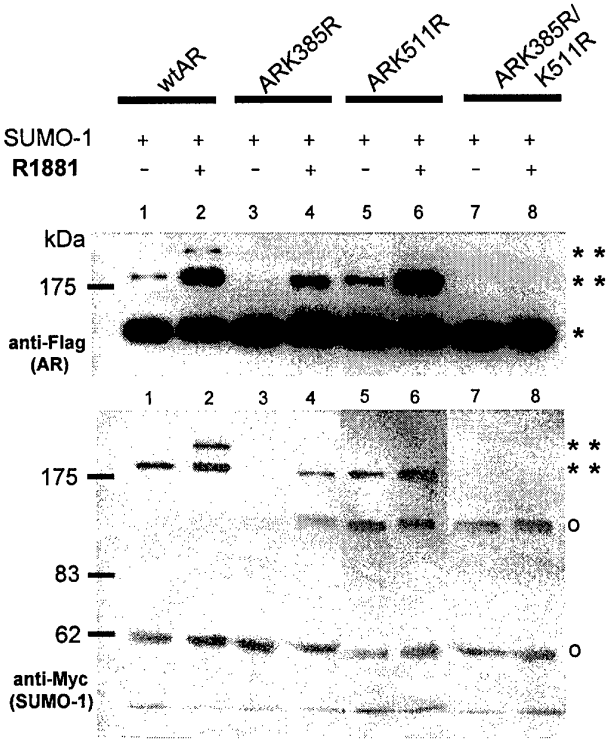
wtAR
ARK385R
ARK511R
ARK385R/
K511R
SUMO-1
R1881
1 2 3 4 5 6 7 8
kDa
175
anti-Flag
(AR)
* *
* *
*
1 2 3 4 5 6 7 8
175
83
62
anti-Myc
(SUMO-1)
* *
* *
o
o

Figure 1B

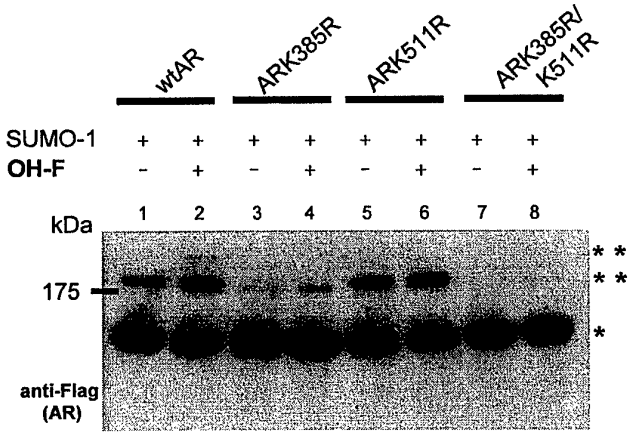
wtAR
ARK385R
ARK511R
ARK385R/
K511R
SUMO-1
OH-F
1 2 3 4 5 6 7 8
kDa
175
anti-Flag
(AR)
* *
* *
*

Figure 1C

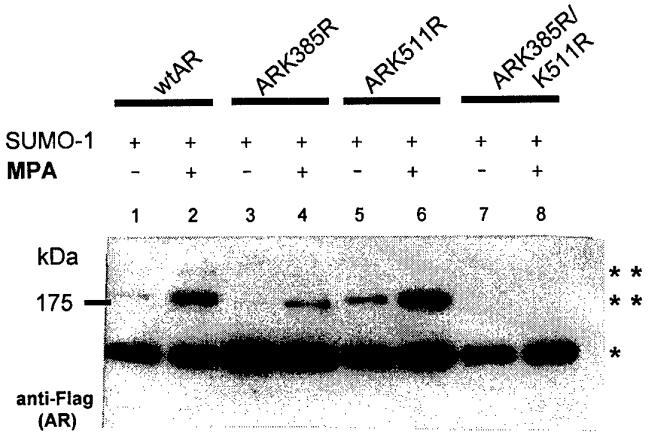
wtAR
ARK385R
ARK511R
ARK385R/
K511R
SUMO-1 + + + + + + + +
MPA - + - + - + - +
1 2 3 4 5 6 7 8
kDa
175
anti-Flag
(AR)
* *
* *
*

Figure 2A

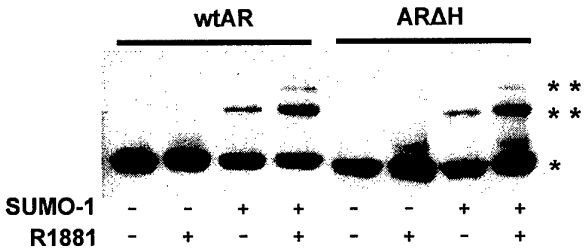

figure 2B

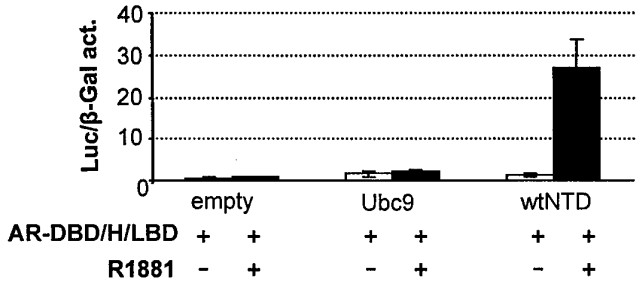

Figure 2C

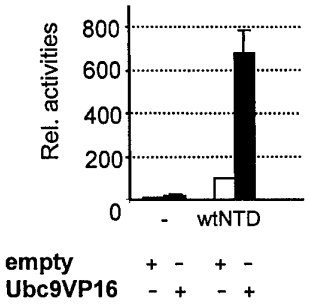

figure 2D

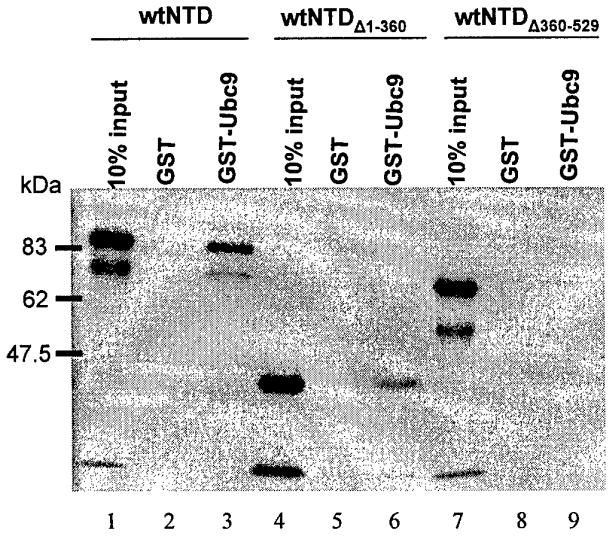
wtNTD
wtNTD$_{\Delta 1-360}$
wtNTD$_{\Delta 360-529}$
10% input
GST
GST-Ubc9
10% input
GST
GST-Ubc9
10% input
GST
GST-Ubc9
kDa
83
62
47.5
1 2 3 4 5 6 7 8 9

Figure 3

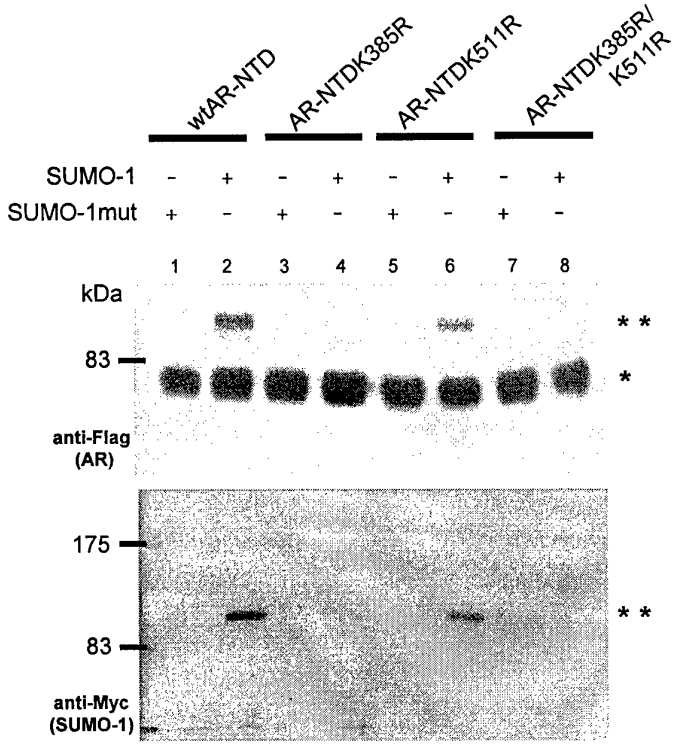
wtAR-NTD
AR-NTDK385R
AR-NTDK511R
AR-NTDK385R/
K511R
SUMO-1 - + - + - + - +
SUMO-1mut + - + - + - + -
1 2 3 4 5 6 7 8
kDa
83
anti-Flag
(AR)
* *
*
175
83
anti-Myc
(SUMO-1)
* *

Figure 4

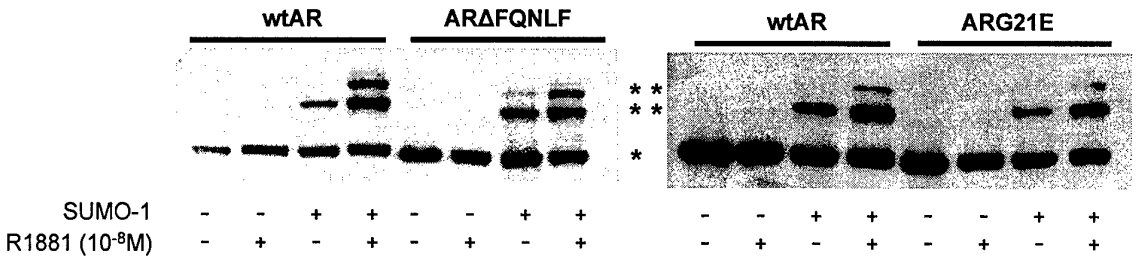

Figure 5A

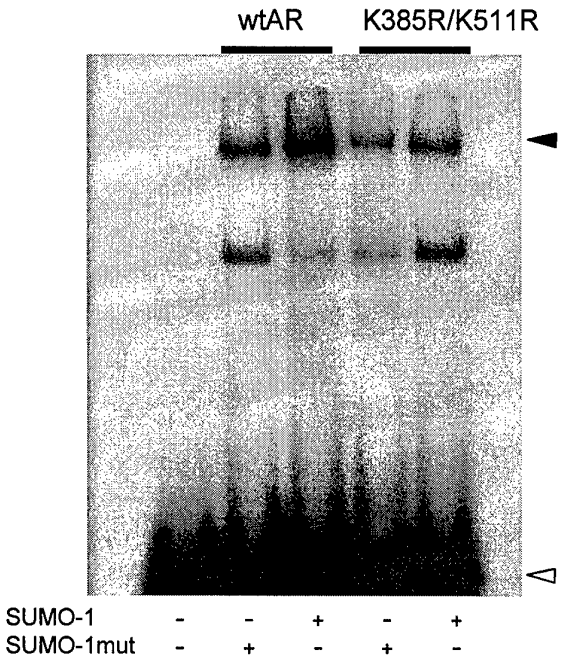

Figure 5B

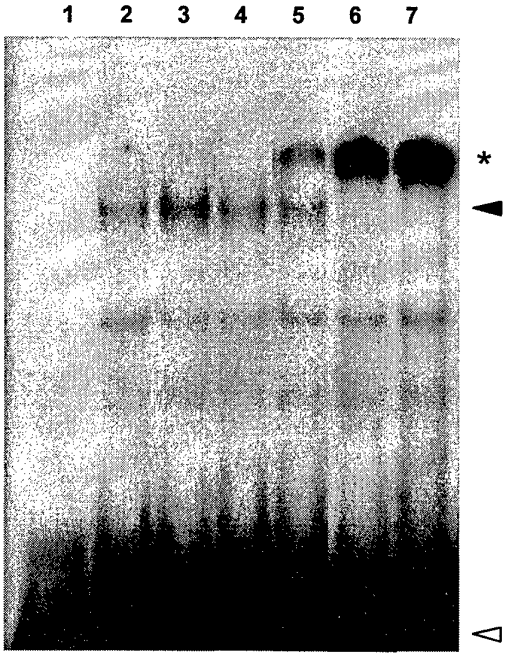

wtAR	-	+	+	+	+	+	+
SUMO-1mut	-	+	-	+	-	+	-
SUMO-1	-	-	+	-	+	-	+
anti-Flag	-	-	-	+	+	-	-
anti-AR	-	-	-	-	-	+	+

Figure 6A

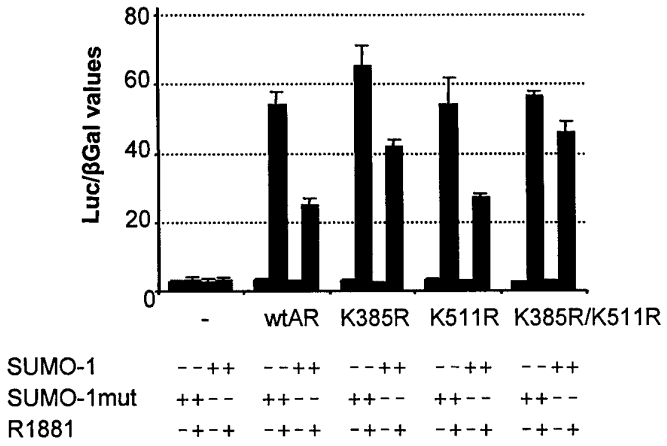
80
60
40
20
0
Luc/βGal values
-
wtAR
K385R
K511R
K385R/K511R
SUMO-1 --++ --++ --++ --++ --++
SUMO-1mut ++-- ++-- ++-- ++-- ++--
R1881 -+-+ -+-+ -+-+ -+-+ -+-+

Figure 6B

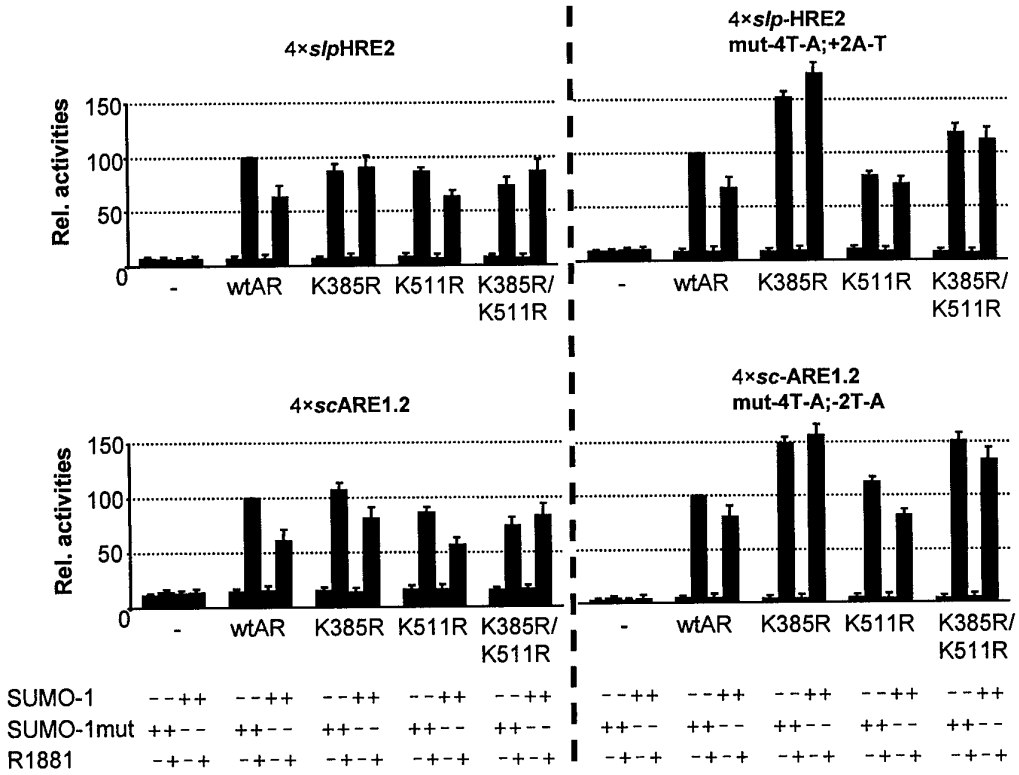
4×slpHRE2
4×slp-HRE2
mut-4T-A;+2A-T
Rel. activities
150
100
50
0
-
wtAR
K385R
K511R
K385R/
K511R
4×scARE1.2
4×sc-ARE1.2
mut-4T-A;-2T-A
SUMO-1 --++ --++ --++ --++ --++ --++ --++ --++ --++ --++
SUMO-1mut ++-- ++-- ++-- ++-- ++-- ++-- ++-- ++-- ++-- ++--
R1881 -+-+ -+-+ -+-+ -+-+ -+-+ -+-+ -+-+ -+-+ -+-+ -+-+

Figure 7

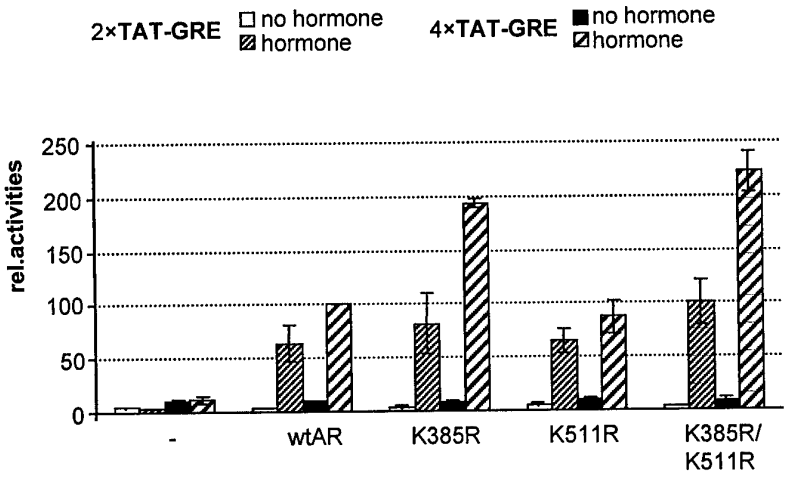
2×TAT-GRE
no hormone
hormone
4×TAT-GRE
no hormone
hormone
rel.activities
250
200
150
100
50
0
-
wtAR
K385R
K511R
K385R/
K511R

Figure 8A

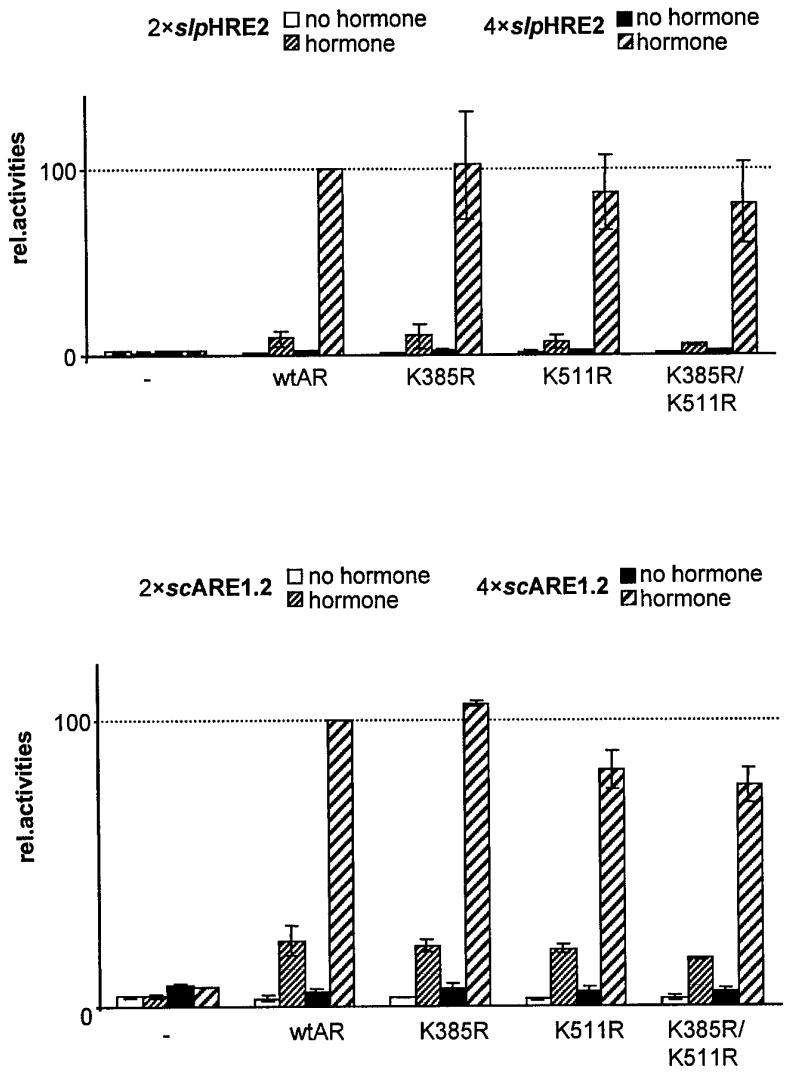
2×slpHRE2
no hormone
hormone
4×slpHRE2
no hormone
hormone
rel.activities
100
0
-
wtAR
K385R
K511R
K385R/
K511R
2×scARE1.2
no hormone
hormone
4×scARE1.2
no hormone
hormone
rel.activities
100
0
-
wtAR
K385R
K511R
K385R/
K511R

Figure 8B

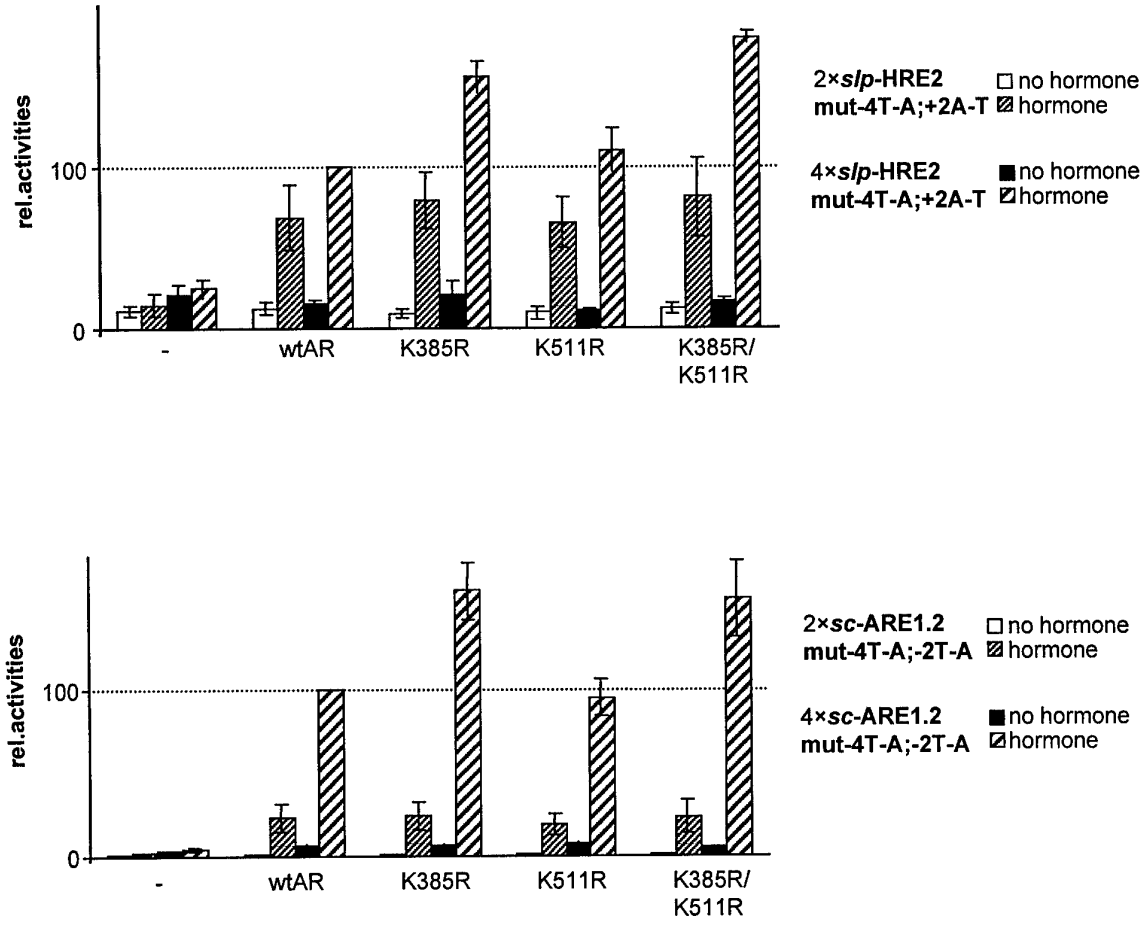
rel.activities
100
0
-
wtAR
K385R
K511R
K385R/
K511R
2×slp-HRE2
mut-4T-A;+2A-T
no hormone
hormone
4×slp-HRE2
mut-4T-A;+2A-T
no hormone
hormone
rel.activities
100
0
-
wtAR
K385R
K511R
K385R/
K511R
2×sc-ARE1.2
mut-4T-A;-2T-A
no hormone
hormone
4×sc-ARE1.2
mut-4T-A;-2T-A
no hormone
hormone

The hinge region of the androgen receptor plays a role in proteasome-mediated transcriptional activation

Tamzin Tanner, Frank Claessens and Annemie Haelens

Biochemistry Division, Laboratory of Molecular Endocrinology, Catholic University of Leuven, Campus Gasthuisberg O&N, Herestraat 49, Leuven, 3000, Belgium.

Keywords

androgen receptor, hinge region, proteasome, PEST sequence, transcription regulation

Address for correspondence: Frank Claessens. Biochemistry Division, Laboratory of Molecular Endocrinology, Catholic University of Leuven, Campus Gasthuisberg O&N, Herestraat 49, Leuven, 3000, Belgium. e-mail: Frank.Claessens@med.kuleuven.ac.be ;Tel: +32 16 347205; Fax: +32 16 345995.

Introduction

The human androgen receptor (AR) is a member of the nuclear receptor superfamily. It has a modular structure and comprises 919 amino acids. It is composed of a long N-terminal domain (NTD) with a transactivation function AF-1, a central DNA-binding domain (DBD), a hinge region and a C-terminal ligand-binding domain (LBD) with an additional transactivation function AF-2 [1]. Initially, the hinge region was considered as a non-functional linker between the DBD and the LBD. However, recent results indicate that the hinge region is a multifunctional region involved in DNA-binding [2, 3], nuclear localisation [4] and modulation of transactivation [5, 6]. The hinge region is also a phosphorylation [7] and acetylation [8, 9] target-site and is an interaction domain for several proteins [10].

Results and Discussion

In this study we investigated in more detail the role of the hinge region (amino acids 628-669) in the transactivation of the AR. Transfection experiments using COS-7 or HeLa cells and androgen responsive reporter constructs were performed. We found that the AR deleted of amino acids 628-646 (ARΔH) is at least three times more potent than the wild-type AR (wtAR) when tested in both COS-7 and HeLa cells (figure 1). This is in agreement with a previous report [6]. Our data indicate that the hinge region plays an important role in controlling the transactivation potential of the AR. These results are surprising since the nuclear localisation signal and a region involved in DNA binding are partially deleted in ARΔH. However, the mutated receptor can still activate transcription, thus both of these functions must still be present to some extent.

Analysis of the amino acid sequence of the AR hinge region reveals the presence of a putative PEST sequence, between amino acids 638 and 658, which is conserved between different

species [11]. PEST sequences are amino acid stretches (rich in proline, glutamate, serine and threonine residues) that are involved in targeting proteins for degradation by the 26S proteasome [12]. For the AR, degradation has been shown to be regulated by the ubiquitin-proteasome pathway [13]. As the PEST sequence is partially deleted in ARΔH, degradation by the proteasome may be hindered resulting in an increase in protein levels which would then explain the increased potency observed in transfection experiments. To study the effect of the proteasome on the expression and activity of the wtAR and ARΔH proteins, we made use of the proteasome inhibitor MG132.

Western analysis revealed that in the presence of androgen, 1 nM R1881, both wtAR and ARΔH expression levels increased (figure 2A, lanes 1 and 2), and that this hormone-dependent stabilisation was more pronounced for the latter. Addition of MG132 did not result in a substantially higher wtAR level, but positively affected the level of ARΔH (figure 2A, lanes 3 to 8). Surprisingly, at higher concentrations (10 μM MG132), this effect was much lower. Our data suggest that the hormone-induced stabilisation of the wtAR is mildly proteasome-dependent, since addition of MG132 had only a weak influence on the hormone effect. On the other hand, it seems that the deletion of the hinge region induces an increased sensitivity of the AR to proteasome-mediated degradation (compare lane 2 with lanes 3 and 6, figure 2A).

Transfection experiments were carried out to determine whether or not the changes detected at the protein level have any influence at a transcriptional level as shown for the estrogen receptor α (ERα), where transcriptional activity is interdependent on proteasome-mediated degradation [14]. For wtAR, MG132 had no net effect on its transactivation properties (figure 2B, light grey bars). However, in the presence of MG132, the potency of ARΔH was reduced

to the levels of wtAR (figure 2B, black bars). At 10 μM MG132, the level of ARΔH expression was very similar to the condition without MG132 (figure 2A), while its transactivation potential was much lower (figure 2B). Similar results were obtained when cells were stimulated with 1 nM (figure 2B) or 10 nM (data not shown) R1881. Collectively, these results imply that there are at least two interdependent effects of MG132 on ARΔH. We would suggest that not only is the proteasome involved in maintaining the steady state of ARΔH, but that it also affects the transactivating potential of this protein. In regards to transcriptional activation, it has previously been demonstrated that proteasome function is involved in the recruitment of the AR, in complex with coactivators, to enhancers [15]. In that system it was further demonstrated that when proteasome function is inhibited by treatment with MG132, the release of the receptor from the promoter is inhibited, and this correlates with a suppressed AR activity. Similarly, MG132 has been shown to suppress AR transactivation in the two prostate cancer cell-lines, LNCaP and PC-3 [16]. Therefore, our results obtained with ARΔH could be explained by a proteasome function in AR transcription complex formation, in our assays however, treatment with MG132 does not suppress wtAR transcriptional activity. Although we cannot explain these differences, our data indicate that the hinge region plays a crucial role in proteasome-mediated transactivation by the AR.

The precise manner in which the proteasome regulates AR activity is still unclear and may indeed involve multiple mechanisms and different co-factors [14]. Identification of some of these processes will involve a more detailed structure-function analysis of the hinge region of the AR, as well as a clear mapping of its interacting proteins.

Acknowledgements

We thank R. Bollen, K. Bosmans and H. Debruyn for their excellent technical assistance. This work is supported in part by grants from 'Fonds voor Wetenschappelijk Onderzoek, Vlaanderen', 'Geconcerteerde Onderzoekactie van de Vlaamse Gemeenschap', 'Congressionally Directed Medical Research Program: Prostate Cancer Research Program' Award n° DAMD17-02-1-0082, and 'Interuniversity Poles of Attraction Program, Belgium State, Prime Minister's Office, Federal Office for Scientific, Technical and Cultural Affairs.'

References

1. Evans, R.M.. 1988. The Steroid and Thyroid Hormone Receptor Superfamily. Science **240**: 889-894.

2. Haelens, A., G. Verrijdt, L. Callewaert, V. Christiaens, K. Schauwaers, B. Peeters, W. Rombauts & F. Claessens. 2003. DNA recognition by the androgen receptor: evidence for an alternative DNA-dependent dimerization, and an active role of sequences flanking the response element on transactivation. Biochem. J. **369**: 141-151.

3. Schoenmakers, E., P. Alen, G. Verrijdt, B. Peeters, G. Verhoeven, W. Rombauts & F. Claessens. 1999. Differential DNA binding by the androgen and glucocorticoid receptors involves the second Zn-finger and a C-terminal extension of the DNA-binding domains. Biochem J. **341**: 515-521.

4. Zhou, Z.X., M. Sar, J.A. Simental, M.V. Lane & E.M. Wilson. 1994. A ligand-dependent bipartite nuclear targeting signal in the human androgen receptor. Requirement for the DNA-binding domain and modulation by NH2-terminal and carboxy-terminal sequences. J. Biol. Chem. **269**: 13115-13123.

5. Moilanen, A., N. Rouleau, T. Ikonen, J.J. Palvimo & O.A. Janne. 1997. The presence of a transcription activation function in the hormone-binding domain of androgen receptor is revealed by studies in yeast cells. FEBS Lett. **412**: 355-358.

6. Wang, Q., J. Lu & E.L. Yong. 2000. Ligand- and coactivator-mediated transactivation function (AF2) of the androgen receptor ligand-binding domain is inhibited by the cognate hinge region. J. Biol. Chem. **276**: 7493-7499.

7. Zhou, Z.X., J.A. Kemppainen & E.M. Wilson. 1995. Identification of three proline-directed phosphorylation sites in the human androgen receptor. Mol. Endocrinol. **9**: 605-615.

8. Fu, M., C. Wang, A.T. Reutens, J. Wang, R.H. Angeletti, L. Siconolfi-Baez, V. Ogryzko, M.L. Avantagiata & R.G. Pestell. 2000. p300 and p300/cAMP-response element-binding protein-associated factor acetylate the androgen receptor at sites governing hormone-dependent transactivation. J. Biol. Chem. **275**: 20853-50860.

9. Fu, M., C. Wang, J. Wang, X. Zhang, T. Sakamaki, Y.G. Yeung, C. Chang, T. Hopp, S.A. Fuqua, E. Jaffray, R.T. Hay, J.J. Palvimo, O.A. Janne & R.G. Pestell. 2002. Androgen receptor acetylation governs trans activation and MEKK1-induced apoptosis without affecting in vitro sumoylation and transrepression function. Mol. Cell Biol. **22**: 3373-3388.

10. http://ww2.mcgill.ca/androgendb/

11. Sheflin L., B. Keegan, W. Zhang & S.W. Spaulding. 2000. Inhibiting proteasomes in human HepG2 and LNCaP cells increases endogenous androgen receptor levels. Biochem. Biophys. Res. Commun. **276**: 144-150.

12. Rechsteiner, M. & S.W. Rogers. 1996. PEST sequences and regulation by proteolysis. Trends Biochem. Sci. **21**: 267-271.

13. Lin, H.K., L. Wang, Y.C. Hu, S. Altuwaijri & C. Chang. 2002. Phosphorylation dependent ubiquitylation and degradation of androgen receptor by Akt require Mdm2 E3 ligase. EMBO J. **21**: 4037-4048.

14. Reid, G., M.R. Hubner, R. Metivier, H. Brand, S. Denger, D. Manu, J. Beaudouin, J. Ellenberg & F. Gannon. 2003. Cyclic, proteasome-mediated turnover of unliganded and liganded ERα on repsonsive promoters is an integral feature of estrogen signalling. Mol. Cell **11**: 695-707.

15. Kang, Z., A. Pirskanen, O.A. Janne & J.J. Palvimo. 2002. Involvement of proteasome in the dynamic assembly of the androgen receptor transcription complex. J. Biol. Chem. **277**: 48366-48371.

16. Lin, H-K., S. Altuwaijri, W-J. Lin, P-Y. Kan, L.L. Collins & C. Chang. 2002. Proteasome activity is required for androgen receptor transcriptional activity via regulation of androgen receptor nuclear translocation and interaction with coregulators in prostate cancer cells. J. Biol. Chem. **277**: 36570-36576.

Figure legends

Figure 1: The hinge region limits the transactivation potential of the AR at androgen responsive reporters.

COS-7 and HeLa cells were seeded into 96-well plates at 10^4 cells/well and $1.5x10^4$ cells/well, respectively. Twenty-four hours later cells were transfected with 100 ng reporter, 10 ng appropriate receptor and 10 ng β-galactosidase expression vectors using FuGENE6 reagent (Roche Molecular Biochemicals) according to the manufacturer's instructions. Twenty-four hours post-transfection, cells were refreshed with medium ± androgen (R1881) at the indicated concentrations and incubated for a further 24 hours, after which cells were lysed with Passive Lysis Buffer (Promega) and assayed for luciferase (Luciferase Assay Reagent; Promega) and β-galactosidase (Galacto Reaction Buffer; Tropix Inc.) activities. Graphs depict induction factors for increasing concentrations of R1881; at two androgen responsive reporters in both COS-7 cells (left panel) and HeLa cells (right panel). Reporters used: a luciferase reporter gene driven by the mouse mammary virus long-terminal repeat, MMTV-luc (**A** and **B**) and a luciferase reporter driven by an ARE of the C3(1) gene of prostate binding protein, C3(1)ARE-luc (**C** and **D**) [2]. Results represent pooled data from at least three independent experiments with each condition in duplicate.

Figure 2: Amino acids 628-646 of the hinge region play a role in proteasome-mediated transcriptional activation by the AR.

(A) Western Blot. HeLa cells were seeded into 24-well plates at 10^5 cells/well. After 24 hours cells were transfected with 200 ng of the appropriate flag-tagged receptor expression vector using FuGENE6 reagent. Twenty-four hours post-transfection, cells were stimulated with or

without androgen (1 nM R1881) in the absence or presence of increasing concentrations of MG132 (Calbiochem). MG132 was added either together with the androgen or 6 hours after addition of androgens, resulting in an incubation time of 24h and 18h, respectively. Total cell extracts were obtained by lysing cells, after 24h of hormone stimulation, with lysis buffer (5% NP40, 1/200 protease inhibitor mix in 1xPBS) and equal amounts of extracts were loaded onto a 10% SDS-polyacrylamide gel, electrophoresed and blotted onto Hybond-P nitrocellulose membrane (Amersham Biosciences). Membranes were probed with anti-flag anti-body, receptor proteins detected by ECL and autoradiography performed. **(B)** Transfection. HeLa cells were seeded into 96-well plates at $1.5x10^4$ cells/well. Cells were transfected as described in figure 1 with 100 ng MMTV-luc reporter, 10 ng appropriate receptor and 10 ng β-galactosidase expression vectors. Cells were stimulated as described for the Western blot (A). Assays were performed and graphs depict induction factors. The left panel shows results for when MG132 was added together with the androgen (24h incubation) and the right panel depicts MG132 added 6h after androgen stimulation (18h incubation). Results represent pooled data from at least three independent experiments with each condition in duplicate.

Figure 1

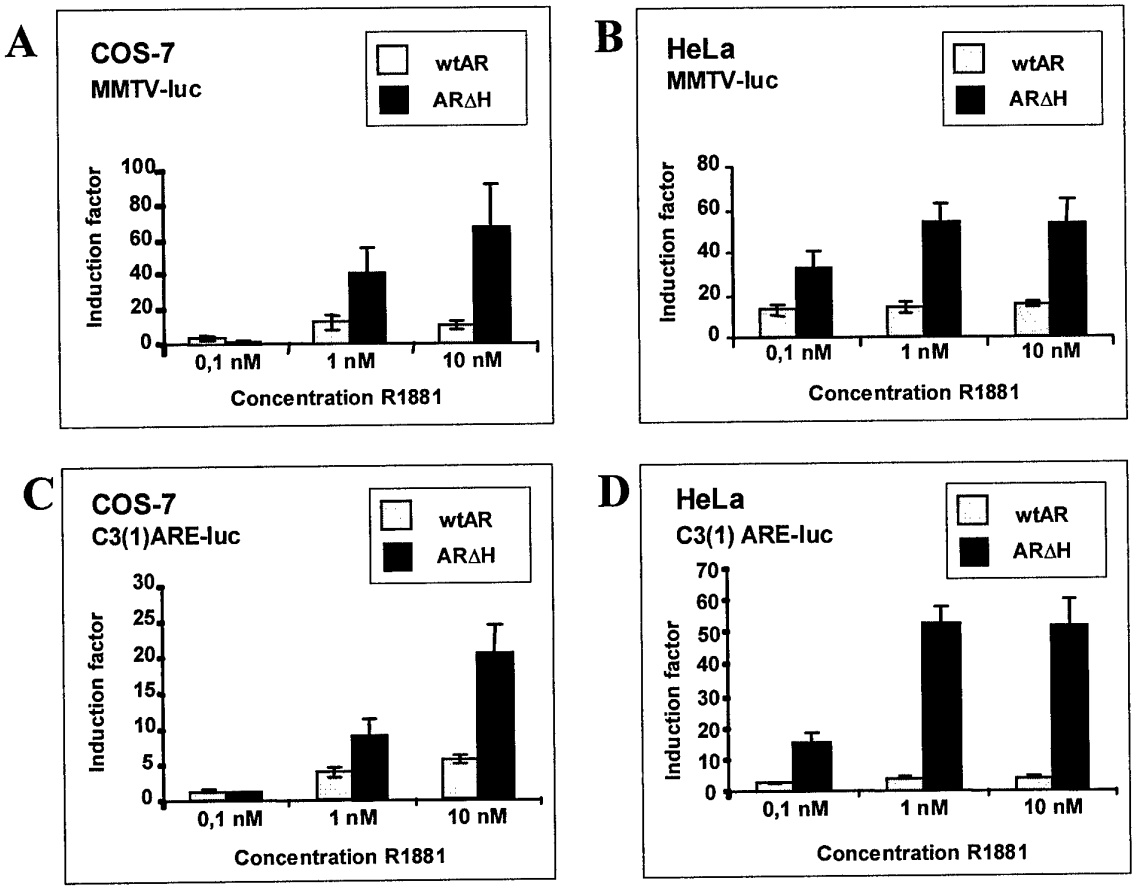
A
COS-7
MMTV-luc
wtAR
ARΔH
Induction factor
100
80
60
40
20
0
0,1 nM
1 nM
10 nM
Concentration R1881
B
HeLa
MMTV-luc
wtAR
ARΔH
Induction factor
80
60
40
20
0
0,1 nM
1 nM
10 nM
Concentration R1881
C
COS-7
C3(1)ARE-luc
wtAR
ARΔH
Induction factor
30
25
20
15
10
5
0
0,1 nM
1 nM
10 nM
Concentration R1881
D
HeLa
C3(1) ARE-luc
wtAR
ARΔH
Induction factor
70
60
50
40
30
20
10
0
0,1 nM
1 nM
10 nM
Concentration R1881

Figure 2

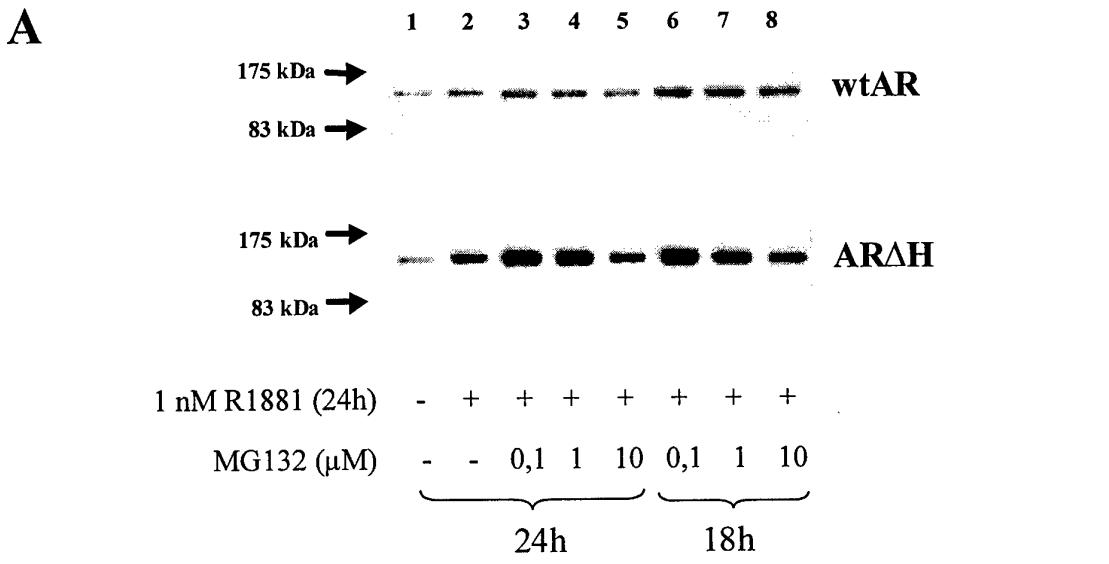
A
1 2 3 4 5 6 7 8
175 kDa
83 kDa
wtAR
175 kDa
83 kDa
ARΔH
1 nM R1881 (24h) - + + + + + + +
MG132 (μM) - - 0,1 1 10 0,1 1 10
24h
18h

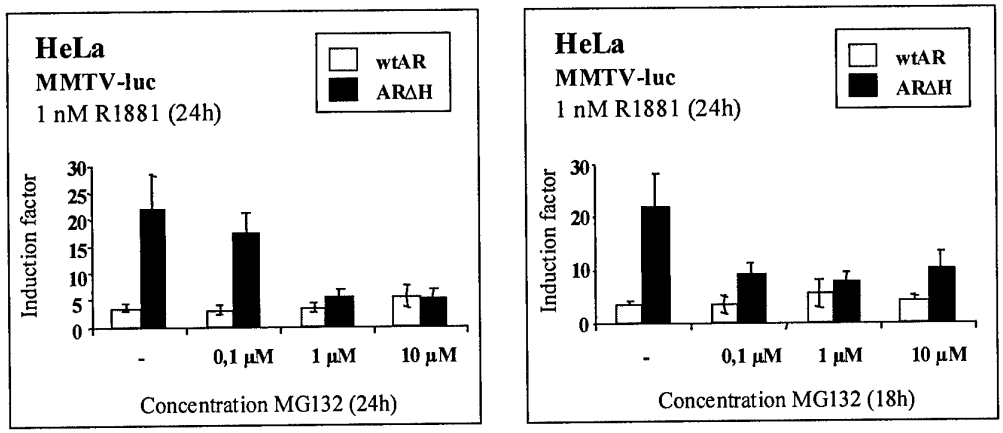
B
HeLa
MMTV-luc
1 nM R1881 (24h)
wtAR
ARΔH
Induction factor
30
25
20
15
10
5
0
-
0,1 μM
1 μM
10 μM
Concentration MG132 (24h)
HeLa
MMTV-luc
1 nM R1881 (24h)
wtAR
ARΔH
Induction factor
30
20
10
0
-
0,1 μM
1 μM
10 μM
Concentration MG132 (18h)